DELIVERABLE

European physical vulnerability models

Work package	WP26 (JRA4: Risk Modelling Framework for Europe)
Lead	UPORTO
Authors	Xavier Romão, University of Porto
	José Miguel Castro, University of Porto
	Nuno Pereira, University of Porto
	Helen Crowley, EUCENTRE
	Vitor Silva, GEM Foundation
	Luis Martins, GEM Foundation
	Daniela Rodrigues, EUCENTRE
Reviewers	Management Board
Approval	Management Board
Status	Final
Delivery deadline	30.04.2019
Submission date	30.04.2019
Intranet path	DOCUMENTS/DELIVERABLES/SERA_D26.5 Physical_Vulnerability

Table of Contents

Summary

This deliverable presents the methodology that is being used to develop a vulnerability model of the residential, commercial and industrial building stock in Europe. The vulnerability model describes the value of expected economic losses and the expected number of fatalities associated to a given level of the ground motion intensity, and aims to cover the physical assets identified in the exposure model which currently covers 46 European countries. The methodology builds upon an extensive review of existing fragility and vulnerability models and is based on a robust framework that accounts for and propagates all the sources of uncertainty affecting the problem, including the building-to-building variability, the uncertainty about the record-to-record variability and the uncertainty about the damage states. The robustness of the framework is also set by a systematic validation methodology recently developed that aims to verify the internal (within the set of fragility functions) and external (testing against damage scenarios) validity of the fragility functions and of the vulnerability models that are being developed. The vulnerability models currently being developed will be one of the inputs to the European seismic risk model.

1   Introduction

A probabilistic seismic risk assessment involves the estimation of the probability of damage and losses resulting from potential future earthquakes. This damage and loss might occur to buildings, infrastructure, people or even the environment. Within the European risk framework that is being developed within SERA, the focus is being placed on estimating damage and loss for residential, commercial and industrial buildings (and their occupants), involving a consistent risk-assessment that is in line with the Global Seismic Risk Map v2018.1, as denoted in Deliverable D26.7 (Crowley et al., 2019c).

Various initiatives were conducted in the past to characterize the seismic vulnerability of physical assets within the Pan-European region. Among those, a European wide probabilistic seismic hazard assessment methodology was developed by the SHARE project (2009-2013), leading to the new European seismic hazard map ESHM20 that is currently being developed within the SERA project. The European FP7 NERA project summarized the state-of-the-art knowledge on Exposure by collecting building stock information at the national level from building or population/dwelling censuses and national records about construction practices performed by statistical or financial services of the country (Crowley et al. 2012). Within SERA, significant efforts are being made to improve and systematize the Exposure model for the Pan-European region. A prior comprehensive building type classification for Europe was also proposed in the RISK-UE project (2001–2004) (Mouroux and Brun 2006) that included fragility and vulnerability models developed for assessing risk for earthquake scenarios at the city scale. Similar scenarios were also analysed within the LessLoss project (Calvi and Pinho, 2006). The SYNER-G project developed a new methodological framework for the systemic assessment of physical seismic vulnerability, including not only residential buildings, but also industrial facilities and infrastructures (Pitilakis et al. 2013). Additional data about the vulnerability of industrial buildings and components of non-nuclear facilities was provided by the STREST project. Despite the large amount of information available from past European projects on the seismic risk assessment, Corbane et al. (2017) pointed out that none of the initiatives succeeded in assessing seismic risk at the European level, and mentioned the challenges of combining different exposure datasets with considerable heterogeneity, different formats and levels of details. The referred exposure heterogeneity and gap of information that vary from country to country are aspects that may also limit the development of a continental risk model, given the several sources of uncertainty affecting simultaneously exposure, fragility and vulnerability models. Recent studies such as the South America Risk Assessment (SARA) project (https://sara.openquake.org/) highlighted several issues on how an

efficient vulnerability assessment could be made, and identified the main aspects that should be taken into account: the adequate treatment of building-to-building variability, the incorporation of record-to-record variability and of the uncertainty about the damage states, and the selection adequate of validation strategies for the fragility and vulnerability models.

As part of the European risk framework work package of SERA (JRA4), efforts are being made to develop a standardized and robust approach for deriving a set of fragility functions and vulnerability models for the most common building classes in Europe. The main objectives that were set are first to evaluate and share existing data for the European building stock, and then develop a framework incorporating the main sources of uncertainty: building-to-building variability, uncertainties about the building class taxonomy, record-to-record variability and uncertainty in the definition of the damage. The framework has several validation levels which include consistency checks with the results of studies conducted in other regions of the globe (e.g. with the models developed in the SARA project) and comparisons across building classes (which are possible given the robust ground motion intensity measures that are being used). Furthermore, the framework also uses a key validation component that is based on the robust methodology proposed by Silva and Horspool (2019) and can be used to calibrate the existing exposure and/or the fragility and vulnerability models.

The current report summarizes the main data of the review of previous studies conducted for the Pan-European region, and presents the methodology that was developed and that is being used to define the SERA fragility functions and vulnerability models database. Due to the importance of the exposure data in the definition of the standardized approach, Section 2 summarizes the main features of the exposure model v0.1 presented in Deliverables D.26.2 and D.26.3. Section 3 presents a review of the main attributes that must be included within the fragility and vulnerability models as part of the uncertainty of the exposure model v0.1, namely the effect of attributes that were collapsed in the classification adopted in Deliverables D.26.2 and D.26.3. Furthermore, the effect of the country-to-country heterogeneity and of the collapsed taxonomy string (see Brzev et al. 2013 for a conceptual definition) is further assessed in terms of variations of fragility functions and capacity curves, and a database was compiled with data from several literature studies and past research projects. Section 3 also describes the existing fragility and vulnerability models that were developed by GEM for the v0.1 exposure model, and that were used in the Global Seismic Risk Map v2018.1. Finally, Section 3 also summarizes the main vulnerability studies that are available for industrial buildings.

Based on this review, modifications were made to the v0.1 European Exposure Model, namely to optimize the mapping of the available exposure information to the building classes for which fragility and vulnerability models are being developed in SERA. Section 4 presents the main modifications that were made to the exposure model to increase its resolution for engineered building classes. Section 5 presents the systematic and robust methodology that is being used to generate the SERA vulnerability models, including the specific variants that are adopted for the different building typologies. Finally, Section 6 presents the specific methods that will be used for the testing and validation of the fragility and vulnerability models that are being developed within SERA.

2   European Exposure Model v0.1

The development of a European exposure model, i.e. the spatial distribution of the residential, commercial and industrial building count, population, and replacement cost - characterized in terms of building classes - follows two main steps: i) modelling the distribution of the number of buildings across different building classes within urban and rural areas, and in some cases also historical centres and large cities, ii) modelling the spatial distribution of the number of buildings, replacement cost and number of occupants (for residential buildings) within each building class across a given country, by combining a number of different public sources of data.

European residential and non-residential exposure models are being derived in the SERA project (as outlined in Deliverables D26.2 and D26.3: Crowley et al., 2018 and Crowley et al., 2019a, respectively) based on the latest national housing censuses, socio-economic indicators (e.g. labour force, population and floor area per worker per economic sector), and mapping schemes (also referred to as inference rules) developed by the authors together with local experts. In December 2018 the Global Earthquake Model (www.globalquakemodel.org.) released a Global Seismic Risk Map v2018.1 (GEM 2018) that made use of version 0.1 of the European Exposure Model developed within SERA.

The buildings in the exposure model are classified according to their seismic performance using a building taxonomy that is based on an updated version of an international standard (the GEM Building Taxonomy, Brzev et al., 2013, as updated by Silva et al., 2018) that allows buildings to be classified according to a number of structural attributes. The following main attributes were selected for the consistent definition of building classes across Europe in the v0.1 exposure model:

- Main construction material (reinforced concrete, unreinforced masonry, reinforced/confined masonry, adobe, steel, timber).
- Lateral load-resisting system, LLRS (infilled frame, moment frame, wall, dual frame-wall system, flat slab/plate or waffle slab, post and beam).
- Number of storeys.
- Ductility level (non-ductile, low, moderate and high ductility).

A description of some of the main residential, industrial and commercial building classes found across Europe (in terms of main construction material, LLRS and number of storeys) can be found in Tables 1, 2 and 3 of Deliverable D26.3. The building classes in each country in the v0.1 model were identified from local expert judgment and peer-reviewed publications. The ductility level has been inferred from the level of seismic design used at the time of construction and the hazard level (as described in Deliverable D26.2). The spatial distribution of the material of construction in the v0.1 Exposure model has been mapped at a national level in terms of the population, number of buildings and replacement cost. Figure 1 shows an example of the pie charts of construction material distribution in terms of replacement cost.
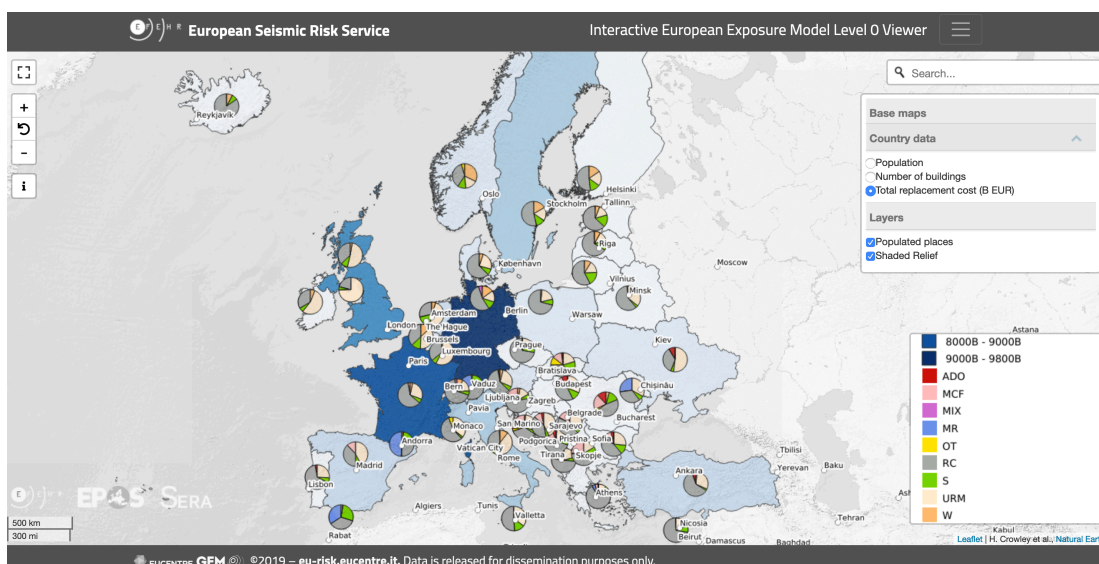

Figure 1: Distribution of construction material across the European countries in the v0.1 exposure model according to total replacement cost (https://maps.eu-risk.eucentre.it/map/european-exposure-level-0/#4/51.33/6.78).

3   Overview of existing fragility functions and vulnerability models for Europe

The SERA exposure models for residential buildings (v0.1; Crowley *et al.* 2018b, summarized in Section 2) and for commercial and industrial buildings (Crowley *et al.*, 2019b) provide the geographical location and distribution of the buildings and occupants (for residential buildings) exposed to seismic hazard in Europe. The physical characteristics of the buildings at risk were then defined following the GEM building taxonomy (Brzev *et al.,* 2013), using a combination of databases and mapping schemes. Nevertheless, due to the limited data available on a number of attributes to be able to make this classification at a continental level, a collapsed taxonomy was adopted instead. This implies that the remaining unknown properties have to be implicitly accounted for in the subsequent tasks of the risk analysis. In particular, these uncertainties about the building classes can be incorporated into the fragility functions and vulnerability models that are defined for each building class of the exposure model. The following sections illustrate these issues and identify the building attributes for which there is insufficient information in the exposure models, by referring to the several building classes that are relevant to the v0.1 exposure models. In addition, a database with this vulnerability data was developed to estimate the epistemic uncertainty associated to the unknown attributes of building classes, which must be included in the fragility/vulnerability modelling.

3.1   Overview of methodologies and guidelines for developing fragility functions and vulnerability models

Fragility functions establish the probability of exceeding/attaining a given damage state for a given intensity level of ground motions, whereas physical vulnerability models provide, for the same intensity, the probability distribution of loss ratios. Fragility functions can be developed using three different types of methods: 1) analytical methods; 2) empirical and expert elicitation approaches; 3) hybrid methodologies. Analytical methods rely on numerical models that simulate the seismic capacity of each building class, involving the complete nonlinear static or dynamic analysis of a representation of the structure. Methods involving different levels of complexity and comprehensiveness are available and guidelines for the analytical derivation fragility functions were recently proposed by GEM (D'Ayala et al., 2014; Porter et al., 2014; STREST 2015). Empirical fragility models rely on data collected in post-earthquake scenarios, using damage records and the recorded ground motion intensities. Colombi et al. (2008) and Rossetto et al. (2013) provided guidelines on how to use empirical data to define sets of fragility functions. Finally, a combination of these methods define the so-called hybrid approaches (Singhal and Kiremidjian, 1997; Kappos et al., 2006).

Empirical and analytical methods can also be used to derive vulnerability models. In the first case, loss data is used to set the probability of different loss ratios. In the second case, numerical models are used to establish directly (correlating the values of engineering demand parameters with repair costs and fatalities, e.g. see FEMA P-58, 2012) or indirectly (combining the damage states for which fragility functions were derived with consequence models) the losses for different ground motion intensity measure levels (IM_L). Direct methods rely on structural and non-structural component fragility data and repair costs to quantify the loss distributions. On the other hand, indirect methods couple the fragility and vulnerability by defining, for a given damage state, the corresponding consequences (using damage-to-loss consequence models). Vulnerability models are often represented by the variation of the expected value of the losses with the ground motion IM_{Ls}. D'Ayala et al. (2014) provide guidelines for the derivation of vulnerability models.

Studies performed in the past at the continental or global scales (e.g. projects RISK-EU (Mouroux et al., 2004), SARA (Villar-Vega et al., 2017), Global Seismic Risk Model v2018.1 (Martins and Silva, 2018) adopted analytical methods based on the nonlinear dynamic analysis of equivalent single-degree-of-freedom (SDOF) systems using real ground motion records. The properties of the equivalent SDOF system formulated in the ADRS format (i.e. spectral displacement vs spectral acceleration) are based on the results of modal and nonlinear pushover analyses performed in multi-degree-of-freedom structure (MDOF) structures. Among these results, the roof displacement (D_{roof}) of the MDOF system and the first mode participation factor (Γ) are used to establish the spectral displacements Sd and the spectral acceleration Sa in the ADRS format by:

$$S_d = \frac{D_{roof}}{\Gamma},$$

(1)

$$S_a = S_d \left(\frac{2\pi}{T}\right)^2,$$

(2)

The behaviour of the SDOF system in the ADRS format is then represented by capacity curves that can have multiple configurations. The simplest capacity curves consider a bilinear model defined as a function of the yield period (T_y), the yield displacement (Sd_y), the ultimate displacement (Sd_u) and the corresponding spectral accelerations, Sa_y and Sa_u. Capacity curves with three and four branches can also be found in the literature, depending on the characteristics of the building class. These curves can include a residual capacity (Sa_r) after the deformation Sd_r is observed and/or that extend the response until a final deformation Sd_f representing the full mobilization of the structural capacity, as illustrated in Fig. 2. In some cases, the initial branch can also be defined with two different slopes, where the first is proportional to the elastic period (T_1) and the second is proportional to the yielding period (T_y). In this case, the value of T_y is considered to be twice the value of T_1 (Silva et al., 2015).

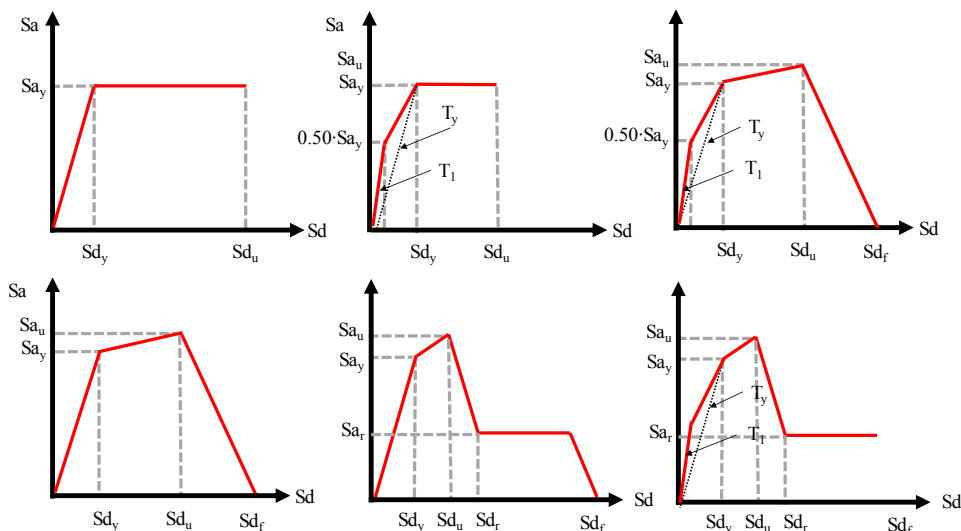Figure 2. Illustration of typical capacity curves defined in terms of spectral acceleration vs. spectral displacement (ADRS format).

3.2   Uncertainty of exposure models associated to missing attributes

The following sections discuss the uncertainty in the classification of different building classes as a result of having insufficient information about some of the attributes that are important to determine the

fragility and vulnerability of these buildings classes. These attributes are parameters or properties that can be common to several building classes, irrespective of the construction material, or that can be specific for the building classes associated to a certain construction material. The number of storeys or the type of design code that was used to design the building are examples of the former, while the type of mortar or the concrete strength are examples of the latter for masonry and reinforced concrete buildings, respectively.

Aside from the uncertainty resulting from insufficient knowledge about these attributes, building classes also include another source of uncertainty that is related to the intrinsic variability of building configurations. For example, a portfolio of RC buildings from a given class can have a multitude of in-plan configurations, which cannot be classified in terms of a meaningful set of attributes of that class. These features are an intrinsic component of the portfolio under analysis, while the previously referred attributes are related to uncertainties about the building taxonomy that can be disaggregated if additional information is available. Both sources of variability/uncertainty, however, have to be included as part of the building-to-building variability when developing or selecting consistent fragility functions or vulnerability models. In the following sections, the main attributes of each building class included in the exposure model v0.1 are listed and analysed in order to identify the sources of uncertainty about the building classification scheme adopted in the exposure model.

3.2.1 Uncertainties about the classification of Pan-European residential masonry buildings

Residential (RES) masonry buildings (M) are known for their large number of attributes that make the taxonomy matrix. This issue is a result of the larger historic period that needs to be considered for the classification of these buildings (when compared to that associated to construction technologies that are more recent such as reinforced concrete) and their larger geospatial variability due to aspects such as the availability of materials or technologies in different regions/countries over time. This latter variability may be associated to the type of LLRS, usually wall systems (LWAL) characteristics of the masonry such as the type of masonry (MTYPE), the material and the geometry of the blocks (BLOCK), the properties of the joints and mortar (MORT), the type of wall-to-wall connections (WWC), the type of wall-to-floor connections (WFC), and the type of floor/diaphragmatic effect (FLOOR). These variables not only distinguish different buildings across the pan European territory, but they also have different effects on the seismic response of buildings. By combining these attributes with the number of storeys (H) and the design code (CD, when applicable), a global taxonomy string for residential masonry buildings can be defined by as follows:

RES/M/LLRS/MTYPE/BLOCK/MORT/WWC/WFC/FLOOR/H/CD

Globally, the following five major classes of masonry construction (MURTYPE) can often be identified:
- Unreinforced masonry (MUR)
- Reinforced masonry (MR)
- Confined masonry (MCF)
- Mixed masonry-timber (MIX(M-W))
- Mixed masonry-RC (MIX(M-RC))

The MR and MCF typologies are normally associated to engineered buildings in the sense that their design relies on engineering principles rather than on empirical and vernacular concepts, such as those used in the construction of older unreinforced buildings. This vernacular character leads to a large variety of structural configurations. Furthermore, depending on the seismicity of a given region, a

seismic culture that led to the development of several damage preventing techniques is sometimes found (Ferrini, 1998), such as the adoption of metallic tie rods to connect the walls, the use of buttresses to increase the lateral strength or the use of lightweight diaphragm systems that increase the box-type behaviour. The MCF and MR building classes usually also refer to buildings whose overall design strategy accounted for seismic provisions.

MIX buildings may refer to 1) timber-laced masonry buildings (M-W), frequently found in the Balkans, in Northern Greece (Karantoni et al., 2016) and in Turkey (Gulkan and Langenbach, 2004); 2) timber framed masonry buildings (W-M/LFM), typically found in older buildings in seismic-prone areas, such as the *Pombalino* buildings in Portugal; 3) masonry buildings with top floors made of timber frames (M-W). MIX(M-RC) buildings normally refer to structural systems with masonry walls along the perimeter of the building combined with interior RC frames, or to masonry buildings with RC floors. Finally, the MUR building class refers to unreinforced masonry buildings where there is no mixture of materials in the LLRS.

Lagomarsino and Cattari (2014) summarized the main attributes of masonry building classes following the taxonomy adopted by the SYNER-G project (Pitilakis et al., 2014). These classes accounted for the possibility of having six different types of masonry units:

- Adobe (ADO)
- Fire clay solid bricks (CL)
- Stone (ST) – dressed (STDRE), uncut (STUC) or rubble (STRUB)
- Hollow clay bricks (HCL) - High percentage of voids (HCL%H), Low percentage of voids (HCL%L)
- Concrete blocks (CB)
- Autoclaved Aerated Concrete (AAC)

as well as for the possibility of having four main types of mortars:

- Lime mortar (LM);
- Cement mortar (CM);
- Mud mortar (MM);
- Hydraulic mortar (HM)

These variables are some of the main attributes of masonry buildings since they can significantly affect their response. The failure modes of these buildings are often connected to the in-plane (IP) or out-of-the-plane failure of walls (OP), depending on the existence, type and effectiveness of connections between them, on the distance between load bearing walls, and on the stiffness of horizontal diaphragms. These factors, together with the existence (and actual level of degradation) of tie rods (WT) and ring beams (WRB), are important to prevent OP failure modes. As mentioned by Lagomarsino and Cattari (2014), WT and WRB often trigger different failure modes, either by creating a strong spandrel (for WRB) or a weak spandrel (for WT) failure mode. As a result, the lateral response of these buildings (particularly MUR buildings) can be further disaggregated in cases with:

- No tie rods or ring beams (WoT and WoRB)
- Tie rods (WT)
- Ring beams (WRB)

Each one of these attributes can be further associated with a given level of quality of the detailing (high quality details, HQD; low quality details, LQD) and of maintenance (good maintenance, GM; poor maintenance, PM). Furthermore, the percentage (high, %H and low, %L) of voids in the walls due to the existence of doors and windows also influences the type of failure mechanism of the structure and,

consequently, its lateral capacity and ductility. The response of masonry buildings is seen to also vary with the number of storeys:

- Low-rise (1–2 storeys) (L)
- Mid-rise (3–5 storeys) (M)
- High-rise (6–7 storeys) (H)
- Tall (8+ storeys) (Ta)

with the type of floor system, which affects both the weight and the stiffness of the structure:

- Reinforced concrete (RC)
- Steel (S)
- Timber (T)
- Vault (V)

with the existence of irregularities in plan and in elevation, and with the design code level, in case of engineered building classes:

- No-code (NC)
- Low code (LC)
- Moderate code (MC)
- High code (HC)

Characterizing each of the referred attributes and their levels is possible when analysing a single building. However, the amount of data needed to perform this characterization for the Pan-European territory is currently unavailable. These limitations were highlighted in Deliverables D26.1 (Crowley et al. 2017) and D26.2 (Crowley et al. 2018) when defining the SERA exposure model (see Section 2). Accordingly, the collected information only allowed for a disaggregation of this type of buildings based on the number of storeys, type of masonry, type of masonry unit and expected ductility level. Table 1 summarizes the attributes considered in the building classes defined for the SERA exposure model v0.1.

Table 1. Main attributes included in the SERA exposure model v0.1 for masonry buildings.

TYPOLOGY (MTYPE)	MASONRY UNIT (BLOCK)	NUMBER OF STOREYS (H)	DUCTILITY LEVEL (DC)
Unreinforced masonry (MUR) Reinforced masonry (MR) Confined masonry (MCF)	Adobe (ADO) Fire clay unit, unknown type solid bricks (CL99) Fire clay solid bricks (CLBRS) Stone, unknown technology (S99) Regular cut stone (STDRE) Rubble stone (STRUB) Concrete blocks (CB)	H:1 to 2 (L) H:3 to 5 (M) H:6 to 7 (H) H:8+ (Ta)	Non-ductile (DNO) Low Ductility (DUCL) Medium Ductility (DUCM) High Ductility (DUCH)

By adopting the taxonomy presented in Table 1 (RES/M/LWAL/MTYPE/BLOCK/H/DC), the attributes type of mortar, percentage of voids in the masonry units, regularity in plan and in elevation, type of floor, existence of tie rods and ring beams, quality of the detailing are implicitly considered (i.e. collapsed) in the simplified building classes. Furthermore, information about several other micro-level attributes is also collapsed in the fragility functions and vulnerability models, namely the material

properties of the masonry, the thickness of the walls, the footprint of the building, the ratio between area of walls and the in-plan area of the building, etc. These characteristics are an intrinsic component of the portfolio under analysis and must therefore be included within the building-to-building variability, along with the effect of the collapsed attributes.

3.2.2 Uncertainties about the classification of Pan-European residential RC buildings

As for the masonry buildings, the taxonomy of reinforced concrete (RC) buildings is diversified and includes multiple attributes and attribute levels. Many studies have been conducted for these types of structures using empirical (e.g. Rossetto and Elnashai, 2003), analytical (Silva et al., 2015) or hybrid (e.g. Kappos et al., 2006) methodologies. The RC technology dates back to the beginning of the 20th century, with the first guidelines and RC standards for design starting to be developed across Europe between 1900 and 1920. Therefore, it is considered that RC building classes only involve engineered buildings. These buildings can be designed only to sustain gravity loads such as the self-weight, service or snow loads, or they can be designed in order to have lateral strength to cope with wind and earthquake loading. This means that a significant geographical and temporal variation of the design solutions may be expected across Europe, especially due to the non-uniform distribution of earthquake hazard.

The several types of RC building typologies that are found in Europe depend on local/national construction practices, on the level of systematization introduced by urbanization plans, on the effects and influence of man-made or natural events, and on sociological aspects related to risk awareness, namely in terms of the effectiveness of design code drafting and enforcement. The FEMA/NIBS standardized methodology (HAZUS; FEMA, 2004) subdivided the RC building stock based on the type of design into RC frame buildings (C1), RC wall buildings (C2) and RC frame buildings with unreinforced masonry infill walls (C3). In the RISK-EU project, these 3 classes were expanded, leading to the adoption of a building taxonomy matrix with moment frame RC buildings (RC1), RC wall buildings (RC2), RC frame buildings with regular or irregular distribution of infill unreinforced walls (RC3), RC frame buildings with dual structural systems (RC4), pre-cast tilt-up walls (RC5) and pre-cast concrete frames with RC shear walls (RC6). Similar classifications were used in the LessLoss (Calvi and Pinho, 2004) project, while the Syner-G project (www.vce.at/SYNER-G) established a new taxonomy in parallel (and partly in collaboration) with the development of the GEM taxonomy matrix (Brzev et al., 2013). The latter includes a larger set of attributes than the previous cases, going beyond the LLRS to classify the building and including a formal structure where other attribute levels are also considered in the classification. Among these attributes, relevance has been given to the type of floor (SLAB), type of beams (BEAM), the expected ductility level (DUC), the concrete compressive (fc), the reinforcing steel yielding strength (fsy), the type of rebar (BAR), the distribution over height (INFD) and the strength (INFTYPE) of infill walls. The resulting generic taxonomy string, which also includes the number of storeys (H) as a key attribute, can be defined as:

RES/RC/LLRS/SLAB/BEAM/DUC/fc/fsy/BAR/INFD/INFTYPE/H

With respect to the LLRS, RC buildings can be essentially disaggregated among 8 classes:
- RC frame buildings (LFM)
- RC frame buildings with infill walls (LFINF)
- RC wall buildings (LWAL)
- RC wall-frame dual buildings (LDUAL)
- RC wall-frame dual buildings with infill walls (LDUALFINF)
- RC buildings with flat/waffle/ribbed slabs (LFLS)

- RC buildings with flat/waffle/ribbed slabs with infill walls (LFLSINF)
- RC tunnel-form buildings (T)

The main difference between the LFM and LFINF classes, the LDUAL and LDUALFINF classes, and the LFLS and LFLSINF classes is the existence of infill walls, usually made of clay bricks (whose properties are often unknown). From a structural engineering point of view, the Eurocode-8/1 (CEN, 2004) approach can be used to distinguish LDUAL and LWAL buildings. According to this approach, buildings can be disaggregated based on the percentage of the total base shear (V_{total}) supported by walls (V_{wall}) using the following criteria:

- $0.35 \cdot V_{total} \leq V_{wall} \leq 0.50 \cdot V_{total}$ (LDUAL; frame-equivalent)
- $0.5 \cdot V_{total} \leq V_{wall} \leq 0.65 \cdot V_{total}$ (LDUAL; wall-equivalent)
- $V_{wall} \geq 0.65 \cdot V_{total}$ (LWAL)
- $V_{wall} \approx \cdot V_{total}$ (T)[1]

Tunnel-form buildings represent a particular case where the total base-shear is usually supported by walls. These buildings are wall-slab-wall structures made of walls and slabs cast in one stage (box-type construction technique).

Based on these classes, multiple building subsystems can be found in the Pan-European territory. These may involve different types of slabs (SLAB), namely in terms of their typology and orientation. The common types of slabs that can be found in RC buildings are:

- Solid two-way cast-in-situ slabs (SS2)
- Solid one-way cast-in-situ slabs (SS1)
- Composite slabs with pre-fabricated joists and ceramic blocks (HS)
- Waffle (two-way) or ribbed (one-way) slabs (WS)
- Flat slabs (FS)

The main difference between these types of slabs lies in the load-bearing system that is involved, which implies that different permanent load values and structural systems may be triggered depending on the orientation of the ground motions. The type of beams (BEAM) supporting each type of slab system can also vary and depends on the geometry and slab typology. Typically, the type of beams that make the floor system can be:

- Emergent beams (EB)
- Wide embedded beams (WB)
- No beams, with embedded rigid bands only (NB)

Based on common structural engineering principles, some beam types and slab typologies are seen to be incompatible. Floor systems with SS2 slabs usually have EB beams supporting the slab, while floors with HS slabs can have either EBs or WBs supporting beams. Floor systems with WS or FS slabs are directly supported by columns and/or walls.

The geometry of beams, columns and walls depends not only on the properties of the slab system but also on the seismic design level that is adopted. As shown in Crowley et al. (2017; 2018), the exposure model includes these features by considering a design ductility level (DUC) which has three main classes, and by combining the type of design code that is involved with the design peak ground acceleration for an average return period (TR) of 500 years (PGA_{500}):

---

[1] The classification of cast-in-place tunnel-form buildings (T) was introduced herein for completeness since this building class is not included in the Eurocode 8/1 classification.

- Pre/low code or moderate/high code with $PGA_{500} < 0.1g$ (DUCL)
- Moderate code with $PGA_{500} > 0.1g$ or high code with $0.1 < PGA_{500} < 0.3$ (DUCM)
- High code with $PGA_{500} > 0.3g$ (DUCH)

The pre/low code (NC/LC) class accounts for design approaches that do not include seismic provisions, while the moderate code class (MC) refers to design scenarios that are based on the first design code (implemented in a given country) that includes seismic provisions. High code (HC) refers to design approaches that are based on the first modern design code (implemented in a given country) that includes principles similar to those defined by Eurocode-8/1 (CEN, 2004), namely by enforcing capacity design. These rules and the corresponding PGA_{500} influence several features of the buildings, namely the amount of longitudinal reinforcement that is adopted in members ($\rho_{l,tot}=A_{sl}/A_c$, where A_{sl} is the area of the reinforcing steel in the section and A_c is the corresponding cross section area of the member) and the transversal reinforcement ratio of the members ($\rho_w=A_{sw}/s_w \cdot B$, where A_{sw} is the total area of stirrup/hoop bars, s_w is the stirrup spacing and B is proportional to the leg-length of the stirrup).

The taxonomy followed by the Syner-G project (Crowley et al. 2014) also mentions the relevance of the concrete compressive strength, the reinforcing steel yield strength and the type of rebar that characterizes each building class. According to that taxonomy, the concrete strength (fc) was divided into 3 levels:

- Low concrete strength, $f_{cm} < 20MPa$ (LSC)
- Average concrete strength, $f_{cm} = 20-50MPa$ (ASC)
- High concrete strength, $f_{cm} > 50MPa$ (HSC)

Similarly, the reinforcing steel yield strength (fsy) was divided into 2 classes:

- Low reinforcing steel yield strength, $f_{sym} < 300MPa$ (LY)
- Average steel yield strength, $f_{sym} \geq 300MPa$ (HY)
-

and the type of rebars (BAR) was divided into:

- Smooth rebars (SB)
- Ribbed rebars (RB)

Although the effect of infill walls and claddings is usually not accounted for in the seismic design, the presence and distribution of these elements along the height and within the footprint of a building can have a significant impact on its seismic fragility and vulnerability. The importance of these elements was recognized in the RISK-EU building taxonomy matrix by disaggregating the building class RC3 (infilled frames) according to the distribution of infill walls (INFD) as:

- Partially (continuous over the height) infilled frames (PI)
- Partially (discontinuous over the height) infilled frames, e.g. pilotis frames (PIL)
- Fully infilled frames (FI)

More recently, Hak et al (2012) proposed a disaggregation of infill walls made of clay bricks that are widely used in European building practice according to their properties (INFTYPE) into weak (T1), medium (T2) and strong (T3) walls, presenting the typical configuration of these walls and proposing different average stiffness and strength properties that can be used for these classes.

As mentioned before, despite the importance of each of these attributes and their levels, a very large amount of data is required to be able to perform a full characterisation of the building stock at a

continental scale. Due to the fact that only a limited number of attributes can be mapped at the level of the Pan-European region, as highlighted in Deliverables 26.1 (Crowley et al. 2017) and 26.2 (Crowley et al. 2018), a collapsed taxonomy is usually adopted. Consequently, the taxonomy adopted in the exposure model v0.1 included only 3 attributes: the lateral load-resisting system, the design ductility level and the number of storeys. By adopting the taxonomy presented in Table 2, the attributes SLAB, BEAM (when a direct association cannot be made with the type of slab), fc, fsy, BAR, INFD and INFTYPE are all collapsed in the simplified building classes, that have a taxonomy defined by the string RES/RC/LLRS/DUC/H. In addition, due to the characteristics of RC construction, multiple building in-plan configurations can be found in the building stock, that then lead to different column and wall densities, beam spans and slab typologies. These characteristics are an intrinsic component of the portfolio under analysis, and also have to be included as part of the building-to-building variability.

Table 2. Main attributes included in the SERA exposure model v0.1 for RC buildings

LATERAL LOAD RESISTING SYSTEM (LLRS)	NUMBER OF STOREYS (H)	DUCTILITY LEVEL (DUC)
RC frame buildings (LFM)	H:1	Low Ductility (DUCL)
RC frame buildings with infill walls (LFINF)	H:2	Medium Ductility (DUCM)
RC wall buildings (LWAL)	H:3-5	
RC wall-frame dual buildings (LDUAL)	H:6+	High Ductility (DUCH)
RC buildings with flat/waffle/ribbed slabs (LFLS)		
RC buildings with flat/waffle/ribbed slabs with infill walls (LFLSINF)		

3.2.3 Uncertainties about the classification of Pan-European industrial facilities

An industrial plant or facility can be defined as set of integrated components and processes that have interdependences (Erdik and Uckan, 2014). Industrial plants are made of building-like and non-building-like structures. Building-like structures include manufacturing units, offices or storage facilities, while non-building-like structures can be represented by electric power systems (namely distribution and transmission substations), tanks, silos, cooling towers and stacks, pipelines and piping systems. As mentioned in SERA Deliverable 26.1 (Crowley et al., 2017), it is not an objective of the project to develop an exposure model (or risk assessment) for industrial plant components. Therefore, only the taxonomy of two particular components was detailed in that report: gas, water and oil pipelines and storage tanks. Pipelines were defined based on the attributes content (PICT), location (PILOC), pipe barrel material (PIMAT), type of pipeline joints (PIJ), soil type (SOIL) and pipe diameter (PIFI). The generic taxonomy can therefore be defined as:

IND/PIPE/PICT/PILOC/PIMAT/PIJ/SOIL/PIFI

The taxonomy of storage tanks was defined in Crowley et al. (2017) based on the attributes content (TKCT), material (TKMAT), anchorage type (TKANC), shape of the tank, namely the height-to-diameter ratio (TKSH) and the elevation of the tank (TKLOC). The generic taxonomy can therefore be defined as:

IND/TANK/TKCT/TKMAT/TKANC/TKSH/TKLOC

Building-like industrial (IND) structures (hereafter termed industrial buildings) can be disaggregated based on the material/construction technique that is used (MAT), the type of vertical structural system in each direction (LLRS), the number of storeys (H:), the column height (CH), the roof cladding (RCLAD), the type of girder (GRD), type of beam-column connection (BCC), the type of side cladding (SCLAD), the type of base connection (BPC), the crane capacity (CRA), the design code (CD), the concrete class (fc), the steel class (ST), the type of steel rebar (BAR), the seismic design level (PGA), the wind design level (WSPEED), and the snow load (SNOW). Furthermore, contrary to the case of residential buildings, non-structural components and contents play a key role in the seismic vulnerability of industrial buildings. Hence, the damage states and the vulnerability models must be associated to the industrial activity (INDACTI), using a content-to-structure-value ratio (CSVR) to estimate the impact of the loss of contents. The global taxonomy string of an industrial building considering that all these attributes are known can therefore be defined by:

IND/MAT/LLRS/H/CH/GRD/BCC/BPC/fc/ST/BAR/RCLAD/SCLAD/CRA/CD/PGA/WSPEED/SNOW/INDACTI

The industrial activities (INDACTI) can be disaggregated according to:

- Extractive Industries
- Food Industry
- Beverages Industry
- Tabaco Industry
- Textiles Manufacturing
- Clothing Industry
- Leather Industry
- Wood and Cork Products
- Pulp, Paper and Paper Products
- Publishing, Printing and Reproduction of Recorded Media
- Coke and Refined Petroleum Products
- Chemical Products and Fibres
- Pharmaceutical Products
- Rubber and Plastic Products
- Non-Metallic Mineral Products
- Base Metallurgical Industry
- Metal Products (Except Machinery and Equipment)
- Communication, Electronic and Optical Equipment
- Electric Equipment
- Machinery and Equipment Manufacturing
- Motor Vehicles Manufacturing
- Other Transportation Equipment Manufacturing
- Furniture and Mattresses Products
- Other Manufacturing Industries
- Repair, Maintenance and Installation of Machinery and Equipment
- Retail
- Transportation and Warehousing

A CSVR and specific downtimes depending on the structural and non-structural damage states can be associated to each INDACTI. From the structural point of view, MAT is one of the key attributes of the taxonomy of industrial buildings. Therefore, the generic taxonomy string previously defined can be

adapted based on the MAT classes. The SERA exposure model for industrial buildings considers the following three main types of materials:

- Cast-in-place RC buildings (CR+CIP)
- Precast concrete buildings (CR+PC)
- Steel buildings (ST)

Based on the type of material, the generic taxonomy string previously defined can be simplified given that some of the attributes are only relevant for specific MAT classes. Since an exposure model for industrial building-like structures is being developed (v0.1 available in Crowley et al., 2019b), building classes were defined for these elements, using a limited number of attributes (due to the fact that these were defined for a continental scale) and collapsing the remaining attributes, as performed for residential buildings. A list of the more important attributes is shown in the following sections, separating the cases of RC/PC and ST buildings.

3.2.3.1 Industrial Steel Buildings

When considering the buildings classes including only ST industrial buildings, the previously defined generic taxonomy string simplifies to:

IND/ST/LLRS/H/CH/GRD/BPC/ST/RCLAD/SCLAD/CRA/CD/PGA/WSPEED/SNOW/INDACTI

For the case of ST building classes, the LLRS is usually made of two different systems (the in plane, LLRS-IP and out of plane and LLRS-OOP systems) (Fig. 3). These systems are usually one of the following categories:

- Portal frames (PF)
- Lattice trusses (LTS)
- V-Concentric Braced Frames (CBF-V)
- IV-Concentric Braced Frames (CBF-IV)
- SD-Concentric Braced Frames (CBF-SD)
- X-Concentric Braced Frames (CBF-E)
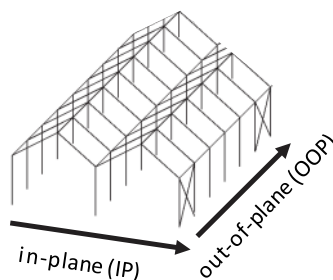- Eccentric Braced Frames (EBF)

Figure 3. Illustration of the in-plane (IP) and out-of-plane (OOP) directions in industrial buildings, adapted from (Alderighi et al. 2010).

The main difference between the VBF, IVBF, NBF and XBF systems lies in the type of bracing system that is adopted, i.e. with V, Inverted-V, N or X shaped systems, respectively. Typically, existing ST industrial buildings in Europe belong to classes IND/PF+CBF99 (as previously mentioned, 99 represents the case where an attribute is of any kind, in this case representing the type of concentric bracing

system). Hence, ST buildings have PF systems as LLRS-IPs and concentric V, IV, N or E braced systems as LLRS-OOPs. Typically, ST industrial buildings have only one storey (H:1). The column height can have a significantly impact in the properties of ST/PF-CBF99 buildings. Araújo et al. (2016) identified statistically significant differences for the in-plane stiffness between ST/PF-CBF99 buildings with CH higher or lower than 5m. Regarding the type of girder, two solutions are often adopted: lattice truss (GLT) or steel beam (GSP). The class of steel strength that is used depends on the year of construction. Normally, steel elements are made of steel with a yield strength lower than 300MPa (STL, usually 235MPA) or higher than 300MPA (STH, typically 355MPA). With respect to the base-plate connections (BPC), three options can be found in industrial ST buildings, based on the corresponding rotation stiffness:

- Fixed (BPC-H)
- Flexible (BPC-M)
- Pinned (BPC-L)

The roof cladding in these buildings can have multiple configurations, which implies that different weights are added to the vertical elements and different types of damage models may be triggered in these elements. According to the PRECASTEEL report (Alderighi et al. 2010), typical roof systems in European buildings include:

- Sandwich panels (RCLAD: SAP)
- Corrugated Metal Sheets (RCLAD: CMSH)
- Precast Concrete Panels (RCLAD: COPA)
- Others (Fibre-cement, aluminium, asphalt) (RCLAD: OT)

Similar classes can be considered for the side cladding (SCLAD) that is attached to side rails, but some buildings also have masonry infilled walls. Hence, the SCLAD is considered to be one of the following types:

- Horizontal cladding panels (SCLAD-H)
- Vertical cladding panels (SCLAD-V)
- Masonry infills (SCLAD-INF)

where the behaviour of SCLAD-H and SCLAD-V is seen to depend on the subtype of SCLAD (SAP, CMSH, COPA or OT, as for the roof systems) combined with the type of fastening used to connect these elements to rail beams.

As seen before for the case of engineered RC residential buildings, the selected design code introduces differences in the building typologies and classes CDN, CDL. CDM and CDH were considered in the taxonomy. Furthermore, the seismicity of the site was also added as an attribute by adopting PGA_{500} as an attribute. For the case of ST industrial buildings, the effect of additional hazards needs to be added to the taxonomy, namely the wind design load and the snow load, given the characteristics of these buildings. Based on the analysis made in the PRECASTEEL project, the following three main classes of WSPEED are considered,

- Vb0<25m/s (WSPEED-L)
- Vb0 between 25m/s and 29m/s (WSPEED-M)
- Vb0>25m/s (WSPEED-H)

while for the case of SNOW, the following three classes can be established based on the characteristic load s_k considered for the roof in design (in kN/m^2):

- $S_k < 0.75$ kN/m^2 (SNOW-L)
- S_k between 0.75 and 1.5 kN/m^2 (SNOW-M)
- $S_k > 1.5$ kN/m^2 (SNOW-H)

For the case of crane loads (CRA), the PRECASTEEL projected distinguished 4 different levels for this attribute based on the maximum crane lifting capacity:

- $F_{crane} = 0$ kN (CRA-N)
- $F_{crane} = 50$ kN (CRA-L)
- $F_{crane} = 100$ kN (CRA-M)
- $F_{crane} = 250$ kN (CRA-H)

The SERA exposure model v0.1 for industrial steel buildings only considers the information that is currently available for the entire Pan-European continent, which limits significantly the number of attributes to be used in the risk analyses. Therefore, the exposure model was defined according to the attributes shown in Table 3, which means that the attributes LLRS, GRD, BPC, ST, RCLAD, SCLAD, CRA, DC, PGA, WSPEED and SNOW representing the uncertainty about the taxonomy and need to be included as part of the building-to-building variability. Other geometrical variables such as the type of steel profiles, the truss configuration, the number of in-plane spans, number of frames in the OOP direction, the spacing between frames, etc., are also parameters that must also be included in the building-to-building variability.

Table 3. Main attributes included in the SERA exposure model v0.1 for IND/ST buildings

TYPOLOGY	NUMBER OF STOREYS, H	DUCTILITY LEVEL
STEEL MOMENT FRAME (S/LFM)	H:1	Low Ductility (DUL)
STEEL FRAME WITH UNREINFORCED MASONRY INFILL WALLS (S/LFINF)	H:2	Medium Ductility (DUM)
STEEL BRACED FRAME (S/LFBR)	H:3	High Ductility (DUH)

3.2.3.2 Industrial RC and PC Buildings

In the case of RC and PC buildings, the taxonomy string is very similar to that defined for the ST buildings (although ST is now replaced by the steel yield strength fsy), and can be generically defined as:

IND/MAT/LLRS/H/CH/GRD/BCC/fc/fsy/BAR/RCLAD/SCLAD/DC/PGA/WSPEED/SNOW/INDACTI

Part of the attributes identified in the taxonomy string are common to those that characterize RC residential buildings, namely fc, fsy, BAR, DC and PGA. Nevertheless, the concrete strength classes have typically larger values than those of (especially older) RC residential buildings due to the precast process which improves the quality of the material. Other attributes and attribute levels are common to the taxonomy of ST buildings, namely the geometrical properties H and CH, and the non-structural properties RCLAD and SCLAD. Hence, the main differences between ST and RC/PC industrial buildings are the properties of the structural system.

In RC and PC buildings, the LLRS can be defined by systems ranging isolated columns (COL), to columns with concrete beams (LPB) and moment resisting frames (LFM), depending on the effectiveness of the beam-column connection (BCC). The LLRS of RC and PC industrial buildings can be disaggregated among the following three classes:

- Partial frame systems made of isolated columns (COL)
- Partial frame systems made of columns and concrete beams (LPB)
- Partial frame systems made of columns and lattice steel girders (COL-LAT)

The difference between LFM and the LLRS reported above is the effectiveness of the beam-column connection (BCC). Beam-column connections can have multiple configurations depending on the existing connection between the girders and the corbels/heads of the precast columns. Typologies such as girders seated on columns with dowels, girders seated on columns without dowels, centering pins, girders seated on fork-shaped columns, Π-shaped girders seated of Π-shaped column-heads with dowels, Π-shaped girders seated of U-shaped column-heads with anchors, among others, have been observed in Europe and their behaviour has been studied within the context of seismic fragility studies (e.g. Deyanova et al 2014). These classes can be disaggregated based on the structural behaviour of the BCC according to:

- Pined connections without friction (BCC-P)
- Pined connections with friction (BCC-PF)
- Pined connections with dowels (BCC-PD)
- Monolithic connection (BCC-MO)
- Fork connections (BCC-FO)

Girders (GRD) can also have multiple configurations, although the importance of this attribute can be limited in comparison with that of BCC. Girders can be disaggregated in precast concrete beams (with various geometries and typologies) or trusses. The latter are associated with COL-LAT LLRSs, while the former are associated to LPB systems.

The SERA exposure model v0.1 for industrial buildings (Crowley et al 2019b) considered the information available for the entire Pan-European region to define a set of building classes as indicated in Table 4. Consequently, the attributes GRD, BPL, fsy, RCLAD, SCLAD, CRA, WSPEED, SNOW and INDACTI must be added to the uncertainty about the vulnerability models for RC and PC industrial buildings since they represent collapsed parameters of the taxonomy.

Table 4. Main attributes included in the SERA exposure model v0.1 for IND/PC buildings

TYPOLOGY	NUMBER OF STOREYS, H	DUCTILITY LEVEL
RC MOMENT FRAMES (CR+CIP/LFM)	H:1	Low Ductility (DUL)
RC MOMENT FRAMES WITH MASONRY INFILLS (CR+CIP/LFINF)	H:2	Medium Ductility (DUM)
RC PRECAST FRAMES (CR+PC/LPB)	H:3	High Ductility (DUH)

3.3 Development of the SERA.REVIEW database

Existing information about the seismic vulnerability of buildings can be seen as a reliable way to infer the impact associated to the collapsed attributes in the exposure model and to perform internal validations of new vulnerability models that are being developed. In light of the importance of this information, the GEM foundation recently promoted an initiative to create a platform that can be used to store, select and analyse fragility functions, vulnerability models, damage limit state and damage-to-loss models, and pushover/capacity curves (Yepes-Estrada *et al.*, 2016).

Within SERA, a literature review was performed to develop the SERA.REVIEW database, a database of existing/literature information which follows the data-structure defined by the GEM platform. This data-structure includes three sets of information: Data, Metadata and Model Information. The *Data* container stores the collected existing fragility functions, damage-to-loss models and capacity curves developed for the Pan-European building stock. The container *Metadata* defines the building class according to the taxonomy of the SERA exposure models v0.1 and the collapsed attributes) for each model of the Data class. Finally, the container *Model Information* stores the main characteristics of each study that could be used to weight their contributions when using logic trees for vulnerability or risk analyses based on the information of the database. The data collected within SERA for this database is presented in the following in terms of capacity curves, fragility functions and vulnerability models for the residential masonry and RC buildings, and in terms of fragility functions and vulnerability models for the industrial building-like structures.

3.3.1 Capacity curves

3.3.1.1 Residential Buildings

A set of 569 capacity curves was collected from the literature for masonry and RC residential buildings. From those, a set (C-MUR) of 189 bilinear capacity curves were collected for masonry residential building classes, including average curves representative of a portfolio of structures and curves for individual buildings. For RC residential buildings, a set (C-RC) of 380 capacity curves were obtained for the database that also includes average curves representative of a portfolio of structures and curves for individual buildings. As opposed to the case of unreinforced masonry buildings, where the use of bilinear capacity curves is normally observed, it is well known (Bal et al., 2010; Silva et al., 2015) that the shape of the pushover and of the capacity curves of RC buildings varies depending on the properties of the building class. In particular, when the building class includes infill walls (LFINF, LDUALFINF, LFLSINF) with a significant strength and stiffness when compared to that of the other vertical elements of the LLRS, a quadrilinear curve is usually observed. Conversely, if the strength/stiffness of infills is not relevant, either a bilinear curve (without strength degradation) or a trilinear curve (e.g. see Kosic et al., 2014) are usually adopted. Given these particularities of RC building classes, 324 bilinear curves, 21 trilinear curves and 35 quadrilinear curves were collected. Figure 4 shows the geographical applicability of these curves. Within the curves that were collected, a subset of 69 capacity curves was found to have been developed in order to include generic characteristics, i.e. not associated to any specific country, and are, therefore, expected to be able to cover the entire continental region.
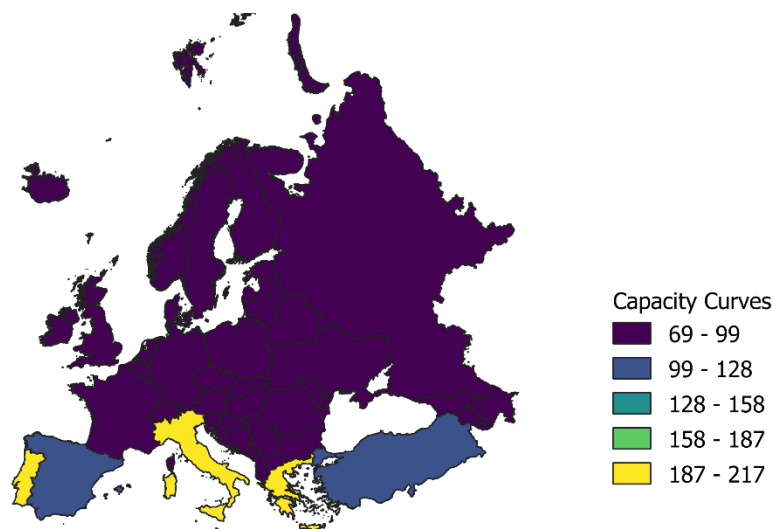

Figure 4. Disaggregation of the capacity curves collected for residential buildings by geo-applicability.

The disaggregation of the capacity curves by region of applicability is presented in Fig. 5. The large majority of the curves found for masonry buildings are seen to be particularly applicable to the Euro-Mediterranean region.
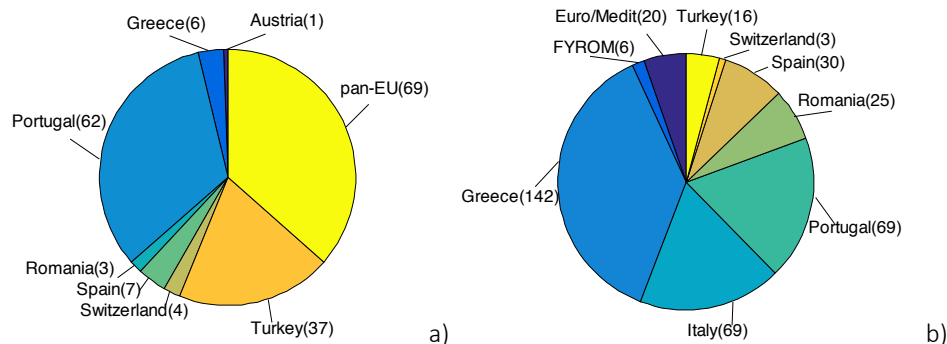

Figure 5. Disaggregation of the capacity curves collected for masonry (C-MUR) (a) and RC (C-RC) (b) residential buildings.

3.3.2 Fragility functions

3.3.2.1 Residential Buildings

Following a strategy similar to that used to identify the capacity curves, a set of 441 fragility functions were collected from the literature for residential building classes. The global vulnerability database (Yepes-Estrada et al. 2016) was used as a reference since it incorporates data from the Global Vulnerability Consortium project (2010-2013) (Porter et al. 2012) launched by GEM, as well as the fragility functions (Crowley et al. 2014) and the methodologies (Silva et al., 2014) analysed within the European project Syner-G. The data collection focussed regions where the seismic hazard level is higher, since these are also the regions that concentrate a larger number of available studies. These regions are mostly those involving Mediterranean countries, as shown in Fig. 6. Within the functions that were collected, a subset of 33 fragility functions was found to have been developed in order to include generic characteristics, i.e. not associated to any specific country, and are, therefore, expected to be able to cover the entire continental region.

In total, 137 fragility functions (set F-MUR) were analysed for masonry buildings, and were disaggregated among six different types of unreinforced masonry (adobe (ADO), rubble stone (STRUB), regular cut stone (STDRE), clay blocks of any type (CL99), concrete blocks of any type (CB99), and unknown type of masonry unit (UKN)) and one type of reinforced/confined masonry (CRM).

For the RC residential building classes, 304 fragility functions (set F-RC) were collected from the literature and analysed based on the classes defined in Table 2. Some of these fragility functions come from the harmonized database developed for the SYNER-G project (Crowley et al. 2014), and are also available in the GEM vulnerability database (Yepes-Estrada et al., 2016). A disaggregation of the fragility functions collected for the masonry (Fig. 7a) and RC (Fig. 7b) buildings classes is shown in Fig. 7. As seen in Fig. 7b, a large percentage of the collected fragility functions apply to buildings constructed according to the design code and the construction practices of different periods in Portugal, Italy and Greece. Furthermore, a large number of fragility curves are also seen to be associated to countries located in the Euro-Mediterranean region (Euro/Medit curves reflect construction practices in Italy and Slovenia).
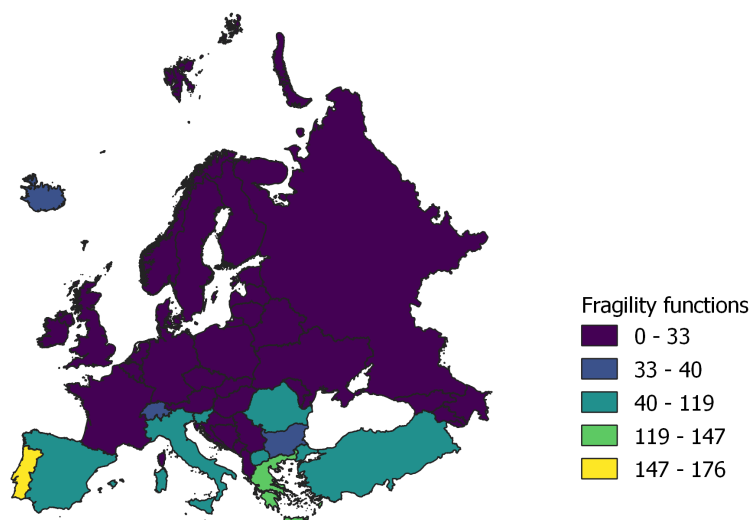
Figure 6. Disaggregation of the fragility functions collected for residential buildings by geo-applicability
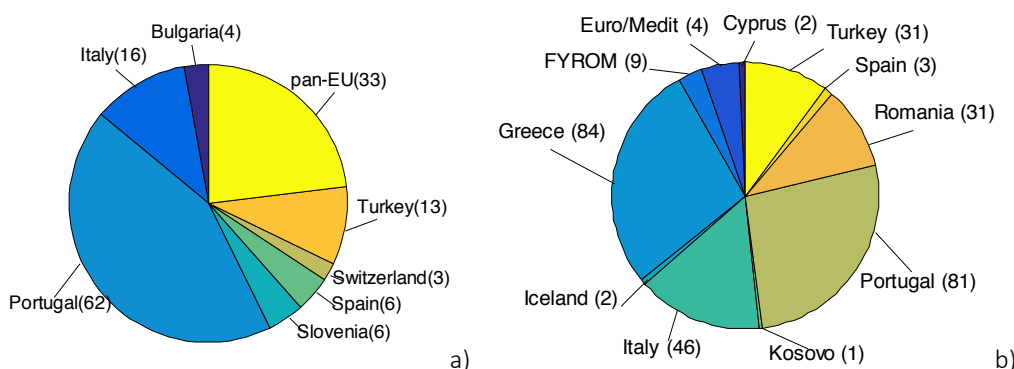

Figure 7. Disaggregation of the fragility functions collected for masonry (a) and RC (b) residential building

3.3.2.2 Industrial Buildings

Currently, the database of industrial building fragility functions includes 55 functions covering IND/PC/LLRS99/H:1/DC buildings and that were obtained based on analytical approaches. Forty of these models represent buildings from Italy, while the remaining 15 models represent Turkish industrial buildings. An additional set of non-structural fragility functions collected from Babič and Dolšek (2016) were also stored. Buratti et al (2017) developed empirical fragility functions based on the aftermath of the Emilia earthquake and concluded that these buildings are more vulnerable than residential ones. A limited number of studies was stored so far for IND/ST/LLRS99/H:1/DC buildings.

3.3.3 Vulnerability models

3.3.1.1 Residential building classes

The repository (V-GEM) of 260 vulnerability models available for the most common building classes in the Global Exposure Map was added to the SERA.REVIEW database. These models were developed based on a uniform approach (Martins and Silva, 2018) accounting for the record-to-record variability, the uncertainty about the damage states and the building-to-building variability. The procedure generally followed for deriving these models is described below:

A repository of over 500 vulnerability functions for the most common building classes in the Global Exposure Map (and thus in the v0.1 European Exposure Model, as described in Section 2) has been developed using a uniform approach (Martins and Silva, 2018; Martins and Silva, 2019). In general, the derivation procedure followed the steps described below:

1. Definition of the structural and dynamic properties of each building class (e.g. yield and ultimate drifts, elastic and yield period of the first mode of vibration, participation factor of the first mode of vibration, common failure mechanisms). These attributes were collected from the literature (e.g. numerical studies, experimental tests, expert judgment, damage observations).
2. Development of representative single-degree-of-freedom (SDOF) oscillator for each building class (using the parameters identified in Step 1).
3. Selection of ground motion records using strong motion databases from the United States, Japan, Chile, Mexico and Europe. The use of a large set of time histories aimed at propagating the record-to-record variability to the vulnerability assessment.
4. Nonlinear time history analysis to evaluate the structural response (i.e. engineering demand parameter (EDP) – maximum displacement and acceleration) of the SDOF oscillators against the selected ground motion records. This step uses the open-source package for structural analysis OpenSees (McKenna et al., 2000), and the Risk Modeller's Toolkit supported by GEM.
5. Estimation of the probability of exceeding a set of damage states (slight, moderate, extensive and complete damage) using cloud analysis (Jalayer and Cornell, 2002), and a damage criterion based on the yielding and ultimate displacement points (e.g. Villar-Vega et al., 2016).
6. The fragility functions were converted into vulnerability functions (i.e. distribution of loss ratio conditional on ground shaking) using a damage-to-loss model (e.g. Yepes-Estrada et al., 2016) for economic losses due to direct damage (structural and non-structural). To produce probability of loss of life conditional on ground shaking, the probability of collapse given complete damage was first estimated (from evidence from past earthquakes as well as recommendations from HAZUS, FEMA 2004) and then the fatality ratios given collapse were taken from the literature (e.g. FEMA 2004; So and Pomonis, 2012).

Figures 8 and 9 illustrate the vulnerability models for common masonry and reinforced concrete building classes in the European exposure model. All of the vulnerability models developed for the Global Seismic Risk Model v2018.1 (GEM, 2018) have been stored using the OpenQuake NRML format, and are being made publicly available through the OpenQuake-platform (https://platform.openquake.org/vulnerability).
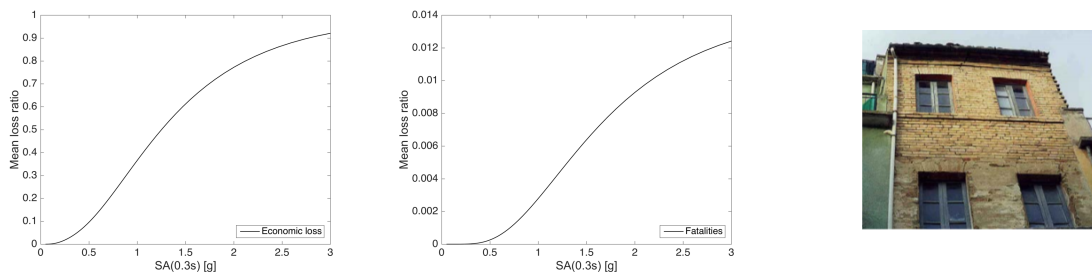

Figure 8. Example of European clay brick masonry building class (MUR+CL99/LWAL-DNO/H2) vulnerability functions
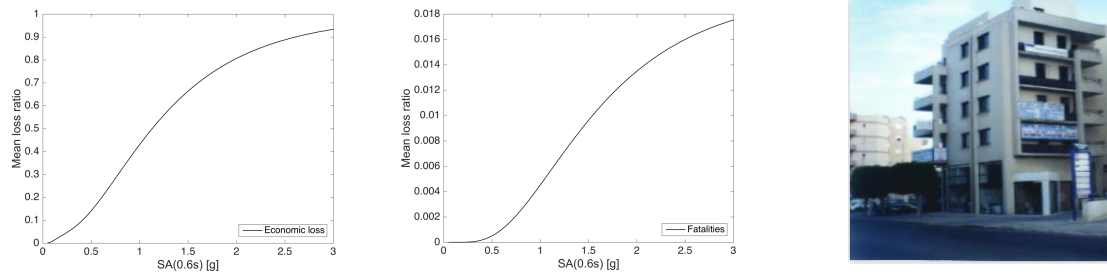
Figure 9. Example of European reinforced concrete infilled frame building class (CR/LFINF-DUL/H4) vulnerability functions

3.3.1.2 Industrial building classes

A repository of vulnerability models for precast industrial buildings was recently developed by Rodrigues et al (2017). These models were developed based on the damage-to-loss models proposed in the STREST project (STREST, 2015) both for structural and non-structural components. The cost of the contents was estimated according to FEMA (2012) while business interruption costs were estimated using the HAZUS methodology (FEMA, 2003). Figure 9 illustrates the vulnerability models proposed by Rodrigues et al (2017).

For the case of ST industrial buildings, a repository of vulnerability models was also recently developed by Araujo (2018), disaggregated according to the type of industry. The structural damage was assessed based on the probability of demolition and on specific limit states defined for steel members, bracings, gusset plates and column base connections. The non-structural damage was estimated according to the HAZUS methodology (FEMA, 2003). The HAZUS model was also used to define the content damage limit states. Content loss was defined based on the content-to-structure value ratio (CSVR) defined for each industrial activity (INDACTI). Araújo (2018) considered downtime and lost production time as measurements of business interruption.
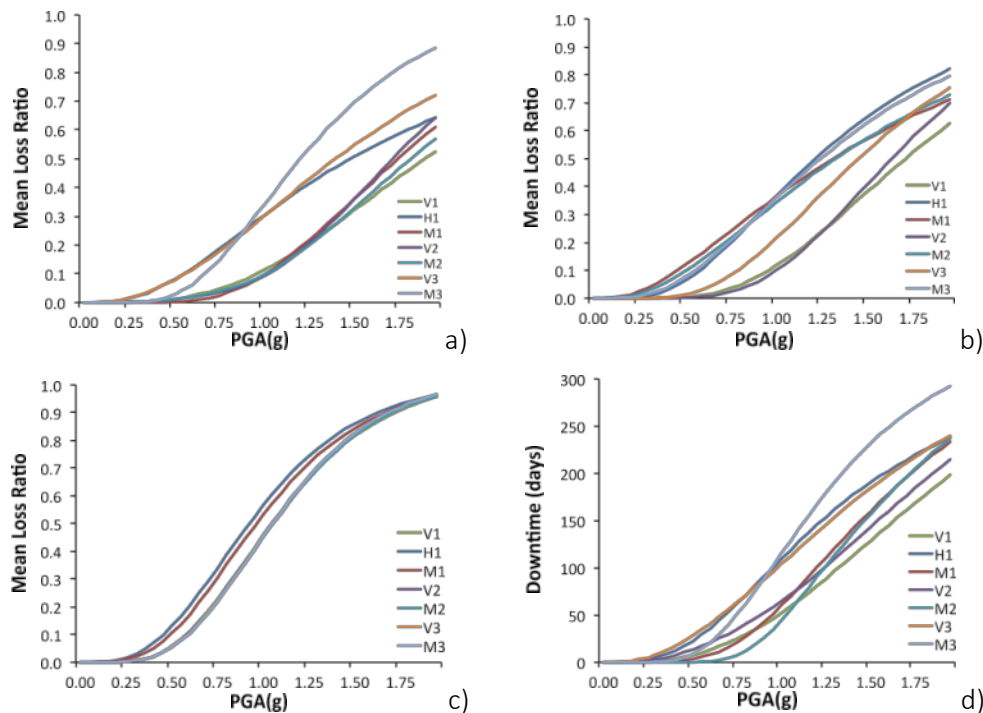

Figure 10. Vulnerability models for PC industrial building classes (adapted from Rodrigues et al., 2018).
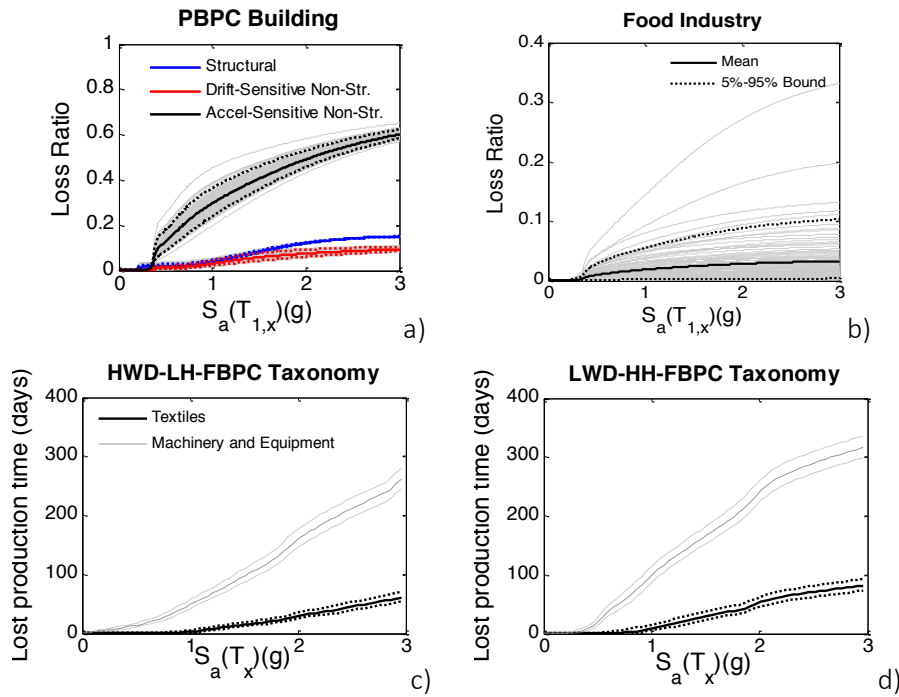
Figure 11. Vulnerability models for ST industrial building classes considering property damage (a), content loss (b), downtime (c) and lost production time (d) (adapted from Araújo, 2018).

3.4   Analysis of the elements stored in the SERA.REVIEW database

The elements stored so far in the SERA.REVIEW database comprise a significant number of fragility functions and capacity curves for residential masonry and RC buildings, reflecting the large amount of studies that can be found in the literature for these type of buildings. On the other hand, only a limited number of fragility functions and capacity curves is available for industrial facilities. Hence, only the database content associated to residential buildings was processed and analysed in the following in order to extract trends and statistical elements that that could be used in the development of the SERA vulnerability models. The following sections present the main results obtained from the analysis of the datasets F-MUR (fragility functions for residential masonry buildings), F-RC (fragility functions for residential RC buildings, C-MUR (capacity curves for residential masonry buildings) and C-RC (capacity curves for residential RC buildings).

3.4.1   Fragility functions

3.4.1.1 Residential masonry buildings (F-MUR)

Figure 12 shows the disaggregation of the F-MUR dataset according to the type of masonry (Fig. 12a) and according to the number of storeys (Fig. 12b). As shown in Fig. 12, no fragility functions were included for confined masonry (CRM) and for the unreinforced masonry ADO referring to European buildings. This trend is consistent with the observations made by Lagomarsino and Cattari (2014) regarding the lower prevalence of confined masonry in Europe (when compared to South America). With respect to the ADO buildings, the lack of fragility functions is, in part, because some of the past research aggregated the data for STRUB and ADO masonry into a mixed STRUB/ADO class. This data was assigned solely to the masonry class STRUB herein. A small number of functions was also found for STDRE masonry buildings, especially when considering the disaggregation among different number of storeys. The larger number of fragility functions found for CL99 buildings is consistent with the exposure

model (see Section 2) and with the multiple variants of this type of masonry building found in the Pan-European territory.
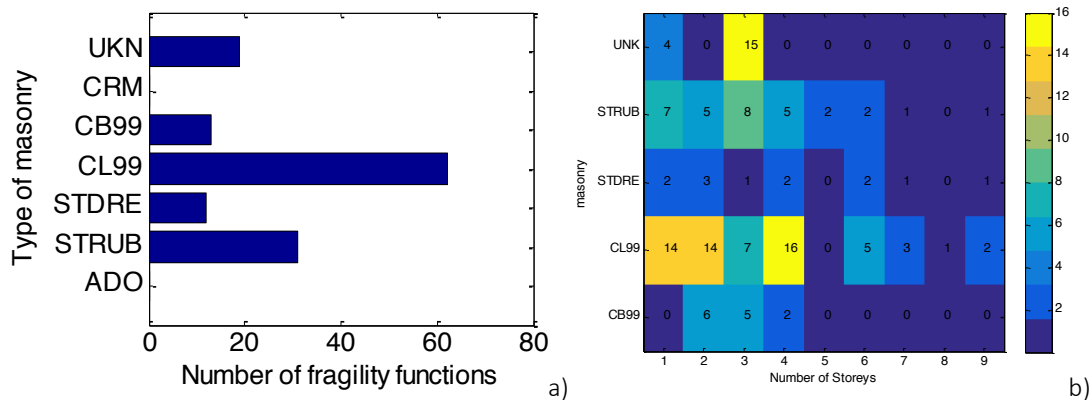

a)

b)

Figure 12. Disaggregation of the 137 fragility functions according to the type of masonry (a) and the number of storeys (b).

Figure 13 shows the disaggregation of the fragility function database in terms of the type of ground motion intensity measure (IM) that is used (Fig. 13a) and in terms of the damage scale that is adopted (Fig. 13b). The three IMs that were found to be used in the studies that are catalogued herein are the peak ground acceleration (PGA) and the spectral displacements at periods T_y and T_{LS}. As can be seen in Fig. 13b, most of the studies adopted a damage scale similar to the one presented in Lagomarsino and Giovinazzi (LG; 2006). Other studies considered the EMS98 scale (Grünthal, 1998), while Borzi et al. (2008a) used an alternative scale.

Figure 14 shows the statistical analyses performed for the central value and the logarithmic standard deviation of the collected fragility functions that use PGA as the IM. The presented values refer to a damage state compatible with an ultimate limit state, which varies depending on the type of damage scale that is adopted. Similar plots are shown in Figs. 15 and 16 for the fragility functions that are based on $Sd(T_y)$ and $Sd(T_{LS})$, respectively. The method of analysis adopted in the assessment presented in Figs. 14-16 is the first approach described by Silva et al. (2015). The main objective of these analyses is to observe the existing dispersion between fragility functions available in the literature and to identify the main research gaps for developing a vulnerability study at a continental scale.
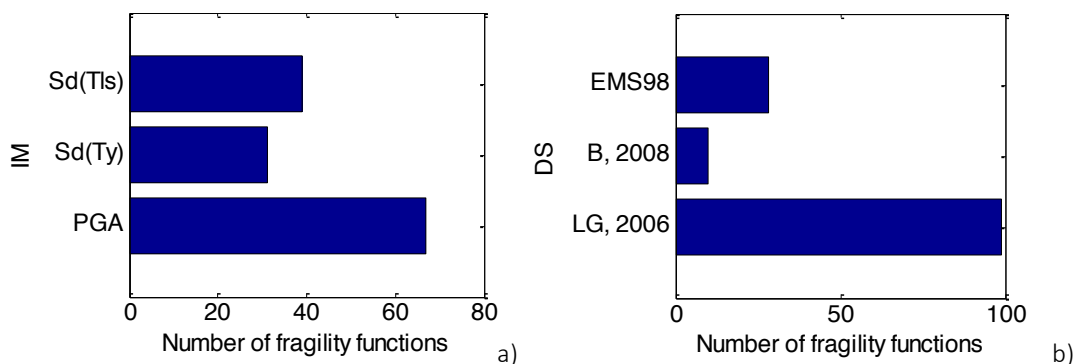

a)

b)

Figure 13. Disaggregation of the 137 fragility functions according to the type of ground motion intensity measure (a) and the damage scale (b).

By analysing the results obtained for the Pan-European database, it can be seen that none of the IMs is able to fully characterize the entire set of building classes that needs to be analysed. Furthermore, the results obtained with $Sd(T_{LS})$ are difficult to harmonize, and highlight the existing dependence between the fragility function and the selected ground motion records and/or the response spectra. The absence of a single damage scale also does not facilitate the use of a consistent definition of damage, which then leads to larger uncertainties in the representation of consequences and risk.
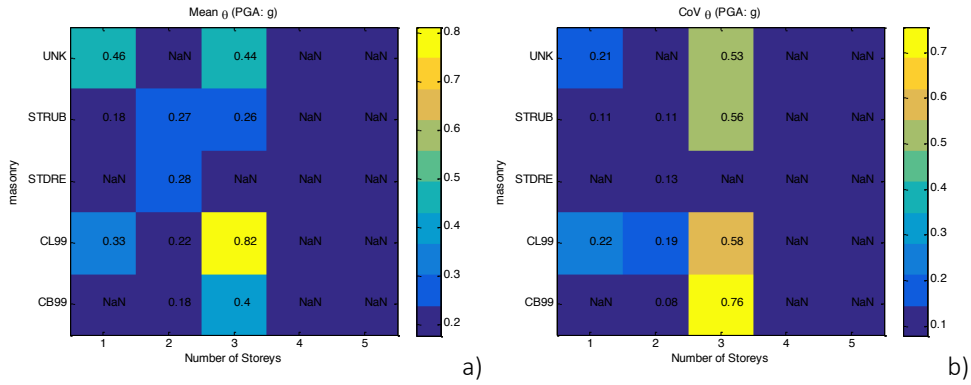

Figure 14. (a) Mean and (b) coefficient of variation (CoV) of the median of the fragility functions included in the database that use PGA as the IM and for a damage state compatible with an ultimate limit state
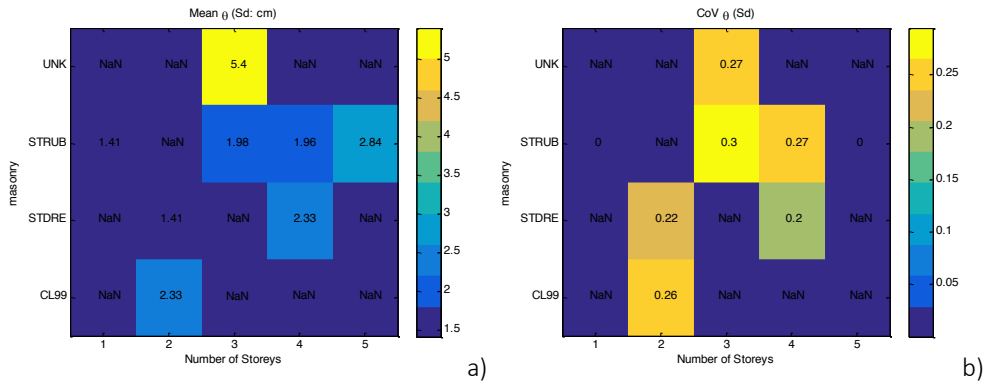

Figure 15. (a) Mean and (b) coefficient of variation (CoV) of the median of the fragility functions included in the database that use $Sd(T_y)$ as the IM and for a damage state compatible with an ultimate limit state
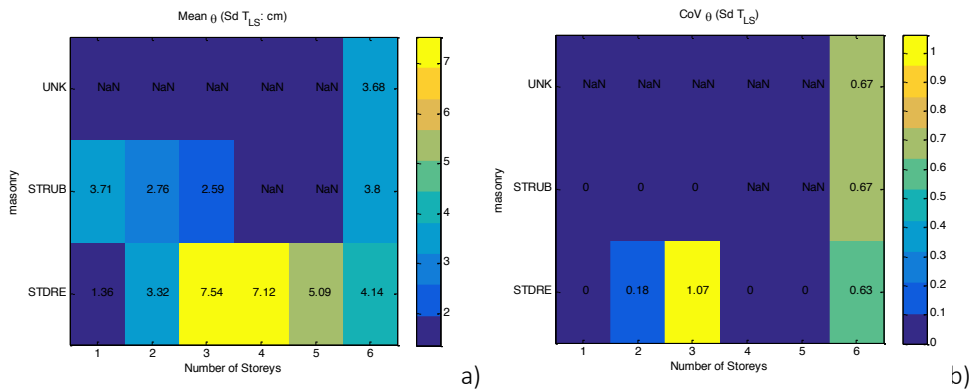

Figure 16. (a) Mean and (b) coefficient of variation (CoV) of the median of the fragility functions included in the database that use $Sd(T_{LS})$ as the IM and for a damage state compatible with an ultimate limit state

3.4.1.2. Residential RC buildings (F-RC)

Figure 17 shows the disaggregation of the F-RC dataset according to the IM adopted in each study. Almost 50% of the proposed models are based on PGA, reflecting the clear preference for this IM against other metrics, as also noticed by Yepes-Estrada et al (2016). Among the other IMs that are used, reference is made to models based on $Sd(T_{LS})$ that are more difficult to harmonize with the remaining ones.
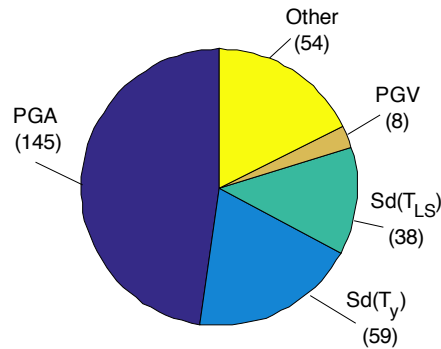

Figure 17. Disaggregation of the 304 fragility functions according to the IM used to define the fragility functions.

Figure 18 shows the disaggregation of the F-RC dataset according to the attributes adopted in the SERA exposure model v.0.1 (Section 2; Crowley et al. 2018). As seen in Fig. 18a, the majority of the functions that were collected refer to building classes that include a bare frame structure (LFM), which reflects the larger incidence of studies available in the literature covering this type of buildings. The number of available fragility functions addressing infilled frame structures (LFINF), wall structures (LWAL) and dual wall-frame systems (LDUAL) is moderate, and the number of fragility functions that were collected covering buildings classes LDUALFINF, LFLS, LFLSINF and T are very limited. Unlike for the case of typically non-engineered masonry buildings, the collected functions are unequally distributed among the 4 categories of design building codes. A relatively small fraction (11%) of the collected functions covers building classes associated with design practices prior to the implementation of seismic design principles (CDN). A second class includes 60% of the collected functions that were classified herein as low code (CDL) based on the reported year or the description of the structural properties found in the corresponding study. The same rationale was then used to classify the fragility functions according to the moderate code (CDM) or high code (CDH) classes, where the latter refers to design procedures similar to those of Eurocode 8/1 (CEN, 2004). The class UKN was used to group fragility functions for which the available information was insufficient to reach an objective classification.
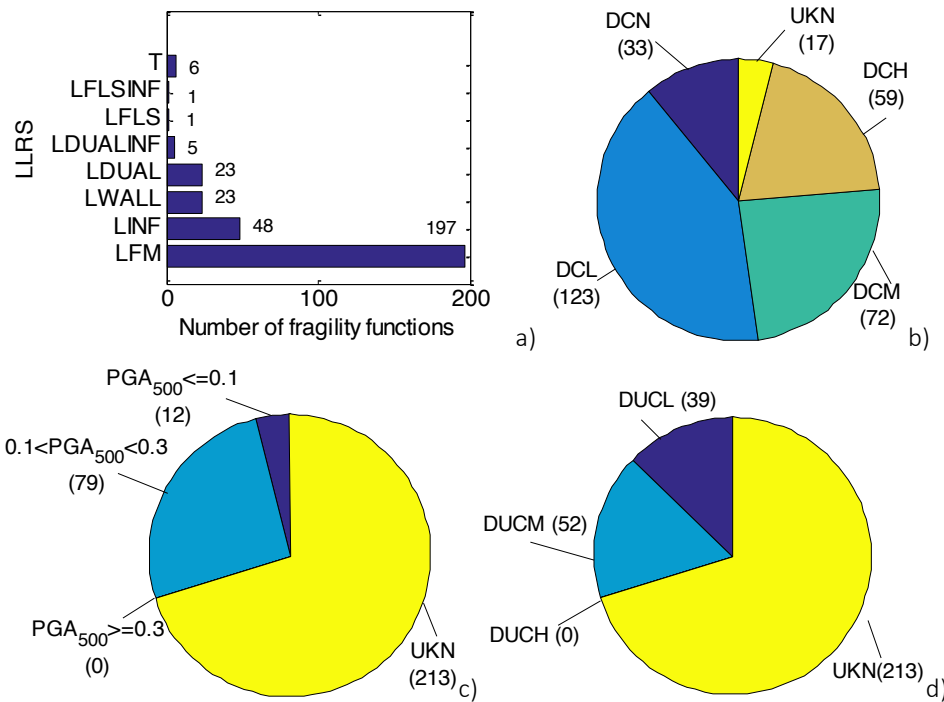
Figure 18. Distribution of the fragility functions based on the LLRS (a), on the type of seismic design code (No-code, NC, low-code LC, Moderate code MC and High code HC) that was adopted (b), on the PGA design level (PGA_{500}) adopted in each study (UKN refers to cases where there is no information about the lateral load coefficient considered in the design) (c) and according to the ductility classes (d) defined in the exposure model v0.1 (see section 3.2.2).

Figures 18c and 18d show the disaggregation of the collected fragility functions based on the reported PGA design levels (PGA_{500}) and according to the ductility classes defined in the exposure model (v0.1). As seen in Fig. 18c, a large part of the fragility functions that were analysed does not provide adequate information regarding the design PGA levels. Figure 18d was obtained by combining this information with the design code level, which demonstrates the current limitations associated to the selection of existing fragility functions that are compatible with the exposure model. In order to have a better understanding about this lack of connection with the exposure model defined in Deliverable 26.2 (Crowley et al. 2018), Fig. 19 shows the disaggregation of the number of existing functions according to the main building classes and attributes included in the SERA exposure model (v0.1). As seen in Fig. 19a, 22 out of the 32 building classes could not be adequately characterized by the database that was collected herein, since less than 10 fragility functions were identified for these classes. By disaggregating these results according to the third attribute that is included in the classification (i.e. the ductility level, DUC; Figs. 19b-c), the coverage that is obtained can be seen to be very low. In particular, no fragility functions covering explicitly the characteristics of building classes that have a ductility level DUCH could be found.

Since the reason for this lack of coverage can be seen to be the result of insufficient available information regarding the design seismicity level (PGA_{500}), Fig. 20 shows the disaggregation of the database based on the design code class (CD; see Fig. 18b). As expected, some of the building classes are able to be analysed using existing fragility functions (particularly those have LFM as the LLRS), since PGA_{500} was seen to be the conditioning variable in the DUC classification. Nevertheless, some of the building classes are still insufficiently covered, even when the design seismicity level is removed from the ductility classification scheme that is used in the SERA exposure model v0.1.
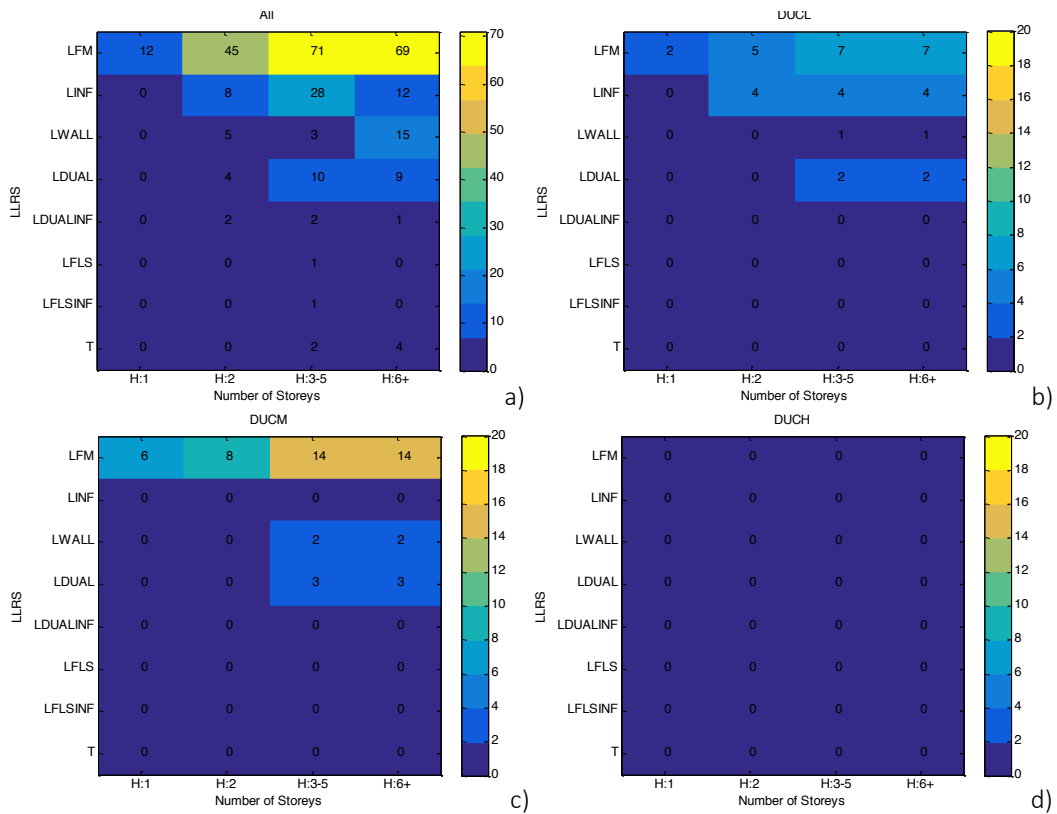
Figure 19. Disaggregation of the available fragility functions according to the RC building classes defined in the SERA exposure model v0.1 (Crowley et al. 2018; Crowley et al. 2019a).
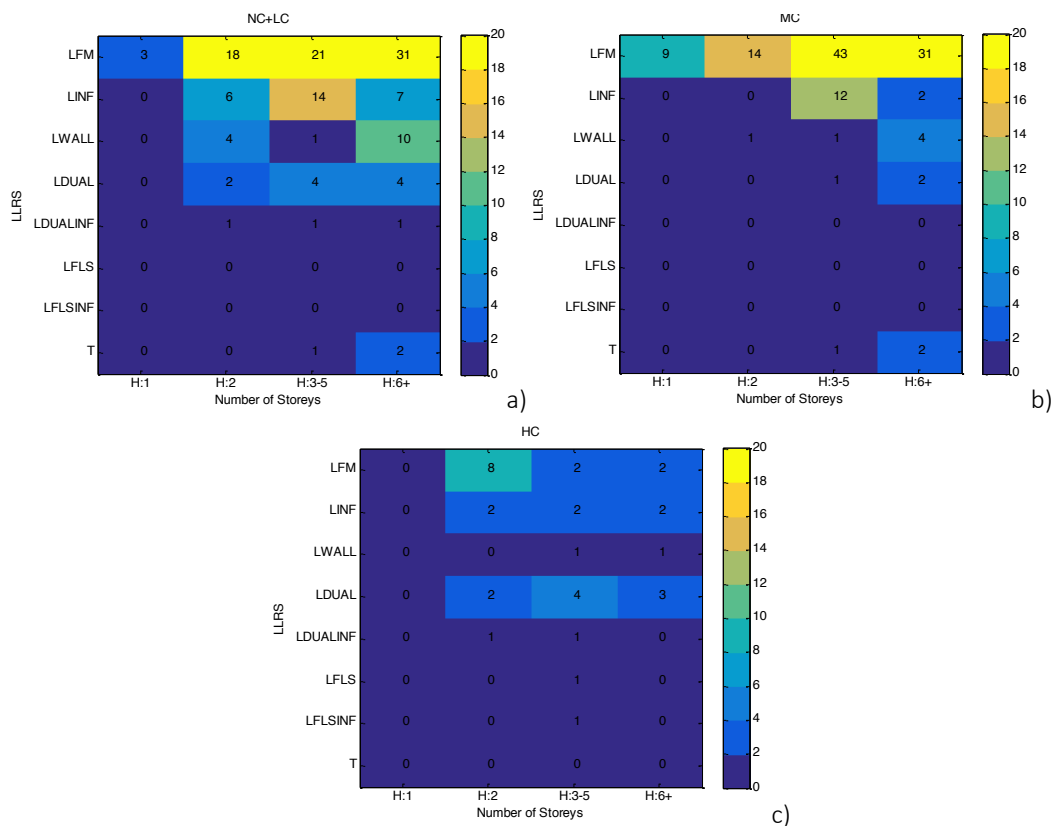

Figure 20. Disaggregation of the available fragility functions for cases with seismic design compatible with the low-code or no-code class (a), the moderate-code class (b) and the high-code class (c), as a function of each combination of number of storeys and type of lateral load-resisting system.

3.4.2. Capacity curves

3.4.2.1 Residential masonry buildings (C-MUR)

Figure 21 shows the histograms and the Kendall rank correlation coefficients between parameters T_y, Sd_y, Sd_u, Sa and S_u of the bilinear capacity curves of the C-MUR dataset. As can be seen, the correlation between some of the parameters of the bilinear capacity curves is significant. Some of these larger correlation levels are expected due to the transformation between the MDOF system and the SDOF system (i.e. the correlations between Sd_y, T_y and Sa_y). The results from the database indicate there is also a significant correlation between Sd_y and Sd_u (Kendall's $\tau = 0.78$). Since capacity curves are assumed to have a perfectly plastic behaviour between Sa_y and Sa_u, a positive and very high correlation is also found between Sa_y and Sa_u (Kendall's $\tau = 0.88$). Slightly larger values were also obtained for the Pearson correlation coefficients (r=0.96 and r=0.95 for the correlation between Sa_y and Sa_u, and between Sd_y and Sd_u, respectively).

Figure 22 shows the disaggregation of the estimates for T_y, D_y, D_u and Sa_y according to the type of masonry. The disaggregation considered five different types of unreinforced masonry (adobe (ADO) with 7 curves, rubble stone (STRUB) with 38 curves, regular cut stone (STDRE) with 40 curves, clay blocks of any type (CL99) with 85 curves, concrete blocks of any type (CB99) with 13 curves), and one type of reinforced/confined masonry (CRM) with 6 curves.

As can be seen in Fig. 22, the results do not show large variations for the median values of each parameter based on the type of masonry. The median value of T_y is found to be 0.39s, 0.49s, 0.32s, 0.48s, 0.51s and 0.17s for the ADO, STRUB, STDRE, CL99, CB99 and CRM masonry buildings, respectively. However, a larger variability of T_y was observed within each class, with values of the CoV of 0.65, 0.71, 0.46, 0.80, 0.71 and 0.39 for the ADO, STRUB, STDRE, CL99, CB99 and CRM masonry buildings, respectively.
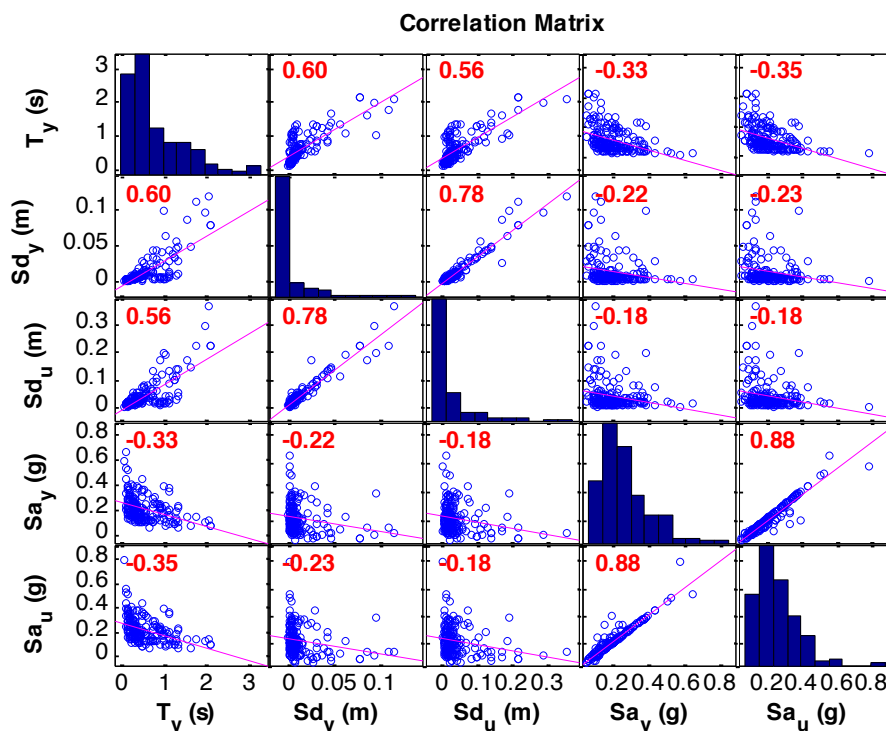

Figure 21. Correlation matrix between the parameters of the 189 capacity curves collected during the literature review (the Kendall coefficients of correlation are shown in red).
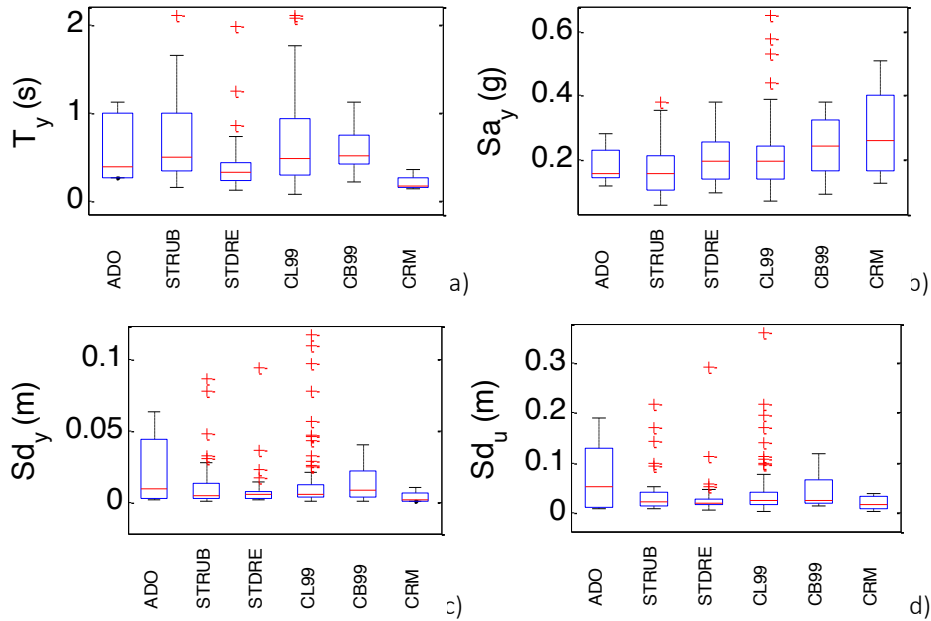
Figure 22. Disaggregation of the estimates for T_y, Sd_y, Sd_u, and Sa_y according to the type of masonry.

Bal *et al.* (2008) noticed that T_y is more influenced by the floor system (timber or RC slabs) than by the type of masonry unit (i.e. solid or hollow clay bricks, or concrete bricks). In this context, Ahmad and Ali (2017) analysed samples of buildings with a total height between 5m and 6m whose characteristics can be fitted into the considered masonry classes and that include cases with timber or RC floor systems. Their analyses include a sample of 50 cases for each type of building and report the mean values and the logarithmic standard deviations of the capacity curves shown in Table 5. As can be seen, a dispersion (β) between 10% and 20% was observed for T_y and Sd_y, where the lower values correspond to the ST99 cases due to the smaller variability of the masonry strength that was considered in the study (i.e. with a coefficient of variation (CoV) of 5%) when compared to the variability of the remaining cases (i.e. with CoVs around 30%).

Table 5. Statistical parameters of the probabilistic capacity curves derived by Ahmad and Ali (2017).

CLASS		Sa_Y (g)		Sd_Y (mm)		Sd_U (mm)	
Masonry	Floor	Mean	β	Mean	β	Mean	β
CL99*	T	0.14	0.12	2.09	0.13	9.91	0.11
CB99*	T	0.22	0.17	3.68	0.23	13.22	0.10
ST99*	T	0.18	0.05	3.08	0.08	18.68	0.08
CL99*	RC	0.19	0.15	3.29	0.19	10.80	0.09
CB99*	RC	0.28	0.18	5.06	0.24	13.87	0.11
ST99*	RC	0.20	0.05	3.52	0.08	19.46	0.08

Classified in this study

The number of storeys (H:) is an attribute that also has a considerable impact in the capacity curve parameters. A disaggregation of the mean and of the CoV of Sd_y, T_y and Sa_y was performed for the 189 capacity curves based on the type of masonry (ADO, STRUB, STDRE, CL99, CB99 or CRM) and on H:, assuming a reference number of storeys when conclusive information about the total height was not available (i.e. for a class of buildings with 3 to 5 storeys, H:4 is considered). Figure 23 illustrates the disaggregation of the results for the different types of masonry, while Figs. 24 and 25 show the mean

and the CoV of Sd_y, T_y and Sa_y obtained after performing statistical analyses of the capacity curves plotted in Fig. 23.
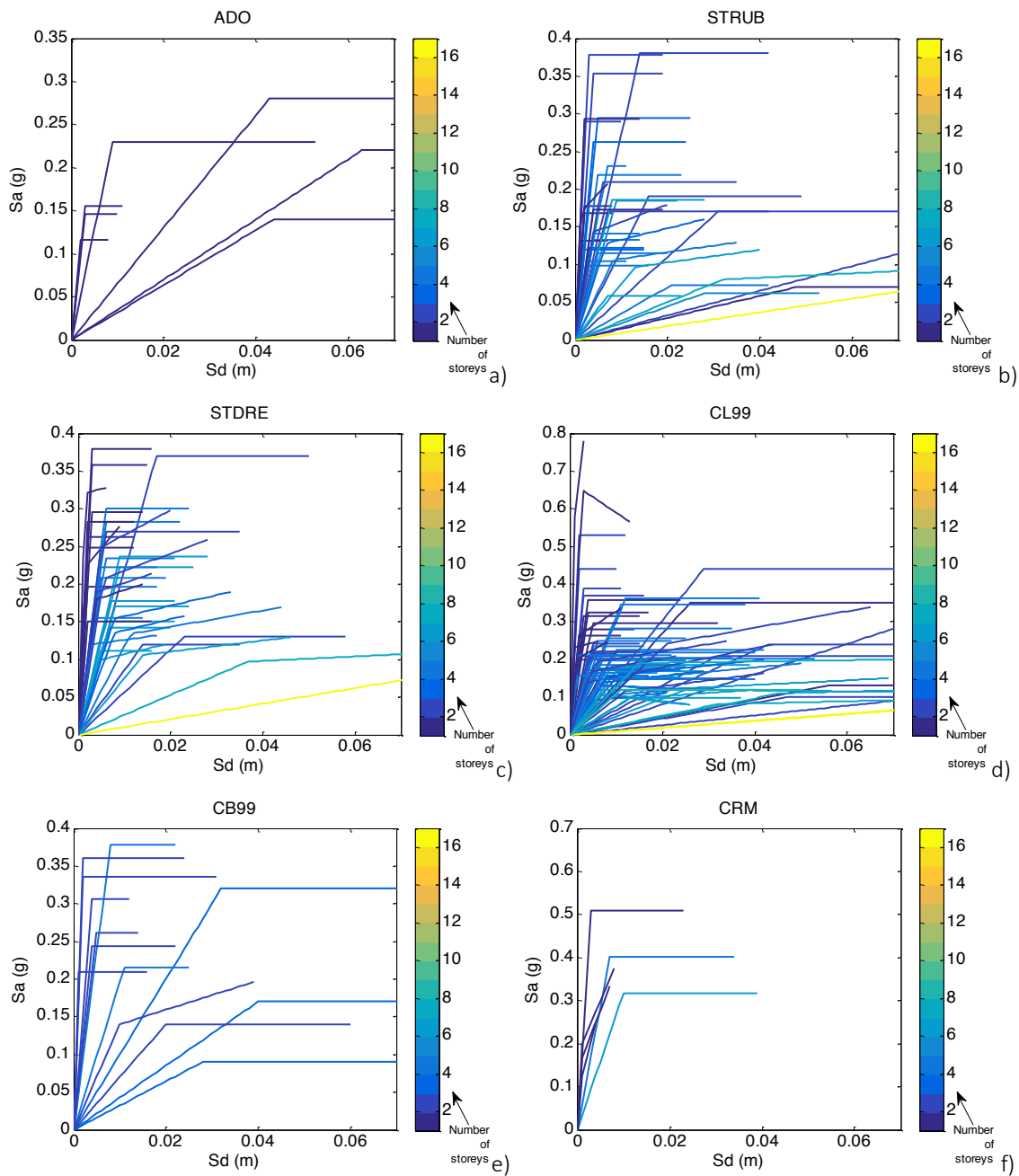

Figure 23. Representation of the capacity curves according to the type of masonry. It is noted that the dataset includes a high-rise(16 storey) masonry building that requires further investigation.

Figures 24a and 25a present the number of curves considered for the calculation of the statistical parameters, which should be used as a robustness indicator for the referred calculations. As seen in Fig. 24a, the ADO buildings only have results for the case of 1 storey because all the buildings found for the class with 1-2 storeys where the information about the number of storeys was unavailable were counted as having one storey. Furthermore, it is noted that the database has a limited number of curves for buildings with 5 storeys. A limited number of studies was also found for reinforced or confined masonry (CRM) buildings, which, as referred previously, is in line with the limited number of buildings found in Europe with this type of masonry (particularly confined masonry), as mentioned by

Lagormasino and Catari (2014). The mean values of Sa_y are typically in the range between 0.15 and 0.30, while typical values of the CoV (considering cases only with sufficient data) are in the range 0.30 to 0.50, with larger CoV values being observed for Sd_y and Sd_u. The sampling uncertainty (the effect of having different number of curves for each building class) and the possible uncertainty about the taxonomy (i.e. the effect of the collapsed attributes) can be observed in the variations of the mean Sa_y with H (Fig. 24b).

Although the number of capacity curves that were collected provide information about the building-to-building variability that can be expected when performing a study at a continental scale, their statistical analysis highlights a few inconsistencies. For example, from a physical point of view, a decrease in the building capacity can be expected when a larger number of storeys is involved (and all the remaining attributes are fixed). However, some of the mean values of Sa_y presented in Fig. 24 do not exhibit this trend. Nevertheless, in global terms, these analyses indicate that a CoV in the order of 0.30 appears to be a representative value for the simulation of Sa_y. Still, larger variations were observed for the yielding and ultimate displacements, which may be due to the possible effect of collapsed attributes such as the type of floor on the building-to-building variability. This type of attributes is difficult to introduce in exposure models and, as a result, must be included in the vulnerability models as part of the building-to-building variability.
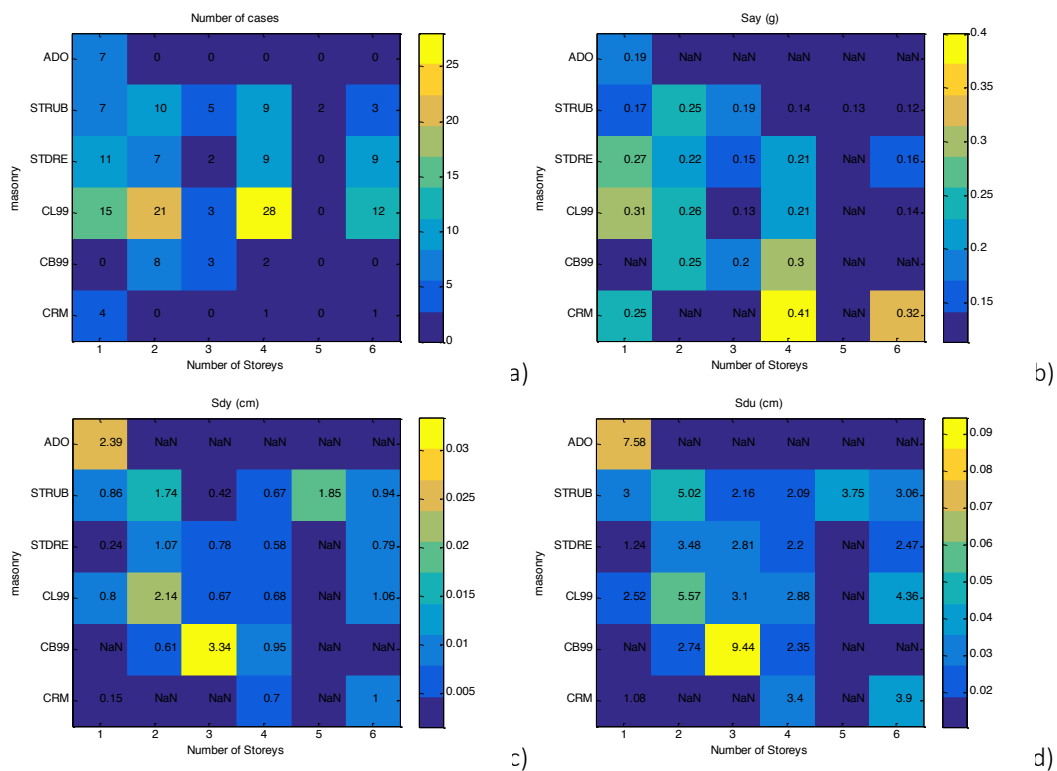

Figure 24. Disaggregation of the mean of the estimates for T_y, Sd_y, Sd_u, and Sa_y according to the type of masonry and the number of storeys.
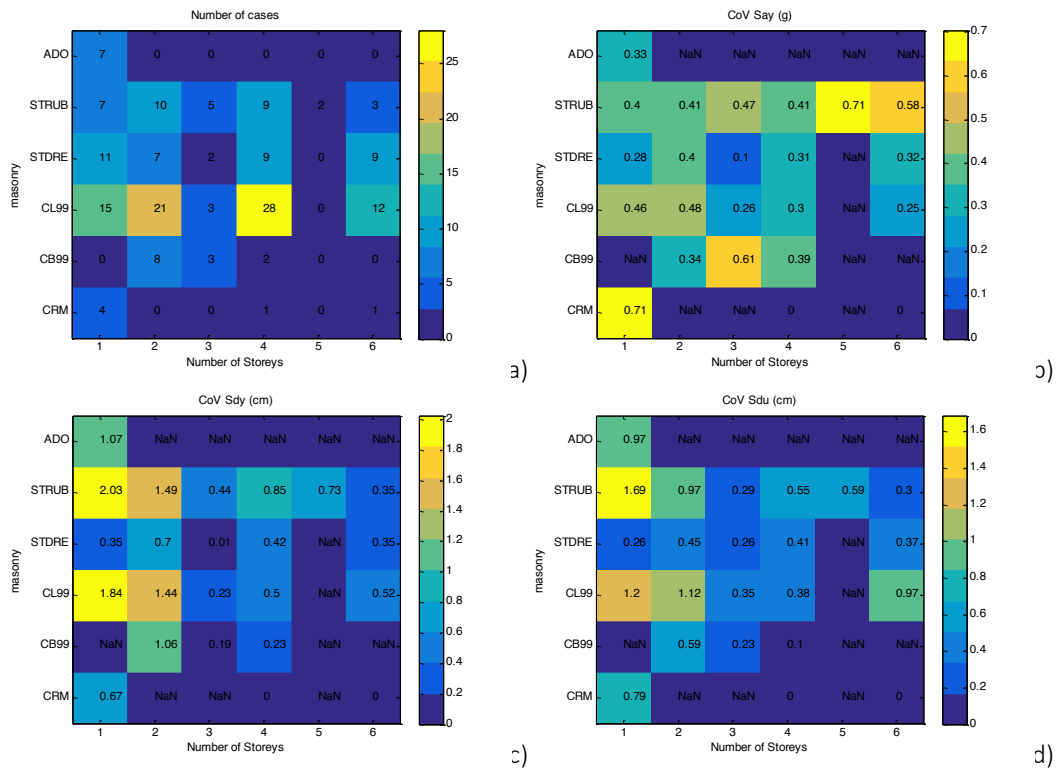
Figure 25. Disaggregation of the CoV of the estimates for T_y, Sd_y, Sd_u, and Sa_y according to the type of masonry and the number of storeys.

Alternatively, regression models can be used to establish a direct connection between Sd_y and Sd_u. The relation between Sd_y and Sd_u involves a significant statistical correlation, as shown in Fig. 21, and, therefore, a global empirical model can be established using linear regression analysis. Figure 26 shows the variation of T_y with the total height of the building according to the gathered data.
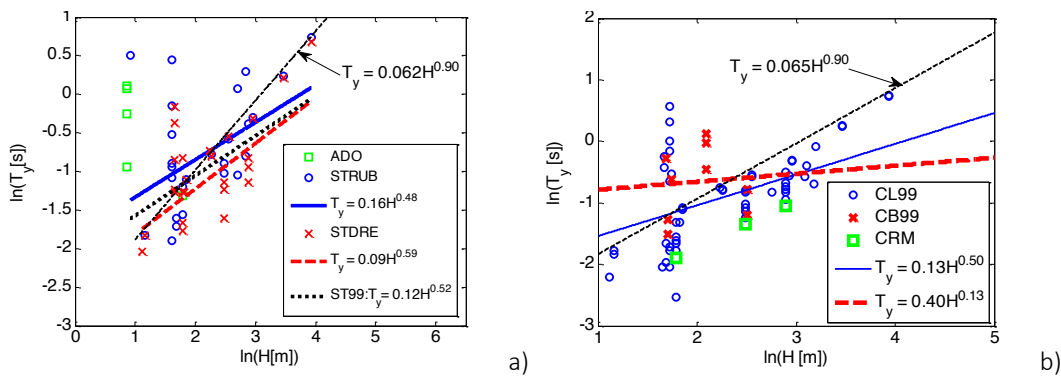

Figure 26. Relation between T_y and the total height of the building based on the available database and comparison with generic models from the literature for a) ABO, STRUB and STDRE and b) CL99, CB99, CRM.

The linear fit in the log-log space shown in Fig. 26 exhibits a goodness-of-fit that is compatible with adjusted R^2 values of 0.18 (RMSE of 0.667) for the STRUB data, 0.41 (RMSE of 0.43) for the STDRE data and 0.57 (RMSE of 0.57) for the ST99 data (that includes both the STDRE and the STRUB datasets). The approximation provided by the model $T_y = 0.062H^{0.90}$ obtained from the literature shows a direct proportionality (in the log-log space) that is not observed in the trend line that was fitted herein (i.e. the lower exponent of the proposed regression implies a higher curvature of the fitted curve). Figure

27a shows the fit obtained to the STRUB dataset after excluding 3 outliers classified as unreliable due to the fact that they present very high periods for typical buildings with 2 storeys. A significant improvement in the quality of fit is observed (adjusted R^2 = 0.76), and the literature model is seen to be adequate given the very close match that is observed. By applying the same filtering approach to evaluate the effect of potential trend outliers on the STDRE dataset, Fig. 27b shows a slight improvement in the goodness of fit (the adjusted R^2 goes from 0.57 (Fig. 26) to 0.65). The main reason for this is the fact that two subsets of points can be observed. The first subset involves the majority of the datapoints and exhibits a very close match with the literature model that is used for comparison. The second subset, however, exhibits lower periods and its trend does not agree with the literature model. Given that similar effective periods can be expected for STDRE and STRUB buildings with similar heights (this is also why the literature model is suggested for both types of buildings), the literature model appears to be consistent with the analysed data.

The results obtained for the CL99 masonry lead to an adjusted R^2 of 0.24 (RMSE of 0.61), while a fit worse than a horizontal line was found for the CB99 masonry. In Fig. 26b, it can be seen that the literature approximation defined by $T_y = 0.065H^{0.90}$ is visually able to fit adequately the bulk of the data belonging to the CL99 and CB99 classes. The approximations shown in Fig. 26 are similar to the proposal of Bal et al. (2008) for CL99 buildings with RC slabs, whereas the same authors proposed the adoption of 0.039H when there are timber floors instead. Naveed et al (2010) calibrated a model fixing the exponent value at 0.75, leading to the approximation $T_y = 0.05 \cdot H^{0.75}$. By removing some outlier points based on the expected physical properties of 1 and 2 storey buildings, it can be seen from Fig. 28 that the reliability of the fitted model significantly improves (the adjusted R^2 goes from 0.24 (Fig. 26) to 0.66) and that the literature models mentioned before are within the 95% prediction bounds of the fitted regression.

Figure 27. Comparison of the prediction bounds of the model fitted after excluding datapoints classified as less reliable with literature proposals based on larger datasets of data for STRUB and STDRE buildings.
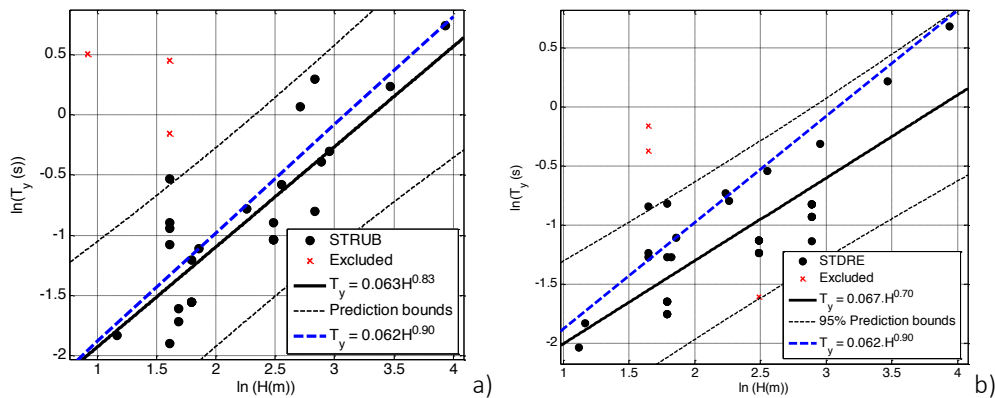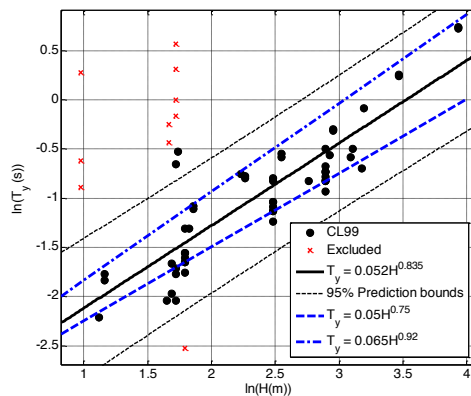

Figure 28. Comparison of the prediction bounds of the model fitted after excluding datapoints classified as less reliable with literature proposals based on larger datasets of data for CL99 buildings.

Figure 29 shows the variation of Sd_u with Sd_y considering the entire database, along with the least squares fit obtained from linear regression. The relation that was obtained ($Sd_u = 1.73 \cdot Sd_y^{0.84} + \varepsilon$) shows an adjusted R^2 of 0.92, with ε being a zero-mean normal distribution with standard deviation 0.014.
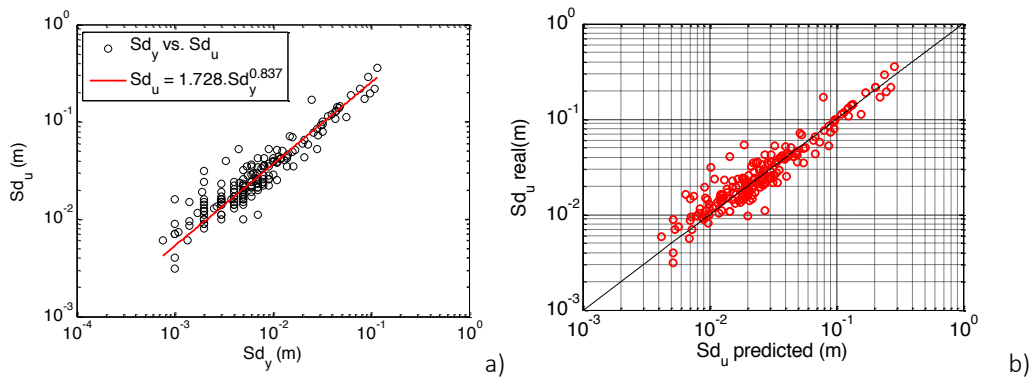

Figure 29. Analysis of the relationship between Sd_y and Sd_u based on the entire database.

3.4.2.2 Residential RC buildings (C-RC)

Figure 30 shows the disaggregation of the capacity curves according to the LLRS and to the type of idealization adopted for the capacity curve. As can be seen, at least 7 capacity curves were included for each LLRS. The larger number of curves corresponds to the LFM system, thus corroborating the trend observed when compiling the existing fragility functions for RC buildings. A large number of studies (104) was also compiled for LFINF systems, while there is a smaller number of cases for the remaining types of LLRS.
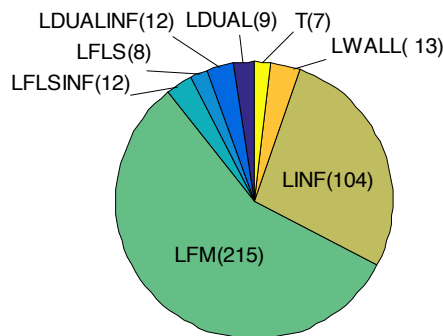
Figure 30. Disaggregation of the capacity curves according to the type of LLRS.

Figure 31 shows the correlation matrix with the histograms and the Kendall rank correlation coefficients between T_y, Sd_y, Sd_u, Sa_y and S_u of the bilinear capacity curves. Similarly, Figs. 32 and 33 show similar correlation matrices obtained when using the data of models with 3 and 4 branches.
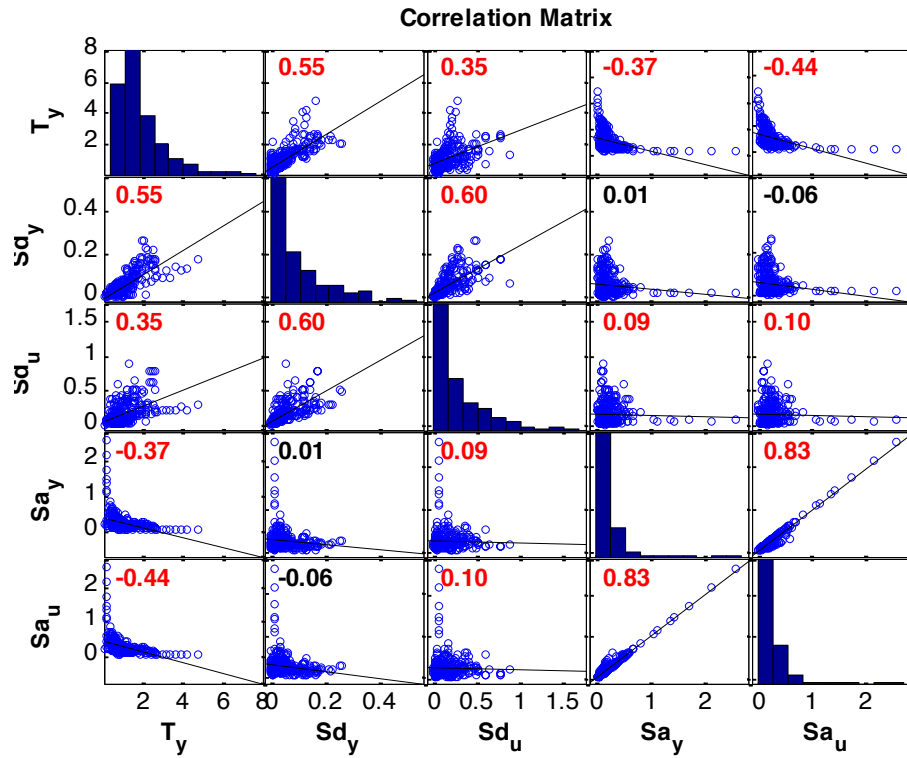
Figure 31. Correlation matrix obtained using the data of bilinear capacity curves from the literature.

Figure 32. Correlation matrix obtained using the data of trilinear capacity curves from the literature.

Figure 33. Correlation matrix obtained using the data of quadrilinear capacity curves from the literature.

The correlation matrix obtained for the bilinear capacity curves (Fig. 31) shows that a Kendall's τ of 0.60 could be identified between Sd_u and Sd_y. The linear correlation level between Sd_u and Sd_y was also seen to be consistent with a Pearson coefficient of 0.70. Most of the models analysed have an elastic-perfectly plastic envelope, a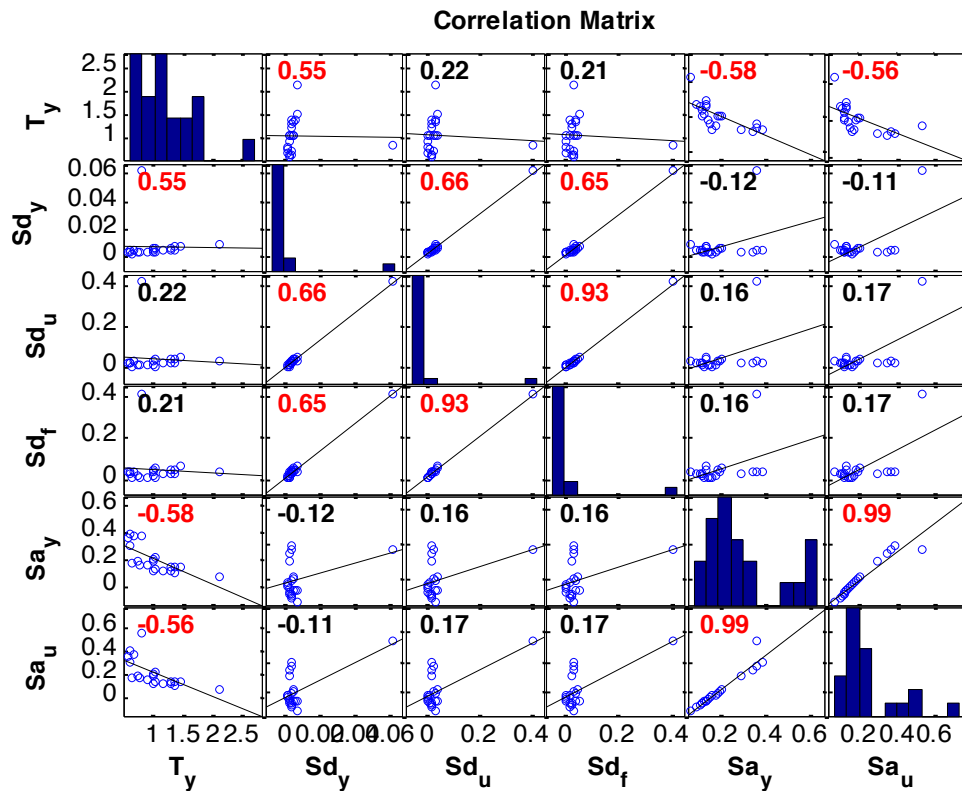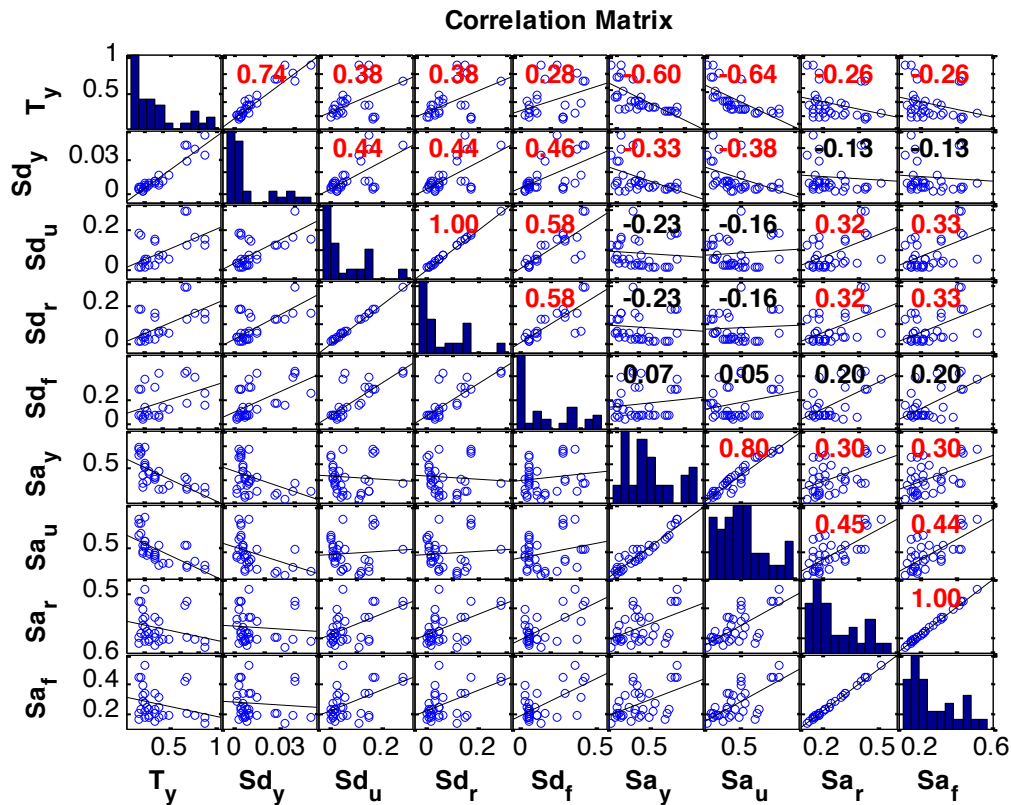s corroborated by the large correlation coefficient found for the relation between Sa_y and Sa_u (Pearson r = 0.98). Similar observations were made when considering the trilinear and quadrilinear curves (Kendall's τ = 0.66 and 0.44), although a lower correlation level was identified in the latter case. Significant correlations were also found between several displacement parameters of the quadrilinear curves. The larger correlation levels that were observed in Figs. 32 and 33 are due to the main assumptions of the models, namely the relations imposed in the quadrilinear model between Sa_r and Sa_f, and between Sa_y and Sa_u. Since the residual Sa level (Sa_r) represents the residual capacity given by the bare frame structure after the drop of strength induced by the failure of the infill walls, no significant correlation level was found between this variable and Sa_y. This fact highlights the duality of the response of these structures due to the interaction between the two systems (RC structure and infills).

Figure 34 shows the boxplots of the parameters T_y (a), Sa_y (b), Sd_y (c) and Sd_u (d), as defined for the different types of capacity curves in Fig. 2, for 45 out of the 96 building classes established in the SERA exposure model v0.1. Due to the lack of available information regarding the PGA levels adopted in the design, the ductility classification was performed based solely on the code class (CDL,CDM,CDH were used as potential indicators of DUCL, DUCM and DUCH buildings).

As shown in Fig. 34, the larger dispersion levels are found for the distribution of the Sd_u values. For Sa_y, CoV values between 5% and 55% are obtained (when the number of observations is higher than 2), with a median of 0.261 and a mean of 0.274. Similar values were observed when analysing the variability of the distribution of T_y (with CoV values between 1% and 0.81, a mean of 0.29 and a median of 0.25).
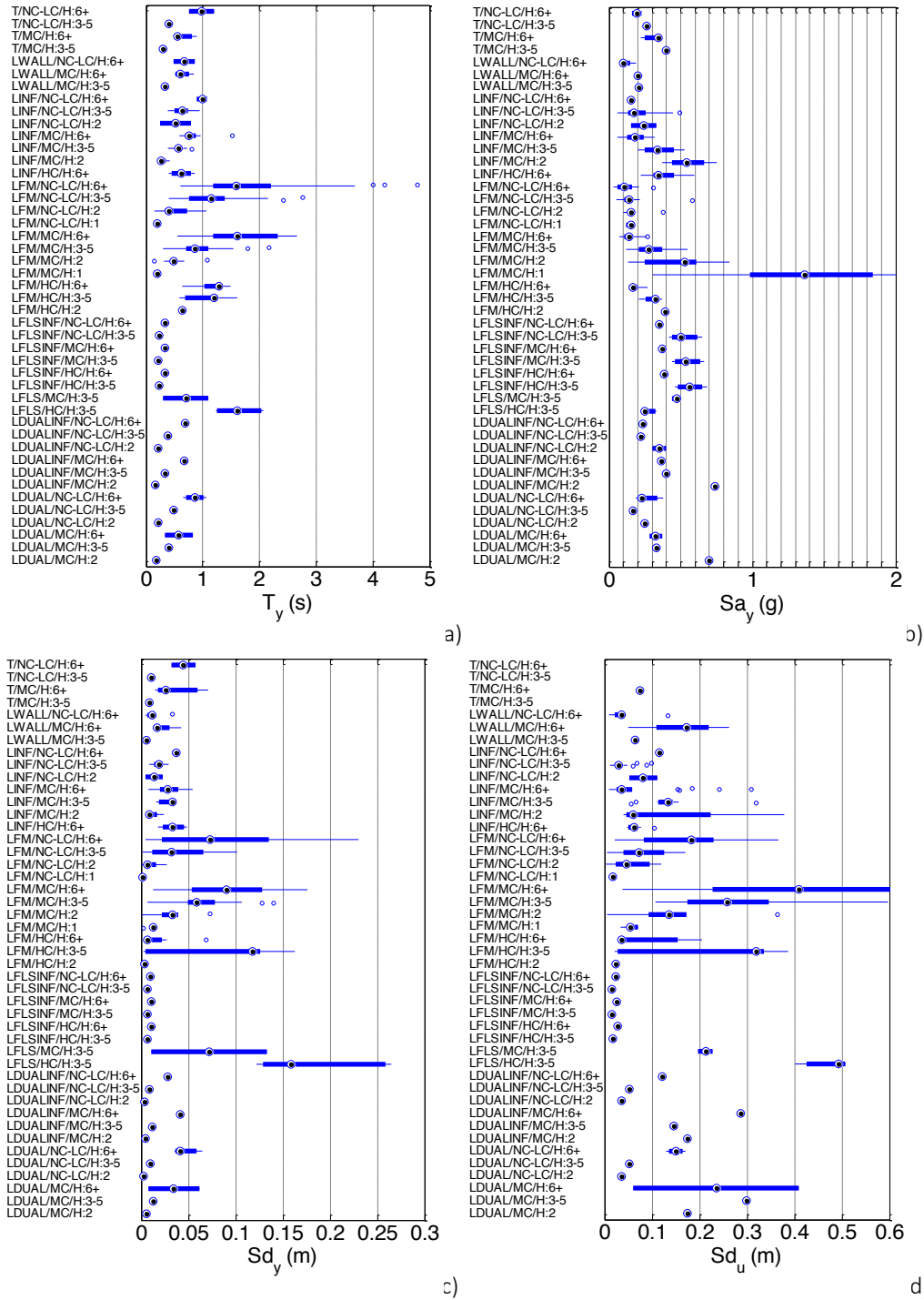
Figure 34. Boxplots of the effective period T_y, Sa_y and the displacement Sd_y and Sd_u (see Fig. 2 for a description) of the different building classes identified in the database following the SERA exposure model v0.1 taxonomy (without including the PGA constraint in the ductility classification).

Figure 35 shows the disaggregation of the effective periods of each capacity curve collected in the database and their comparison with available period-height relationships. The literature models used for comparison are the relation $T_y = 0.10H$ proposed by Crowley and Pinho (2004) for no ductile LFM buildings and $T_y = 0.07H$ for ductile cases, as proposed by Crowley et al. (2008). The models $T_y = 0.042H$ for LFINF and $T_y = 2 \cdot 0.049 \cdot N$ (where N is the number of storeys and where an inter-storey height of 3 m was adopted, leading to the relation $T_y = 0.032 \cdot H$) for LWAL buildings were also used, following the indications provided by Villar-Vega et al. (2017). For DUAL buildings a slightly larger relation was

considered ($T_y = 0.036 \cdot H$). For the case of LFLSINF buildings, the results obtained by De Luca et al (2015) for Spanish buildings were adopted. These authors proposed the consideration of a period-height relationship with the form $T_0 = 0.023 \cdot H/\sqrt{A_{inf}}$, where A_{inf} is the percentage between the infill area along the direction of seismic loading and the building footprint area. For simplicity, it was considered that the value of A_{inf} contributing to the lateral resistance could be assumed as 2.5%, thus leading to the simplified relation $T_y = 0.0146H$. By assuming (as done by De Luca et al. (2013)) that $T_y = = 1.4 \cdot T_0$, the simplified model $T_y = 02H$ was obtained. Finally, for the case of tunnel-form buildings (T), an approximation was considered based on the proposal of Balkaya and Kalkan (2004) assuming that, on average, buildings have an aspect ratio R (i.e. the longer in-plan dimension over the lower in-plan dimension) of 1.0 and the same amount of walls in both directions (Rx=Ry=20%, where Rx and Ry are the ratios between the wall area and the floor area of the building), thus leading to an elastic period of approximately $T_0 = 0.0219H$. A factor of 1.33 was used to convert T_0 into T_y, yielding the approximation $T_y = 0.029H$.
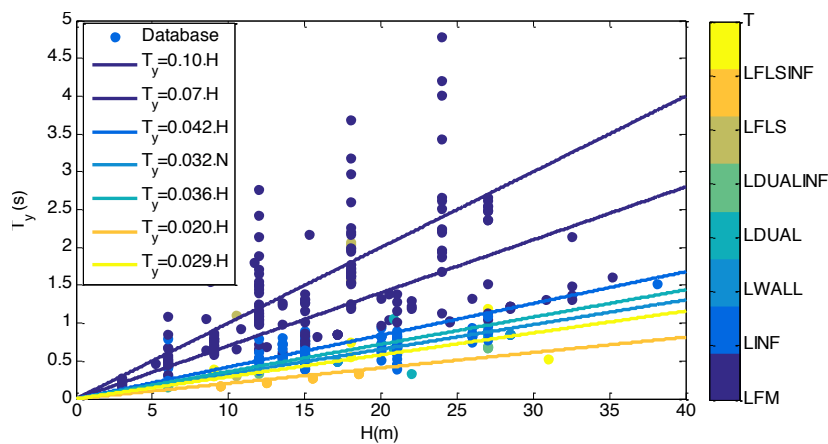

Figure 35. Disaggregation of the effective periods of the capacity curves collected in the database and comparison with period-height relationships available in the literature.

As shown in Fig. 36, the approximations collected from the literature provide, on average, adequate estimates for the effective periods of the different building typologies. The duality observed between the ductile and non-ductile LFM buildings is clear, since the two different lines defined based on Crowley and Pinho (2004) and Crowley et al. (2008) fit different regions of the dataset. These differences can be further analysed in light of the large number of points available for the LFM building class. To do so, Fig. 36 shows the comparison of the LFM data with the period-height relations proposed by Mariniello (2007) and Martins (2018). The main differences between the two approaches refers to how the design code and the seismic hazard were considered when developing these relations: Marinielo (2007) used an old code based on the Italian practices from around the 1960s, using a percentage of the weight as a design metric to reflect the seismic hazard level at different sites; Martins (2018) adopted modern design code practices and used a response spectrum combined with different PGA_{500} values to design the buildings. As can be seen from Fig. 36, considering different design code levels clearly allows capturing the two trends observed before. The effect of using different design codes does not affect significantly T_y in the LFINF buildings, and the approximations proposed by Martins (2018) seem to provide adequate estimates for T_y.
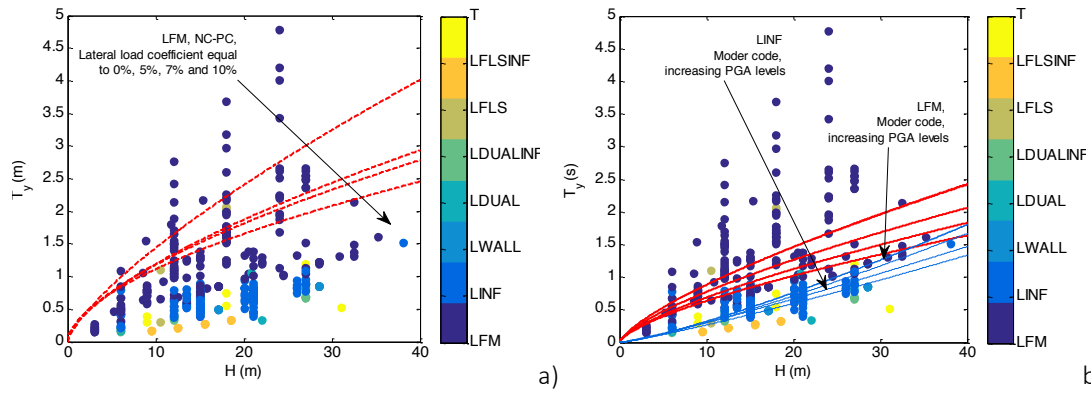
Figure 36. Comparison of the T_y values included in the C-RC dataset and period-height relationships proposed in the literature for LC (a) and MC (c) design classes.

Figure 37 shows the variations of Sd_u with Sd_y based on the capacity curves of the dataset C-RC, disaggregated according to the LLRS and according to the design code class. Part of the database shows a significant increase of Sd_u with smaller variations in Sd_y. Conversely, a second set of points shows an approximate linear relation between Sd_y and Sd_u, thus highlighting the existence of a lower post-peak ductility (Fig. 37a).
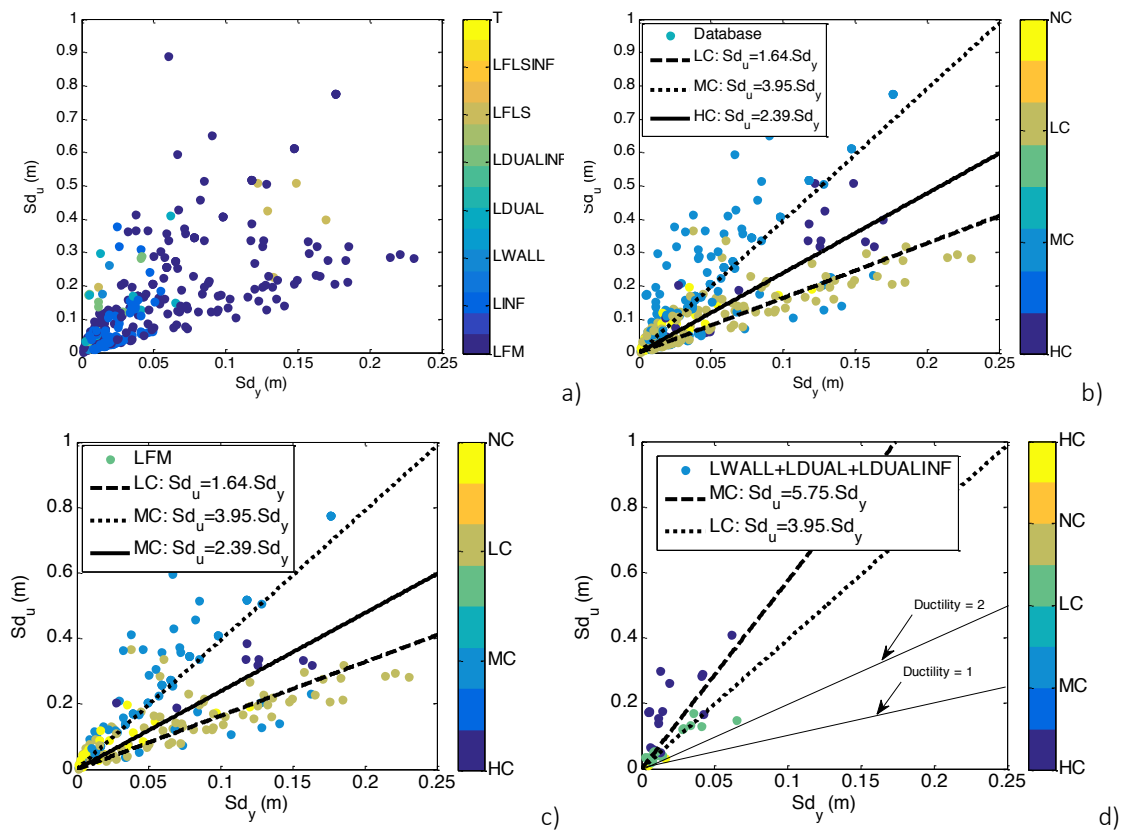
Figure 37. Evaluation of the relationship between Sd_u with Sd_y disaggregated by type of LLRS (a), design code class (b), using only buildings with LFM (c) or with LWAL, LDUAL and LDUALFINF LLRS (d).

A clearer distinction of these two datasets is obtained when the models are separated according to the design code class (Fig. 37b). By doing so, the clusters of points observed in Fig. 30b can be seen to follow essentially three trend lines. By fitting a linear model to the points associated to the LC designs, it can

be seen that Sd_u is on average 1.64·Sdy (R^2=0.62; RMSE=0.05). When selecting the points associated to MC, it is seen that the slope of the relationship changes to 3.95 (R^2=0.55; RMSE=0.1282). A weak variance relation was observed for the HC subset since a limited number of points was considered, which may be related to the lower ductility level observed for these structures. These trends are visually compatible with the subset that includes only the points corresponding to LFM buildings (Fig. 37c). The differences observed between the two lines and the magnitude of the RMSE values suggest that different failure modes are observed. The LC line appears to predominantly capture soft-storey mechanisms, thus leading to lower ductility values (1.64). On the contrary, the MC line appears to capture beam-sway mechanisms, thus leading to the increase of ductility that is observed (from 1.64 to 3.95, on average). Figure 37d shows a similar disaggregation but considering only the classes LWAL, LDUAL and LDUALFINF. It can be seen that two steeper lines were obtained by the regression analysis, with ductility levels higher than those observed in Fig. 37c.

Figure 38 shows the variation of Sa_y with the LLRS and H (Fig. 38a), with the design code class and H (Fig. 38b;d) and with both H and PGA_{500} (Fig. 38c). The results show a considerable dependence of the Sa_y values on H, the design code class and PGA_{500}. The design code effect is evident from the difference between the scale of Sa_y values found for CDN and CDM, along with the lower dispersion obtained when comparing the NC and LC cases. In Fig. 38c, the effect of the design PGA_{500} that is not captured for the MC cases in Fig. 38b is observed, indicating that the development of fragility functions for building classes applicable at a continental level must explicitly take into account both the seismic design hazard level and the type of ductility considered in the design (which is related to the type of design code that is adopted) separately. Globally, the literature Sa_y-H relationships were seen to underestimate the Sa_y.
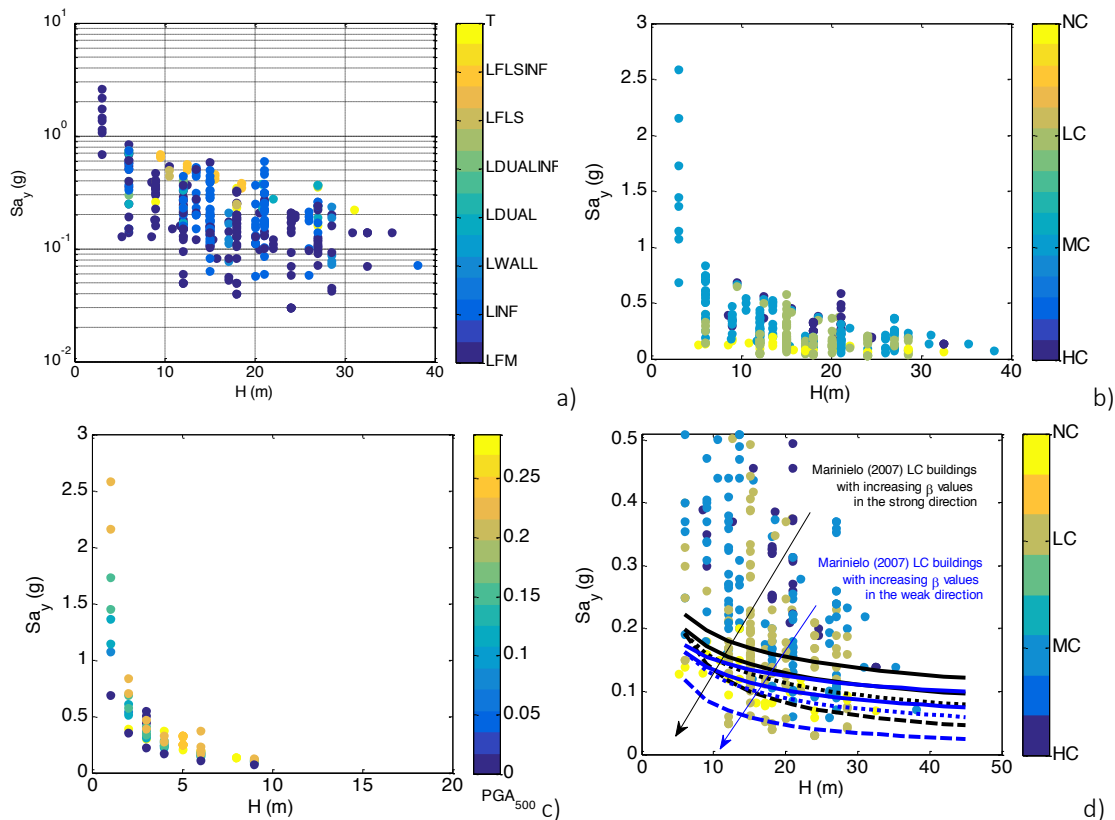

Figure 38. Disaggregation of the relationship between Sa_y and H according to the type of LLRS (a), to the type of design code (b) and according to the level of design PGA_{500} (c) and comparison with the Sa_y-height relationships proposed by Marinielo (2007) for different levels of the design lateral load coefficient for NC/LC buildings (d).

3.5   Limitations of existing fragility functions and vulnerability models

A number of studies covering the fragility and vulnerability of pan-European residential and industrial buildings was reviewed in this task of the SERA project. All the studies and their corresponding data were stored in the SERA.REVIEW database, including a significant number of studies about the fragility and capacity of the residential buildings with larger prevalence in the SERA exposure model. As mentioned before, there is currently a limited amount of data addressing the fragility and capacity of industrial buildings, in part due to the specific paradigm that must be considered when analysing these buildings. Key aspects such as non-structural damage, content loss, downtime and lost time of production have to be incorporated in the analysis, which implies that vulnerability models have to be defined for each type of industry, while fragility functions have to include the damage induced to structural components, non-structural components of the building and contents. Loading conditions, which impact the design of industrial buildings, and design codes/local practices were seen to be the most relevant attributes. On the other hand, the existence of adequate and industry activity-specific damage-to-loss models are seen to be extremely relevant for an adequate quantification of the seismic vulnerability.

Thanks to the literature review that was performed and to the subsequent post-processing of the gathered data for residential buildings, the effect of collapsing attributes was analysed on both the fragility functions and the capacity curves, and a set of statistical distributions that could be used to develop consistent vulnerability models for pan-European building classes was tentatively made.

Still, it was impossible to match directly all the building classes of the SERA exposure model v0.1 with existing fragility functions. Moreover, even for cases where this match was possible, the fact that specific sets of ground motions were used in the development of the existing functions limits the generic character that is needed for a function to be applicable at a continental scale. Fragility functions are also conditioned on the adopted IM to measure the intensity of the ground motions. As a result, fragility functions obtained from the literature and developed for a specific region or country can be generically seen as important data source for internal validation (i.e. for a direct comparison of results obtained with models developed at a continental scale). However, using these functions for regions or taxonomies different from those for which they were developed may imply significant deviations.

The combination of fragility functions following the main principles outlined in Crowley et al (2014) did not allow for a statistical characterization including the building-to-building and country-to-country variability of each building class. In many cases, the incompatibility between IMs and the effect of ground motions selected to match a particular response spectrum were identified as potential conflict arguments when choosing an existing fragility function from the literature.

The efforts undertaken in this task to analyse a comprehensive set of capacity curves allowed for the derivation of general correlation matrices that can be used as a benchmark for the definition of probabilistic SDOF models, which can then be used with fragility derivation strategies similar to those adopted in seismic risk studies performed at continental scale (e.g. SARA; Villar-Vega et al 2017). Several models were tested against the data gathered for masonry buildings, and it was seen that some approximations could be used on average as adequate predictors for T_y.

Capacity curves of RC building typologies highlighted the importance of considering both the design code level (as an indicator for the global ductility and elastic stiffness) and the design ground motion intensity (as an indicator about the available lateral strength). The combined use of Code and PGA_{500} (or design lateral force) in the exposure model v0.1 was seen to be, therefore, an adequate strategy towards the development of models to be combined with exposure models with low resolution. However, as seen from the disaggregation results that were presented, increasing the resolution of the vulnerability model requires a higher resolution exposure model, namely including the mapping of both the design seismic hazard and design code levels, possibly using the year of construction to define mapping schemes, as summarised in the next section.

4   European Exposure Model Updates

The v0.1 European Exposure Model was developed considering ductility as an attribute of the building classes. As mentioned previously, the ductility was inferred from the level of seismic design used at the time of construction and the hazard level. In the v0.2 model that is currently being developed, a decision has been taken by the SERA team to replace the ductility attribute with the following two attributes (in particular for engineered buildings):

- Seismic design code level (CDN: pre-code, CDL: low code, CDM: moderate code, CDH: high code).
- Lateral load coefficient used in the seismic design.

This modification has been made to allow such information (that can be readily obtained by studying the evolution of seismic design codes within each country in Europe) to be explicitly used in the development of the fragility functions, as described further in the next section which outlines the SERA framework for fragility and vulnerability assessment. For a clearer explanation of how these attributes are defined, two examples of the evolution of seismic design codes (in Italy and Serbia) are provided in Crowley et al. (2019a; 2019b).

Although the use of the GEM Building Taxonomy and the addition of the aforementioned attributes leads to a closer match between the building classes in the exposure model and the vulnerability classes for which fragility and vulnerability functions are being produced, the experience obtained during the development of the Global Seismic Risk Map (v2018.1) has shown that it is difficult to obtain a one-to-one mapping. For example, in some countries the data available on the number of storeys is aggregated into groups, whereas the fragility and vulnerability models are developed for each number of storeys separately. Another example is where the material obtained from the census used to develop the exposure model is defined as 'other' or 'mixed' and so it could be mapped to a combination of the fragility and vulnerability models. Plans are currently underway to include a module in the OpenQuake-engine (which is being used for all of the European risk calculations, as described in Deliverable 26.7 – Crowley et al., 2019c) which allows to a one-to-many or many-to-one mapping of the building classes in the exposure model to the vulnerability classes used for the fragility and vulnerability models, with the aim that this will be implemented in time for the v1 European Seismic Risk Model that will be released in April 2020.

5   Proposed framework for seismic physical vulnerability assessment

Based on the review of past studies that was performed and on the improvements currently being made in the resolution of the exposure model for engineered buildings, a set of key points were identified for the definition of the framework for vulnerability analysis. Accordingly, the framework would have to be able to make a systematic many-to-one mapping of the multiple vulnerability classes (defined based on the complete taxonomy strings including all the attributes, as mentioned in Section 3) and the building classes in the exposure models. The design of these many-to-one mapping schemes to create vulnerability models is centred on the robust quantification of the building-to-building variability. This includes not only the general differences between buildings due to random factors such as designer or architectural options, but also the effect of the collapsed attributes, i.e. the variation of a fragility function due to the fact that many attributes that significantly change the seismic response are not known. Hence, the framework developed within the SERA project was envisioned to account simultaneously for the building-to-building variability and the record-to-record variability. Furthermore, it was developed to control and minimize epistemic uncertainties at several levels, namely by adopting

robust and generalized ground motion intensity measures (the average spectral acceleration, AvgSa, defined as the geometric mean of spectral acceleration values over a range of periods), by adding engineering judgement to the treatment and propagation of uncertainties, and by including procedures for validating the fragility and vulnerability models generated at several levels, as further detailed in Section 6. The following sections summarize the general and specific features of the framework, illustrating the proposed general workflow currently being developed for the SERA project that will lead to the final vulnerability and risk calculations (including all the validations and testing).

5.1 General features of the proposed framework

The developed framework builds upon the expandability and collapsibility of properties of the building taxonomy adopted for the Exposure models. Furthermore, it introduces all the source of uncertainty associated to the physical vulnerability assessment, at different scales, and accounts for the possible differences regarding the available information to simulate the seismic fragility. The general workflow of the methodology is shown in Fig. 39.
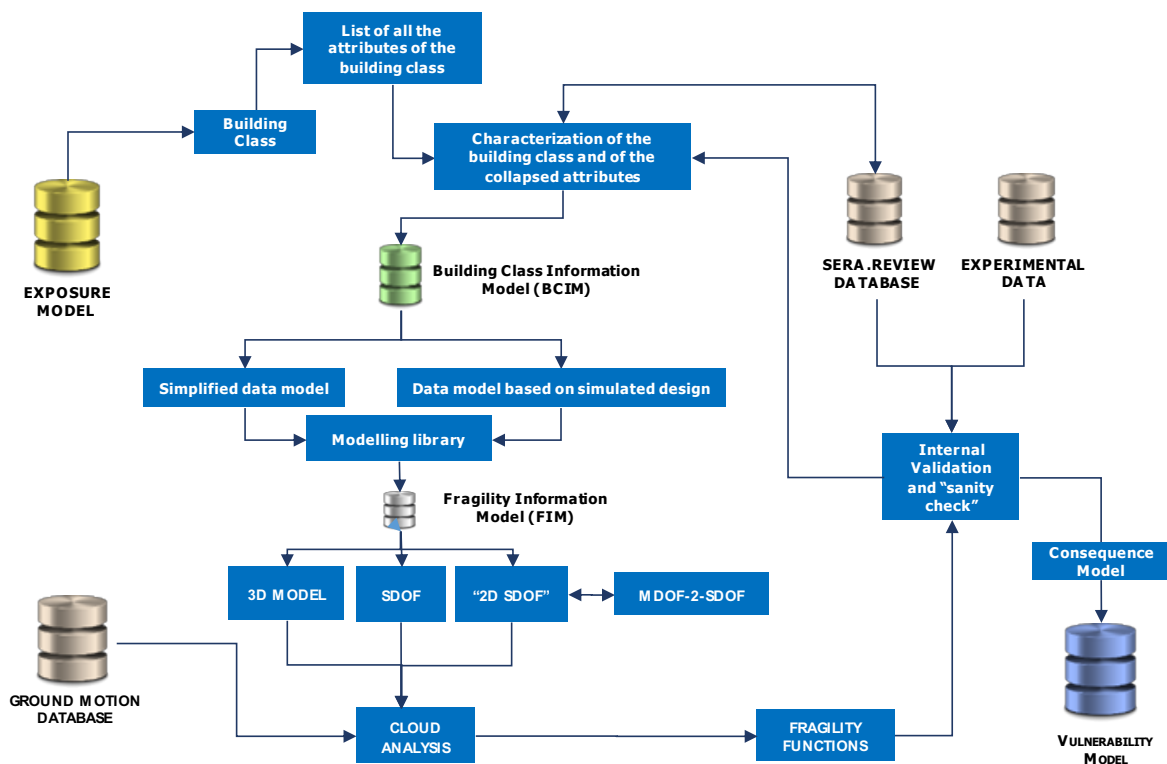
Figure 39. General workflow of the developed framework for seismic vulnerability analysis.

The basic workflow of the framework starts with the definition of the Building Class Information Model (BCIM). The BCIM includes the information that is necessary to compute the total variability of the fragility function associated to a building class. Inside the BCIM, the building class is characterized by its designation (collapsed taxonomy), the information about all the possible combinations of attributes that were collapsed (i.e. the many-to-one mapping of the multiple variants of the taxonomy string into the adopted building class taxonomy) and statistical information about the architectural properties and design assumptions. Furthermore, the BCIM also includes information available in the SERA.REVIEW database regarding the properties of the capacity curves and the attributes that were previously analysed. As an example, the adequacy of several period-height relationships adopted in the Martins

and Silva (2018;2019) repository was confirmed by the SERA.REVIEW database, thus pointing to the consistency of the capacity curves adopted therein and their adequacy to be included as simplified data models for residential buildings in the SERA framework.

Alternatively, the BCIM can include a set of probability distributions defining the geometry of the building and probabilities for the decision tree associated with design, as shown in Fig. 40 for the building class RES/RC/LFM/DUCL/H:4.
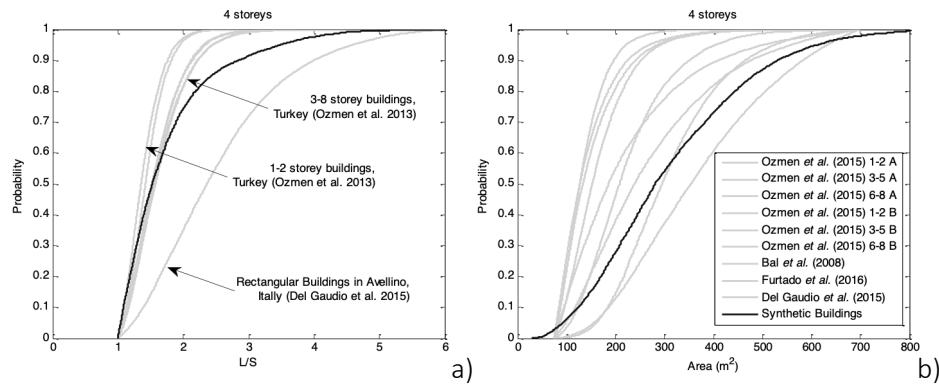

Figure 40. Representation of an example of a distribution of the ratio between the longer and the shorter in plan dimensions (a) and of the footprint area (b) of RES/RC/LFM/H4 buildings included in the BCIM compared with data collected from literature studies.

The propagation of the uncertainties and variability sources included in the BCIM to the fragility function is then performed by developing a set of realizations of the BCIM data that represent several possible building realizations of a given building class. Each realization is then analysed in the modelling module, where either a simplified or a complex model based on a simulated design approach are created. The information of these models is stored into the fragility information model (FIM). The FIM also includes a set of realizations of the BCIM data, each of which is defined by a numerical model and a set of seismic capacity variables derived from nonlinear static analysis. Hence, two types of FIM can be generated by the framework, depending on the type of data stored in the BCIM:

Type 1: The FIM is based on a simplified data model, and is based on the main principles used by Villar-Vega et al. (2017) and Martins and Silva (2018; 2019) to develop existing continental fragility functions. The BCIM information required for applying this method are approximations for the probabilistic capacity curve parameters and correlations (in the ADRS format) for the building class. Hence, a Type 1 FIM is made of sets of probabilistic SDOF model parameters based on information collected from existing studies (namely the SERA.REVIEW and the GEM Vulnerability database (Yepes-Estrada et al., 2016)), further calibrated using experimental data and expert judgement.

Type 2: The FIM is based on a simulated design approach (Verderame et al. 2010; Borzi et al. 2008b), thus targeting mainly engineered buildings (i.e. excluding the MUR building classes). By using statistical distributions for the architectural building parameters and defining the main design assumptions, a set of buildings can be designed for a given design code level (also connected to the age of the buildings considered for each building class). This design is also performed accounting for the seismicity of the site, which can be represented by a lateral load coefficient (β). After designing the buildings, a set of nonlinear models of the buildings are developed and nonlinear static analyses are performed. Hence, the data included in the FIM involves a set of nonlinear 3D models, their corresponding modal properties and statistical distributions of pushover curve parameters. The main steps of a simulated design procedure are defined in Fig. 40.
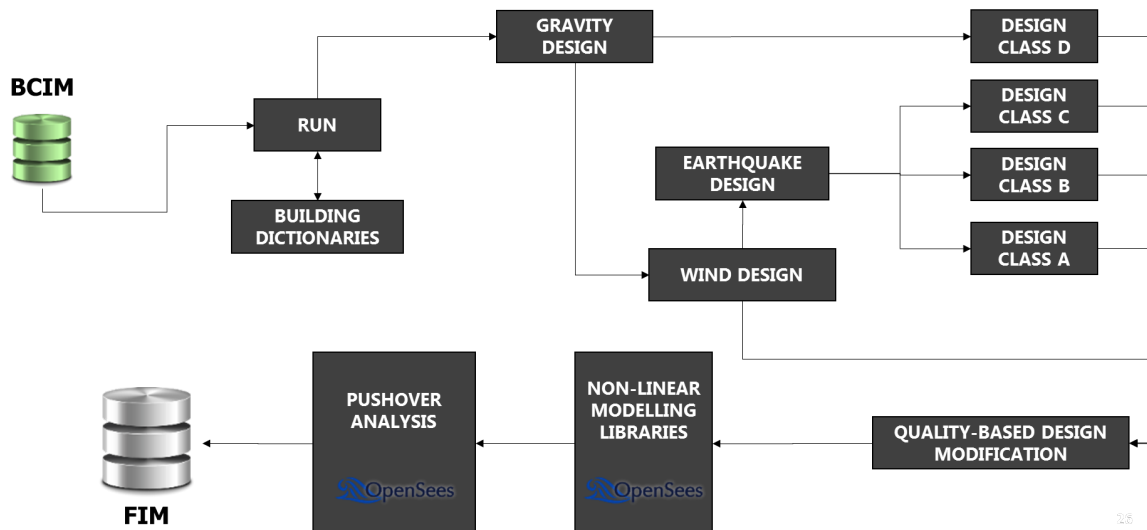
Figure 41. Workflow of the simulated design approach transforming the BCIM data into a Type 2 FIM.

As shown in Fig. 40, the transition between the BCIM and the FIM is defined by a set of design routines combined with a quality-based modification module. The design routines can either include solely gravity or wind design (e.g. for the case of IND/ST buildings where earthquake design is typically less relevant) or include a given class of earthquake design. As discussed in Section 4, four design classes were defined in the SERA framework: CDN, CDL, CDM and CDH. The simulated design philosophy for buildings of design class CDN targets older buildings, prior to the 1960s, and is based on allowable stresses and very low material strength values. The simulated design philosophy for buildings of design class CDL accounts for the seismic action by enforcing values of the seismic coefficient, β. Structural design is based on material-specific standards that use allowable stress design or a stress-block approach. Seismic design including modern concepts of ultimate capacity and partial safety factors is the basis of CDM, including an enhanced definition of material classes and failure modes. The seismic action is also accounted for in the design by enforcing values for the seismic coefficient, β. The ultimate capacity design approach and modern design strength values are adopted. Finally, CDH refers to modern seismic design principles that account for capacity design and local ductility measures, similar to those available in Eurocode 8. As mentioned before, the design classes (CD) are independent of the value of the seismic coefficient β. The fragility functions currently being developed use combinations of β (which can be defined across time and space in the pan-European region) and design code, and will be fully compatible with the Exposure model v0.2, and can also be mapped to the various ductility levels defined in the Exposure model v0.1 (based on PGA rather than on β).

After performing the simulated design, a quality-based modification of the original structure is introduced to account for the potential spatial irregularities (a key element identified by Maio et al., 2016) and existing damage due to aging. Essentially, the quality-based modification module defines, construction quality levels that accounts for the level of conformity of the construction with the design documents. The modified building designs are then transformed into nonlinear models using state-of-the-art modelling libraries.

Each realization of the FIM data model is then analysed using a record-to-record uncertainty propagation method (CLOUD analysis), either using a SDOF, a 2D SDOF or a full 3D MDOF, depending on the complexity of the building class and the existing degree of confidence in the more simplified modelling approaches. A database of recordings has been compiled for the nonlinear dynamic analyses using records with PGA above 0.05g in the European Strong Motion (ESM, Luzi et al., 2016a; 2016b) and the NGA (Chiou et al. 2008) databases, and a maximum scaling factor of 2. The cloud methodology

(see e.g. Jalayer and Cornell 2002) requires to define a best fit curve between the intensity measure level (IML) and an engineering demand parameter (EDP) in the logarithmic space (see Figure 42).

In numerical analysis it can occur that convergence is attained at levels of deformation for which the structure is so severely damaged that for all practical purposes a complete loss must be considered. These high levels of deformation levels are only reached due to limitations in the numerical models, thus including these points in the regression would result in bias in the fragility and vulnerability models. For this reason a censored regression (Schnedler, 2005) approach was followed with the threshold for the censored observations being set at 1.5 times the displacement for the complete damage state. Figure 42 also displays the differences between the regular and censored linear regressions. When applied to seismic fragility assessment, censored regression leads to a shift to the right on the complete damage fragility curve when comparing to the uncensored regression.

A number of different intensity measures can be considered in the regression. As mentioned previously, the SERA methodology proposes the use of AvgSa as it has been shown to be a sufficient intensity measure (e.g. Eads et al., 2015, Kohrangi et al., 2017a) and it also allows for a direct comparison between fragility functions which is useful for validation purposes (see Section 6.1). The AvgSa definition that has been used herein has been taken from the ground motion model of Kohrangi et al. (2017b) such that the resulting fragility functions can be used with this ground motion model (which is already implemented in the OpenQuake-engine, the software that will used for the European seismic risk assessment calculations, as described in Deliverable D26.7).
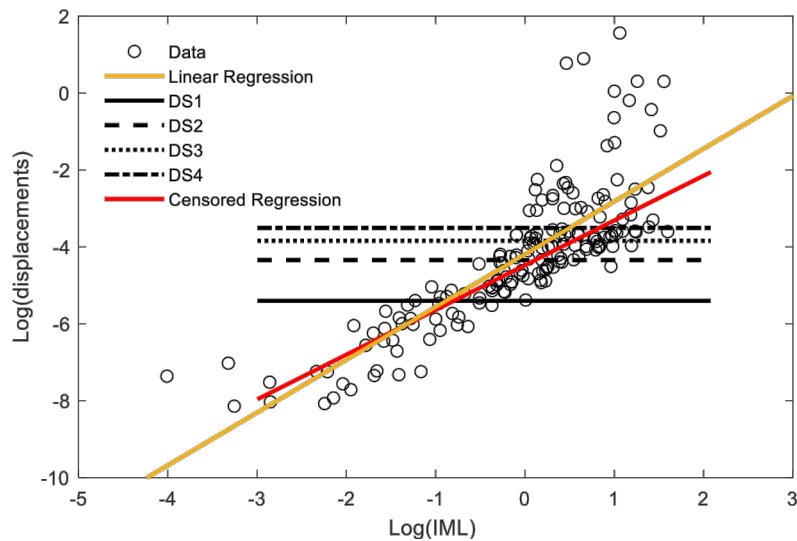
Figure 42. Example of censored regression analysis for MR/LWAL-CDN/H2

For developing fragility functions, the expected value of the natural logarithm of the displacement response (D) given the intensity measure level (IML), $\ln \eta_{D|IML}$, is modelled by the slope and intercept of the linear regression (Figure 42), and the probability of exceeding each damage state (P_{eDS}) is then calculated for a given level of intensity (IML) as follows:

$$P_{eDS} = 1 - \Phi\left(\frac{\ln(DL) - \ln \eta_{D|IML}}{\sigma}\right) \qquad (3)$$

where Φ is the cumulative standard normal distribution function, DL is the damage threshold displacement for each damage state and σ is the standard error of the regression, that can account for both the record-to-record variability and building-to-building variability.

Fragility functions are further checked according to a set of benchmark case studies to assess their conformity ('sanity checks" based on the comparison of fragility functions of different building classes, which is possible within the SERA framework due to the fact that AvgSa is used as a ground motion intensity measure) and their predictability capacity (comparing their results with real data from post-earthquake surveys). If a function provides adequate conformity and predictability levels, it is adopted as a good representation for the fragility of the building class under analysis. Otherwise, an iterative procedure starts that can involve increasing the complexity of the FIM data model and of the techniques used to include record-to-record variability. In case these measures are insufficient, modifications have to be made to the BCIM or FIM models.

5.2 Specific features of the proposed framework for residential masonry building classes

For masonry building classes, the FIM Type 1 approach described above has been used. Nonlinear time-history analyses are performed on equivalent SDOF oscillators, each of which is represented by the mean capacity curve. Given that masonry buildings have a reduction of stiffness due to cracking, a generic trilinear capacity curve has been assumed. The curves have been defined through the yield (Sd_y) and ultimate (Sd_{ult}) displacements and the elastic (T_1) and yield (T_y) periods, where T_y is considered to be double T_1 (Silva et al., 2015). In ADRS format (i.e. spectral displacement *vs* spectral acceleration) the mean capacity is estimated from the roof displacement (D_{roof}) of the multi-degree-of-freedom structure considering the relationships in Equation (1) and (2) presented previously in Section 3.1.
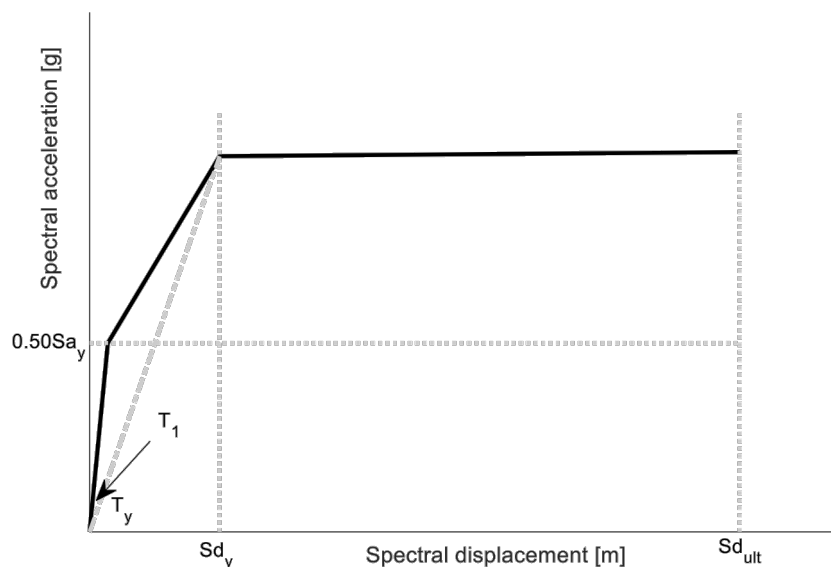
Figure 43. Generic capacity curve format used for masonry building classes

Table 6 lists the parameters used to define the capacity curves of each masonry building class (MUR: unreinforced masonry; MUR+STRUB: unreinforced masonry and rubble stone; MUR+STDRE: unreinforced masonry and dressed stone; MUR+CL99: unreinforced masonry with clay bricks; MUR+CB99: unreinforced masonry with concrete blocks; MUR+ADO: unreinforced masonry with adobe bricks; MR: reinforced masonry; MCF: confined masonry) resulting of the compilation of data coming from research studies and experimental campaigns. It is noted that all of the unreinforced masonry buildings are assumed to have no seismic design (CDN) whereas reinforced and confined masonry (MR and MCR) can either be CDN or CDL. The latter buildings are assumed in the exposure model to be located in the areas of a given country that have been classified as seismic zones. However, unlike for

reinforced concrete buildings, a lateral force coefficient is not assigned to these buildings but they are assumed to have a better performance compared to CDN buildings due to the culture of seismic design that will exist in seismically classified zones.

Table 6. Parameters used to compute masonry capacity curves

BUILDING CLASS	T_Y [S]	NO. OF STOREYS	YIELD DRIFT [%]	ULT. DRIFT [%]	REFERENCES
MUR/LWAL-CDN	$T_y = 0.062H^{0.9}$	1-5	0.14	0.60	Ahmad and Ali (2017); Bal et al. (2010); Borzi et al. (2008a); D'Ayala and Speranza (2003); Lagomarsino and Cattari (2014)
MUR+STRUB/LWAL-CDN	$T_y = 0.062H^{0.9}$	1-5	0.12	0.51	
MUR+STDRE/LWAL-CDN	$T_y = 0.062H^{0.9}$	1-5	0.13	0.54	
MUR+CL99/LWAL-CDN	$T_y = 0.065H^{0.9}$	1-5	0.13	0.57	
MUR+CB99/LWAL-CDN	$T_y = 0.065H^{0.9}$	1-5	0.16	0.69	
MUR+ADO/LWAL-CDN	$T_y = 0.066H^{0.9}$	1-3	0.12	0.55	
MR/LWAL-CDN	$T_y = 0.060H^{0.9}$	1-5	0.17	0.80	
MR/LWAL-CDL	$T_y = 0.058H^{0.9}$	1-5	0.20	0.90	
MCF/LWAL-CDN	$T_y = 0.044H$	1-6	0.19	0.90	Riahi et al (2009)
MCF/LWAL-CDL	$T_y = 0.042H$	1-6	0.24	1.00	
H – HEIGHT [M]					

In the proposed methodology for developing fragility functions, four damage states have been considered ranging from slight (DS1), to moderate (DS2), to extensive (DS3) to complete damage (DS4). To account for damage initiation in non-structural elements (e.g. infill walls), slight damage was assumed to begin at 75% of the yield displacement (Villar-Vega et al., 2017). Complete damage, requiring replacement of the building, is considered to be reached at the ultimate displacement capacity of the structure. The intermediate damage states (i.e. moderate (DS2) and extensive damage (DS3)) were considered evenly spaced between the first and last damage state as depicted in Fig. 44.
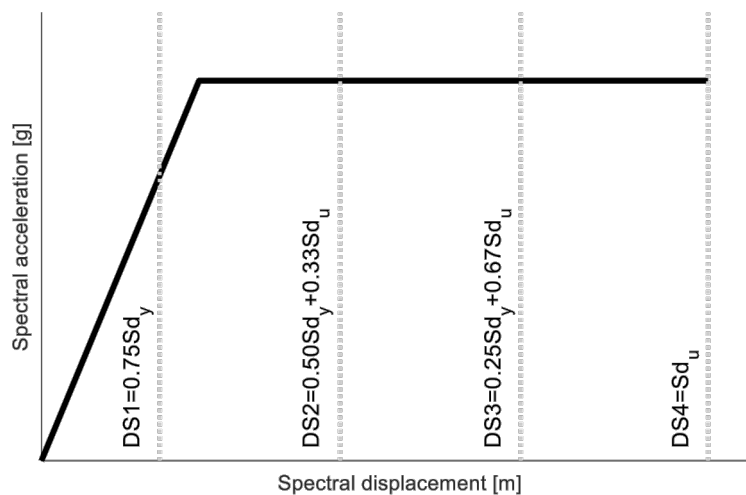
Figure 44. Damage thresholds

Fragility functions are developed considering the damage threshold displacements represented in Figure 44 for each damage state. In terms of parameter σ (see Eq. (3)), its value is defined by Eq. (4) considering that the standard error of the regression (see Figure 42) represents the standard deviation

due to record-to-record variability, σ_{RR}, directly modelled in a cloud analysis, and a standard deviation due to building-to-building variability, σ_{BB}, which has been assumed to be equal to 0.3 (e.g. Borzi et al., 2008a; FEMA 2004).

$$\sigma = \sqrt{\sigma_{RR}^2 + \sigma_{BB}^2} \qquad (4)$$

For masonry buildings, AvgSa is given by the geometric mean of spectral accelerations between 0.2T and 1.5T, where T is given as 0.5s. Figure 45 presents the fragility functions in terms of AvgSa for all masonry classes with two storeys.

Figure 45. Fragility functions for two storey European masonry building classes in terms of AvgSa

However, for compatibility with other ground motion models that will be implemented within the European Seismic Hazard Model (ESHM20) additional intensity measures of PGA, Sa(0.3s), Sa(0.6s) and

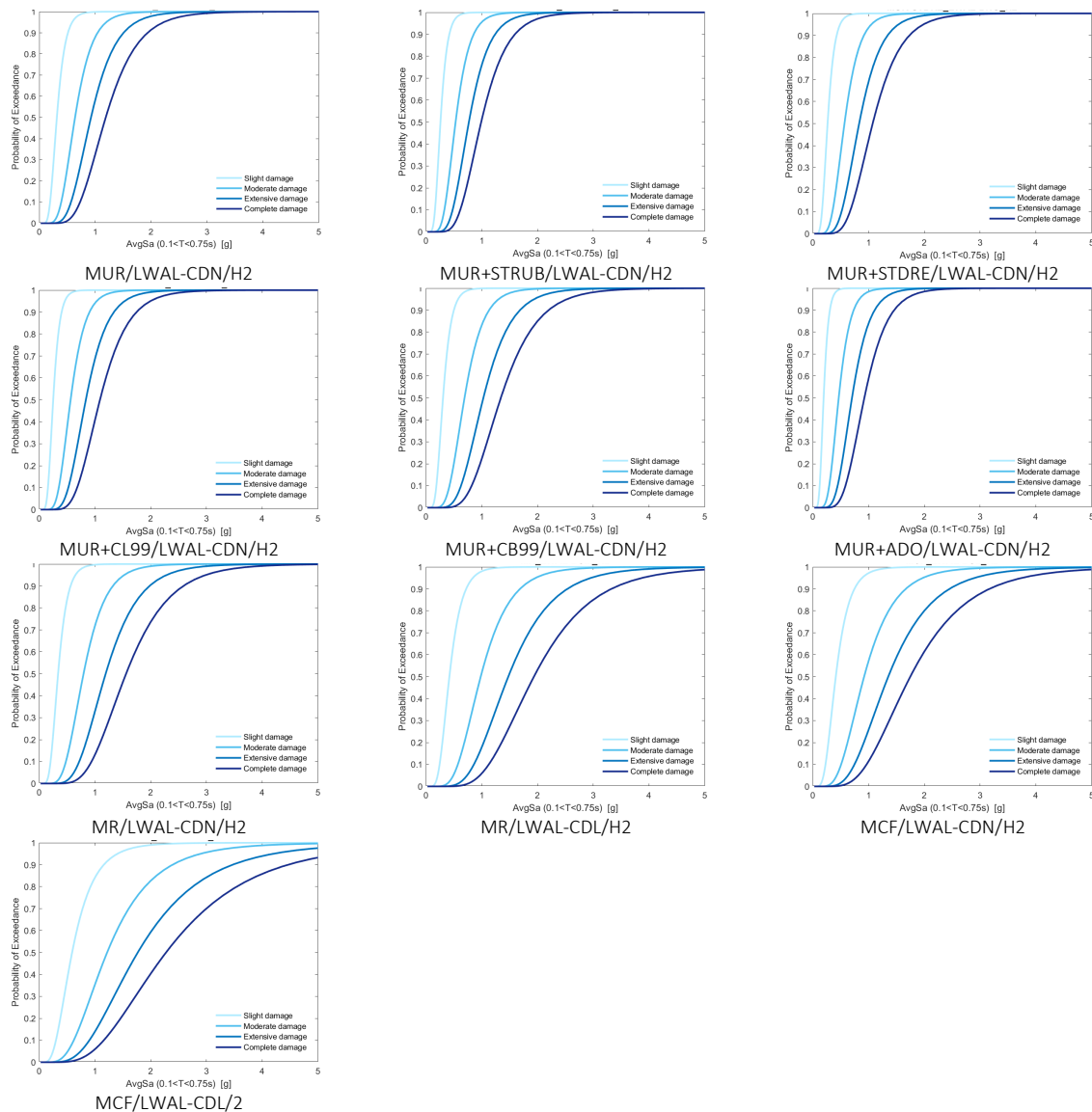Sa(1.0s) are also considered for the regression. The minimum distance between the yield period and the period used to estimate the IM determined the intensity measure to be used in the regression analysis.

5.3 Specific features of the proposed framework for residential reinforced concrete building classes

For RC building classes, both simplified data models and data models based on simulated design are being used in the framework. The simplified data models that are used to develop the Type 1 FIMs adopted in the analyses follow the observations made in the review, and are based on the parameters of the capacity curves calibrated by Martins and Silva (2018). Some of these parameters were seen to be in line with the statistical trends found in past studies (e.g. see Fig. 35). Table 7 shows the parameters used to compute RC capacity curves adapted from Martins and Silva (2018) and that incorporate the main conclusions extracted from the review presented in Section 3.

Table 7. Parameters used to compute RC capacity curves based on the simplified data models

BUILDING CLASS (EXPOSURE MODEL V0.1)	T_Y [S]	NO. OF STOREYS	YIELD DRIFT [%]	ULT. DRIFT [%]
CR/LFM/DUCL-SOS/H	$T_y = 0.10H$	1-12	0.73	1.20
CR/LFM/DUCL/H	$T_y = 0.10H$	1-12	0.73	3.00
CR/LFM/DUCM/H	$T_y = 0.07H$	1-12	0.75	3.20
CR/LFM/DUCH/H	$T_y = 0.07H$	1-12	0.77	3.40
CR/LFINF/DUCL/H	$T_y = 0.046H$	1-12	0.15	1.20
CR/LFINF/DUCM/H	$T_y = 0.044H$	1-12	0.20	1.35
CR/LFINF/DUCH/H	$T_y = 0.042H$	1-12	0.25	1.50
CR/LWAL/DUCL/H	$T_y = 0.032H$	1-12	0.17	1.10
CR/LWAL/DUCM/H	$T_y = 0.030H$	1-12	0.22	1.20
CR/LWAL/DUCH/H	$T_y = 0.028H$	1-12	0.28	1.30
CR/LDUAL/DUCL/H	$T_y = 0.036H$	1-12	0.17	1.16
CR/LDUAL/DUCM/H	$T_y = 0.034H$	1-12	0.21	1.28
CR/LDUAL/DUCH/H	$T_y = 0.032H$	1-12	0.26	1.40
H – HEIGHT [M]				

In the proposed methodology for developing fragility functions for RC buildings using Type 1 FIMs, the method of analysis mentioned in Section 5.1 and the damage models and strategies introduced in Section 5.2 for the assessment of masonry buildings are adopted. The damage model is anchored on the properties of the SDOF, resulting in different damage states when compared to those defined for masonry buildings. Following the principles outlined in Section 5.2, a σ_{BB} of 0.30 can be assumed to account for the building-to-building variability. For RC buildings, AvgSa was defined as the geometric mean of spectral accelerations between 0.2T and 1.5T, where T is set as 1.0s. Figure 46 presents the fragility functions in terms of AvgSa for the RC classes defined in Table 7.
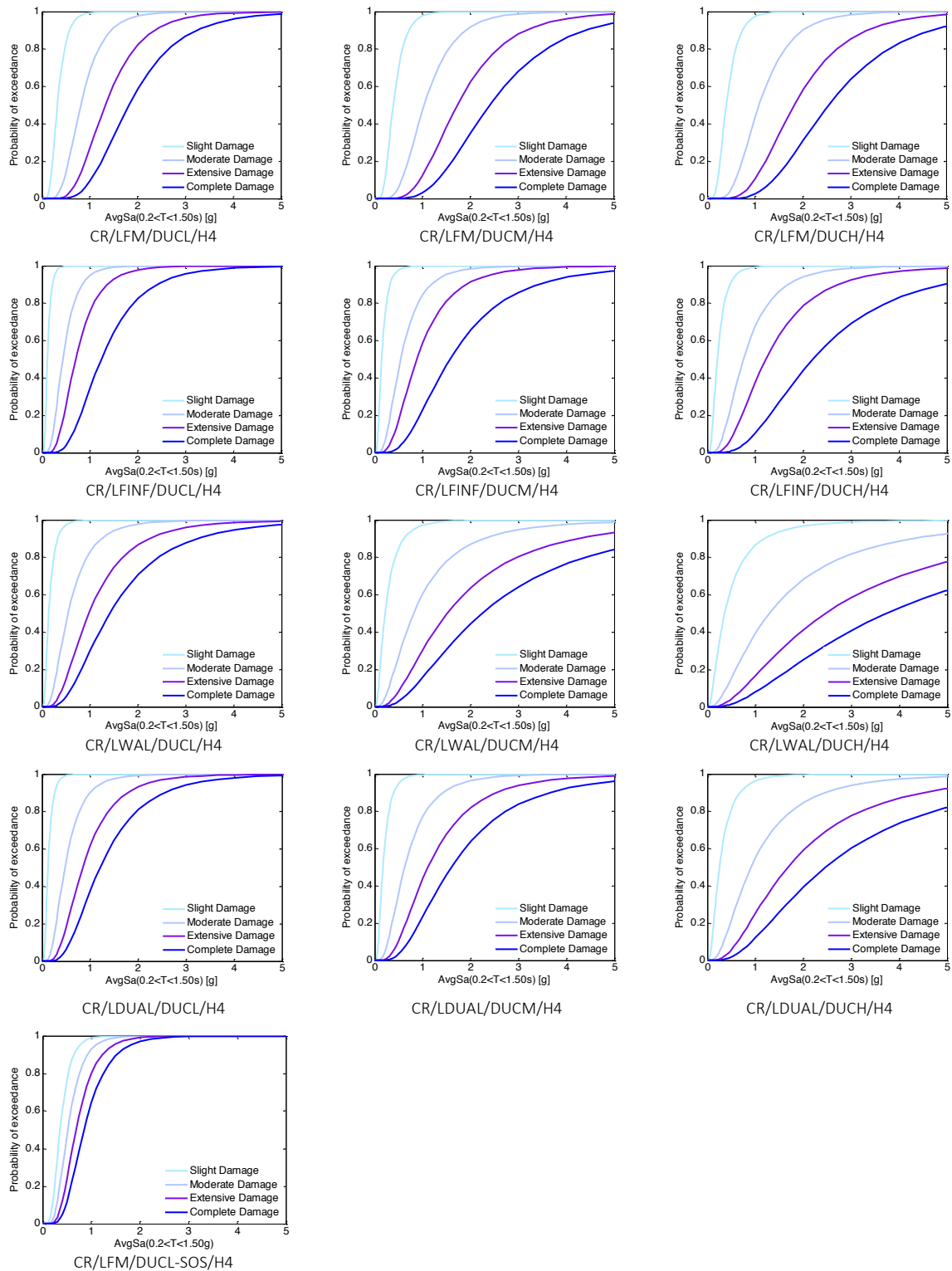
Figure 46. Fragility functions for four storey European RC building classes in terms of AvgSa

Complementary to the simplified data models that are used to compute fragility functions based on the nonlinear time history analysis of equivalent SDOF models, an additional strategy was also developed to improve the resolution of the exposure model by disaggregating the DUCL, DUCM and DUCL into multiple design code classes and include multiple values for the lateral load coefficient, β. The strategy uses a data model based on a simulated design approach. In this case, the derivation of the BCIM data is based on the definition of a set of random generators and decision-tree processes. The random

generators include a set of probabilistic models representing the general characteristics of the building stock. The decision-trees include the correlations between some of these random properties and other characteristics often used to reflect the assumptions made during a design process. An illustration of the decision-tree process is presented in Fig. 47.

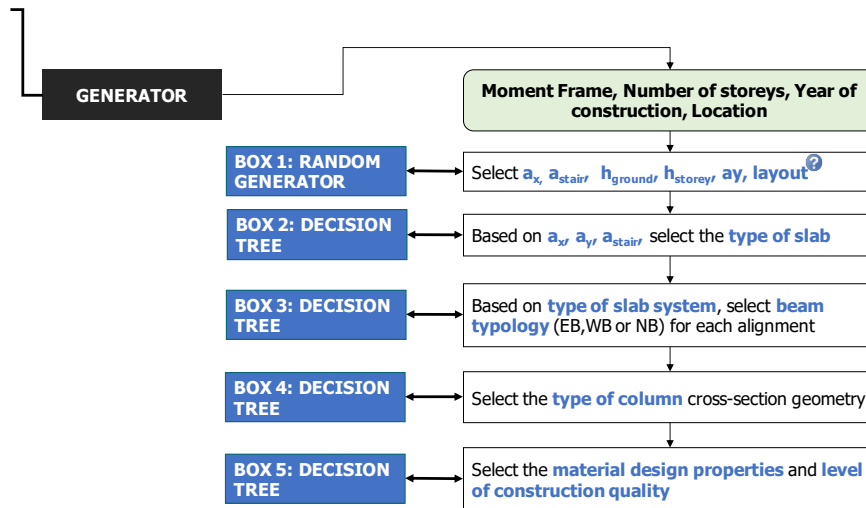Figure 47. Workflow of the simulated design approach transforming the BCIM data into a Type 2 FIM.

After creating the global taxonomy string of each building, that includes all the features needed to start the design process, design routines are called to design each building according to the design code class and the selected value of β. Mapping schemes are also used to define β values based on modern code response spectra including local soil effects. Four design classes were defined based on the historical evolution of RC seismic design and based on an extensive survey whose results are illustrated in Crowley et al (2019b). The simulated design philosophy for buildings of design class CDN targets older buildings, prior to the 1960s, and is based on allowable stresses and very low concrete strength values. The simulated design philosophy for buildings of design class CDL includes the seismic action by enforcing values of the seismic coefficient, β. RC design is based on material-specific standards that consider allowable stress design or the stress-block approach, and global ductility is not considered in the seismic design (i.e. elastic analysis considering a q-factor of 1.0). For class CDM, seismic design includes modern concepts of ultimate capacity and partial safety factors, and an enhanced definition of material classes and failure modes. The seismic action is included in the design by enforcing values of the seismic coefficient, β. RC design is based on the ultimate capacity approach and modern design strength values. Older reinforcing smooth steel bars and/or low steel yield strength values are not used. Global ductility is considered in the seismic design (i.e. considering a q-factor close to 2.5) but no capacity design procedures are involved. Brittle shear failures are avoided as a result of the adopted design strength models. Finally, CDH refers to modern seismic design that includes capacity design procedures and stringent local ductility measures (i.e. similar to the Eurocode 8 procedure). RC design is based on the ultimate capacity approach and modern design strength values, namely steel of class S500 is generally adopted for the reinforcement. Global ductility is considered in the seismic design (i.e. considering a q-factor of 3.5 or above) and it is guaranteed by adopting stringent local ductility detailing rules and by applying capacity design procedures. After performing the simulated design, a quality-based modification of the structure is carried out to account for the potential spatial irregularities (a key element identified by Maio et al., 2016). Essentially, the quality based modification module defines construction quality levels that accounts for the expected real values of the stirrup spacing (s_w), the concrete strength (f_c) and the reinforcing steel yielding strength (f_y). Geometric properties are assumed

to be the same as the design values. Figure 48 shows the adopted strategy that accounts for the quality level assigned to the referred building properties.
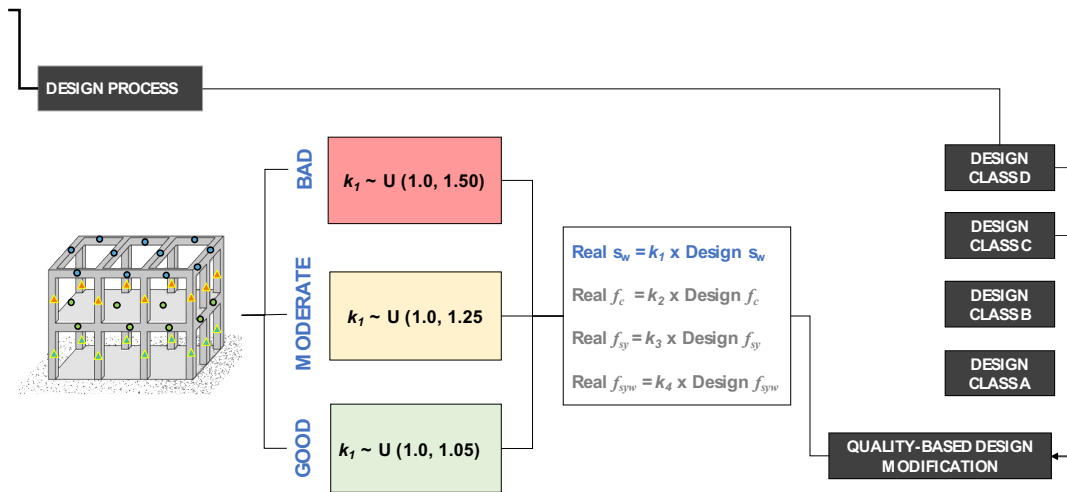

Figure 48. Workflow of the quality-based design modification for RC residential buildings.

The specific methodology developed to compute fragility functions of RC buildings considers adequate nonlinear modelling strategies to simulate the dominant failure modes of the buildings belonging to the design classes previously defined. The main features of the framework for developing the vulnerability model involve performing pushover analysis and creating probabilistic 2D SDOFs representing the response of the building in its two main orthogonal directions. As a result, the FIM data involves a correlation matrix and a set of probability distributions for the capacity curve parameters of the two main orthogonal directions of the building class, developed explicitly using the BCIM and the simulated design routines to calibrate the simplified models. Therefore, the main difference between the new vulnerability modelling strategy and that of the simplified FIM data models is that the probabilistic models (including an explicit definition of σ_{BB}) are directly derived from 3D models and that 3D effects are indirectly accounted for by using the 2D SDOF approach.

To further complement the outputs of the framework, these fragility functions will be compared to the fragility functions obtained from the simplified data models of Table 7. This comparison will map the DUCL, DUCM and DUCH attributes to the new design classes and β coefficients and enable these simplified models to be used in the future.

5.4 Specific features of the proposed framework for industrial steel building classes

For industrial ST building classes, data models based on simulated design are being used in the framework given the significant lack of data in the literature regarding simplified data models for these building typologies. The justification for this can be found on the inherent structural characteristics of industrial steel buildings that are typically composed by different LLRSs in the two main orthogonal directions. As an example, steel portal frame buildings are composed of moment-resisting frames in the transverse direction whereas the lateral resistance in the longitudinal direction is provided by a concentrically-braced system. Other factors, such as the flexibility of the roof structural system and the presence of cranes, which result in structural in-plan irregularities, justify the need to resort to robust numerical models that are able to account for the 3D behavioural effects. In addition, it is important to refer that, to fully represent a Type 2 FIM, the seismic vulnerability analysis of industrial ST buildings

should take into account losses due to damage on both non-structural components and contents. This requires reliable consequence models that are still unavailable in the literature.

Similar to the approach adopted for the RC building classes, the derivation of the BCIM data is based on the definition of a set of random generators and decision-tree processes. The random generators include a set of probabilistic models representing the general characteristics of the industrial ST building stock. The decision-trees include the correlations between some of these random properties and other characteristics often used to reflect the assumptions made during a design process. An illustration of the decision-tree process is presented in Fig. 49.
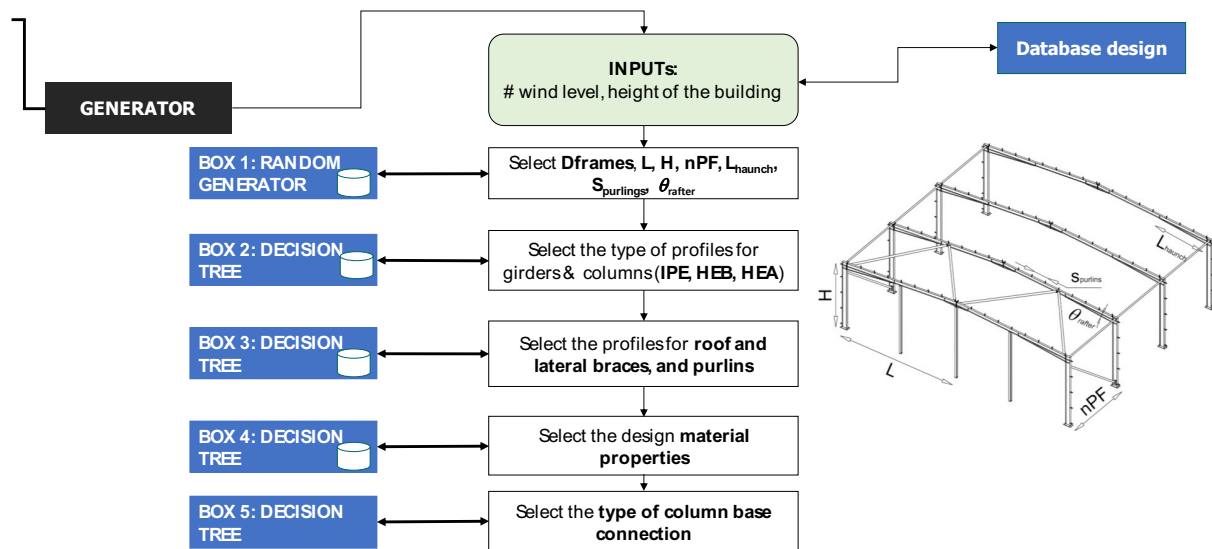
Figure 49. Set of random generators and decision-tree processes considered for the industrial ST buildings.

As shown in Fig. 50, the design process that follows the creation of the global taxonomy string of each industrial ST building involves the gravity and wind load design of each realization of the building class. It is important to note that seismic design is not performed given the fact that this action does not typically govern the sizing of the members. The lateral stiffness and resistance of the building is governed, therefore, by gravity and wind load design requirements.

Figure 50. Workflow of the simulated design approach transforming the BCIM data into a Type 2 FIM.

The fragility analysis that follows the design process involves the development of a 3D numerical model of each realization of the industrial ST building class. Special attention is devoted to the simulation of the structural components where inelastic behaviour is expected to occur, namely the beam and column members, the bracing components and the gusset plate, and the column base connections. State-of-the-art models are adopted to represent the behaviour of these components in the model.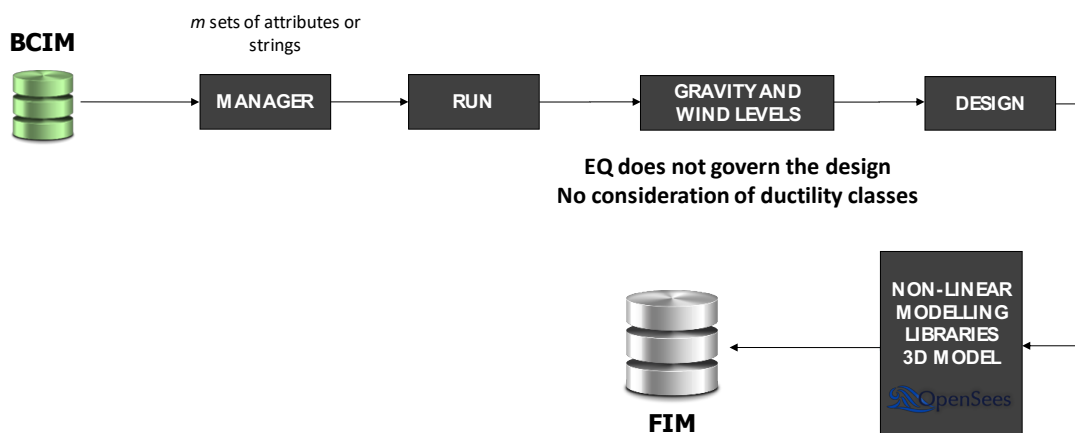 Fragility functions are then derived based on the results of response-history analyses that are performed using CLOUD analysis to account for record-to-record variability.

As referred before, the damage evaluation should consider not only the limit states associated to damage in structural elements, which are explicitly simulated in the numerical model, but also the damage that is estimated to develop in non-structural components and that is induced to contents. To this end, the procedure proposed in HAZUS – MH MR5 is adopted. According to this guideline, non-structural components are divided into two groups: drift-sensitive and acceleration sensitive components. The threshold drift and acceleration limits prescribed in the guideline for three different limit states, namely damage limitation, significant damage and near collapse, are adopted.

5.5   Fragility functions for remaining European building classes

The previous sections have outlined the proposed SERA framework for developing fragility models for European buildings, and a few example fragility functions have been provided. The aim of the coming months will be to apply the framework to a larger number of reinforced concrete frame, steel frame and masonry building classes to increase the coverage of the building classes within the European Exposure Model.

During this period, risk calculations at the European scale will also be undertaken in preparation for the European Risk Workshop, which is planned to take place in Istanbul in September 2019. For any building classes for which SERA fragility models are not yet available (which is likely to be the case for industrial precast reinforced concrete post and beam buildings and residential/commercial reinforced concrete dual frame-wall buildings), the SDOF models developed by Martins and Silva (2018; 2019) and described in Section 3.1 will be used, given that they have already been employed in a risk assessment covering Europe. In order to make them compatible with the framework described herein, the fragility functions for these SDOF models will be re-derived using the same set of records presented previously and using the same intensity measures. Over the course of the final year of the SERA project, the aim will be to replace these simple SDOF models with more refined models developed following the SERA framework described herein.

5.6   Consequence models

Consequence models, or damage-to-loss models, are used to transform the fragility functions (which describe the probability of reaching or exceeding a set of damage states, conditional on a level of ground motion), to vulnerability functions (that provide the distribution of loss ratios conditional on a level of ground motion). The losses that will be considered in the European Seismic Risk Model will be direct economic loss due to structural and non-structural damage (and thus the loss ratios will represent the ratio of cost of repair to cost of replacement of the buildings) and fatalities (and thus the loss ratios will represent the ratio of the number of fatalities to the number of occupants of the buildings).

Converting the fragility functions into vulnerability curves is performed with damage-to-loss models that provide an estimate of the mean ratio of the cost of repair to the cost of replacement for each

damage state. Several analytical tests (Yepes-Estrada et al., 2016) and evaluated claims data been studied by have shown that 5%, 20%, 60% and 100% seem to be realistic (Martins and Silva, 2019).

Table 8. Damage-to-loss model used to derive vulnerability functions in terms of direct economic loss

DAMAGE STATE	MEAN LOSS RATIO [%]
Slight damage (DS1)	5
Moderate damage (DS2)	20
Extensive damage (DS3)	60
Complete damage (DS4)	100

An approach that estimates the fatality risk from the probability of collapse of buildings is being used in the SERA methodology given that it has been observed in past earthquakes that the number of earthquake shaking casualties is driven by the number of buildings that fully or partially collapse, as this is directly linked to the percentage of occupants trapped in the building (Figure 51).

Damage Level: **D5 Collapse**Extent of Collapse: 10% of Volume**M3** (Occupants Trapped) : 10%

Damage Level: **D5 Collapse**Extent of Collapse: 50% of Volume**M3** (Occupants Trapped) : 37.5%(50% of ground floor occupants assumed escaped

Damage Level: **D5 Collapse**Extent of Collapse: 100% of Volume**M3** (Occupants Trapped) : 75%(50% of ground floor occupants assumed escaped before collapse)

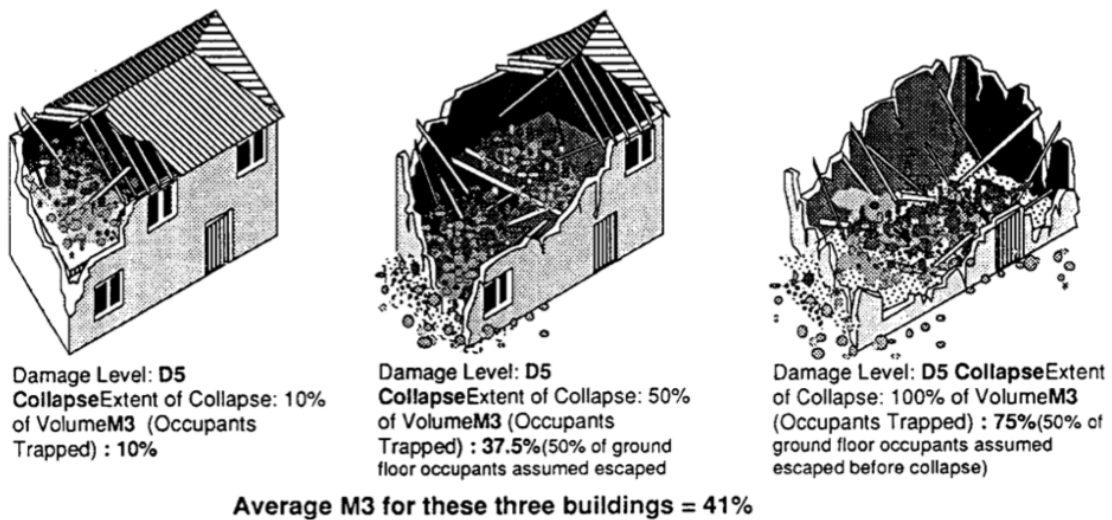**Average M3 for these three buildings = 41%**

Figure 51. Illustration of extent of collapse and its effect on M3 (Coburn et al., 1992)

The fatality vulnerability model is defined as the mean probability of loss of life, given a level of ground shaking. Fatality models for each building class are being developed in SERA by combining the DS4 (i.e. complete damage) fragility functions ($P_{DS \geq DS4|IML}$) with the mean probability of loss of life, given collapse ($P_{LL|DS5}$) and the probability of collapse given that the damage reaches or exceeds DS4 ($P_{DS5|DS \geq DS4}$):

$$P_{LL|IM} = P_{DS \geq DS4|IML} \times P_{LL|DS5} \times P_{DS5|DS \geq DS4} \qquad (5)$$

The mean probability of loss of life, given collapse ($P_{LL|DS5}$) for different building classes can be obtained from various empirical sources (e.g. So and Pomonis, 2012; FEMA, 2004; Coburn and Spence, 2002; Coburn et al. 1992) and new models are currently being developed with fatality and damage data that has been provided by Antonios Pomonis (personal communication). The probability of collapse given DS4 is reached/exceeded can be obtained from damage databases such as the Da.DO database of building-by-building damage data from Italian events (DPC 2018) as well as the aforementioned data provided by Antonios Pomonis. The Da.D.O. database provides a description of the extent of collapse

to vertical, horizontal and roof elements of the buildings, and an investigation into which collapse mechanism correlates best with fatalities will be undertaken. Also, the influence of ground shaking intensity on the probability of collapse, given DS4 is reached/exceeded ($P_{DS5|DS \geq DS4}$)will also be studied with these databases.

6 Procedures to validate fragility and vulnerability functions

Now that the framework for the development of European fragility and vulnerability functions has been finalised, and initial models are being developed, the next step that will be undertaken during the final year of the project will be to test the models using existing studies and empirical damage and loss data. The following sub-sections summarise some of the activities that are planned to test and evaluate the European fragility and vulnerability functions.

6.1 Internal validation and comparison with existing models

An important check that is needed before a set of fragility and vulnerability functions are employed within a seismic risk assessment is an internal validation or 'sanity check'. Although the European seismic risk calculations may need to be undertaken using the fragility and vulnerability functions that were presented previously in terms of spectral ordinates, the simultaneous development of these models also in terms of AvgSa will allow all functions to be directly compared. Such comparison is important to make sure that the relative fragility between different construction materials and lateral load resisting systems matches engineering judgment and observations from past European earthquakes. As an example, Figure 52 presents a comparison of the complete damage masonry fragility functions that were presented previously in Figure 45 and it shows that the trend of fragility is as expected – the most fragile is the adobe building class, and the least fragile is the low code confined masonry. Also, the unreinforced masonry building classes are all more fragile than the reinforced masonry classes.
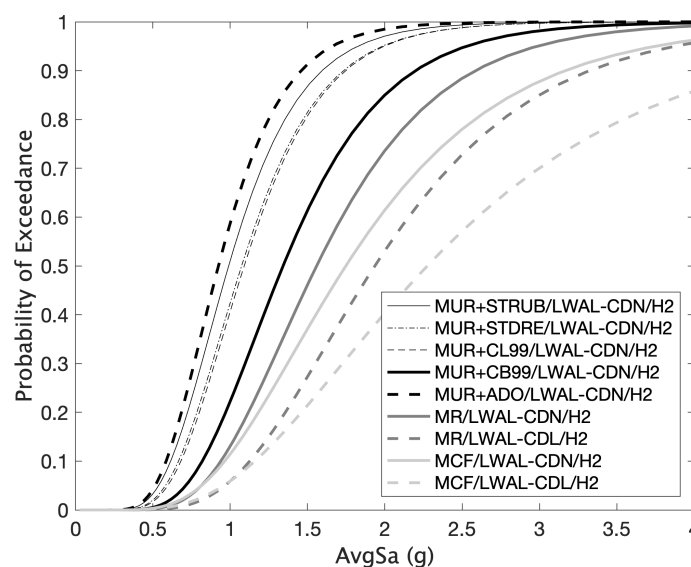

Figure 52. Comparison of the complete damage fragility functions from Figure 45

Furthermore, a comparison with a selection of the existing fragility and vulnerability functions included in SERA.REVIEW and presented in Section 3 will be carried out to make sure that the proposed models are in line with previous studies carried out in Europe. However, differences with respect to past studies are expected given that many of the models in the academic literature have not been calibrated or tested using past earthquake damage and loss data, as described in the next section. Hence, although comparisons with existing models is important as a preliminary step towards validation, it is even more important to make sure that the proposed models are tested against empirical data, as described in the next section.

6.2   Testing and evaluation using empirical damage and loss data

In order to compare the proposed vulnerability models for economic loss and fatalities for a given country with empirically derived models, a mean vulnerability function calculated through an exposure-weighted combination of all the building classes in the country will be undertaken. These vulnerability functions (in terms of both economic loss and fatalities) can then be compared with the empirical models developed by PAGER (Jaiswal et al., 2009; Jaiswal and Wald, 2013). The latter models are in terms of MMI and so, for comparison purposes, all models should be transformed to PGA (or another common intensity measure). The PAGER functions can be transformed to PGA using ground-motion conversion equations (GMICE) whereas the fragility functions can be transformed to PGA based on the relationship between Sa(T) and PGA or AvgSa and PGA as observed in the database of records used for the nonlinear dynamic analyses. Figure 53 shows an example comparison of the mean vulnerability function based on GEM's analytical vulnerability model in terms of fatalities (Section 3.3.3) with PAGER's empirical model for Turkey. It is noted that the Faenza and Michelini (2010) GMICE was used for this comparison and the uncertainty in the conversion as not accounted for, but should be accounted for in the future.
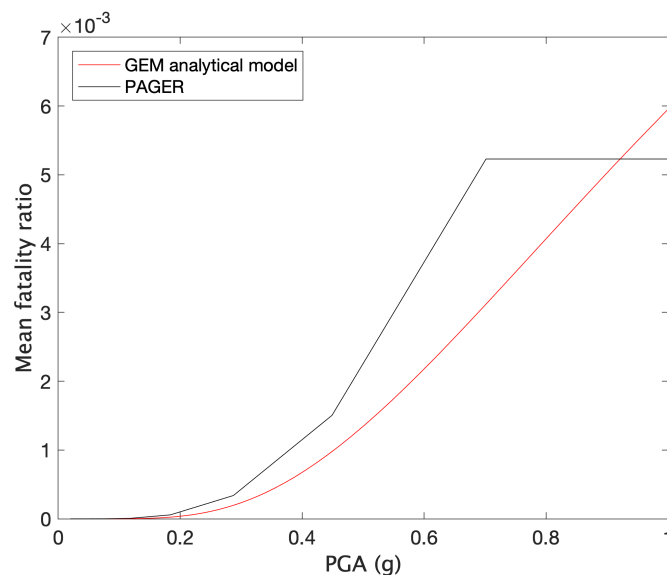
Figure 53. Example comparison of analytical mean vulnerability function for Turkey compared with the PAGER empirical model for fatalities (Jaiswal et al., 2009)

The existing fragility and vulnerability functions developed by GEM and introduced in Section 3.3.3 have been tested using damage and loss data from global past events between 1980 and 2017 from the NatCatService database (MunichRe, 2019). In this process, USGS ShakeMaps were used with the global exposure dataset and the fragility and vulnerability functions in order to estimate the number of

collapsed buildings and direct economic losses, respectively. The framework employed for these calculations is described in Silva and Horspool (2019). A comparison between the estimated and observed losses (adjusted to 2017) for just the European events is depicted in Figure 54. Although a fair agreement between the estimated and observed losses was obtained (with limited bias), there is clearly a large dispersion in the results. Reasons for this variability include differences in the exposure model and the actual built environment, bias in the collection of the observed damage and losses, and large uncertainty in the ground shaking due to lack of recording stations in the affected region (e.g. Villar-Vega and Silva 2017). Such analyses will be repeated with the updated vulnerability models presented herein, once they have been extended to cover all building classes in the updated exposure model.
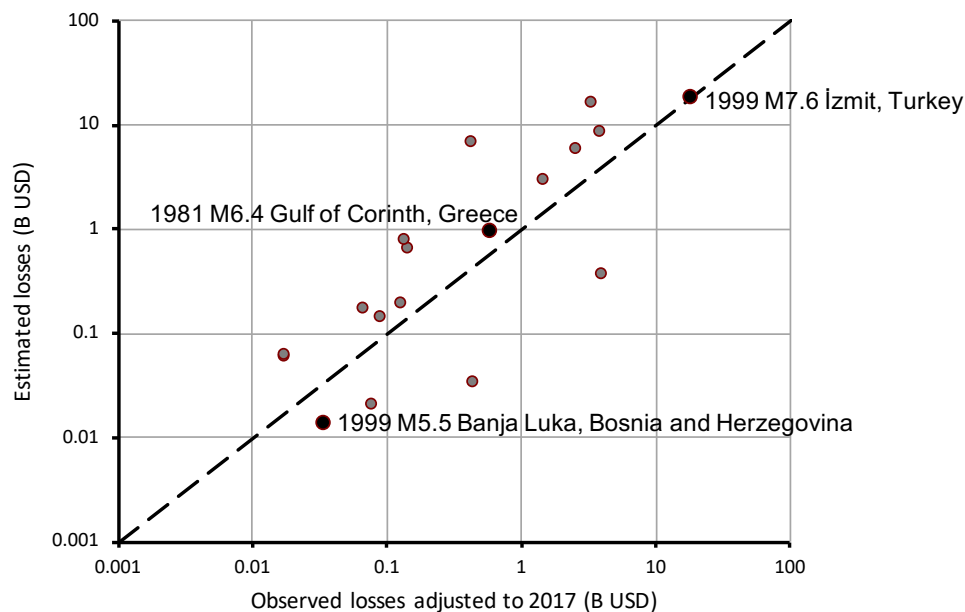

Figure 54. Comparison between estimated and observed losses for over 20 past events in Europe.

Other tests that will be carried out using the Silva and Horspool (2019) framework will be to check predicted damage distributions for specific events against the observed damage distributions. A large database of building-by-building damage data from Italian events (http://egeos.eucentre.it/danno_osservato/web/danno_osservato) is available for this purpose, but as it only includes damaged buildings, and so further elaboration of the database will need to be undertaken in order to include the undamaged buildings. Other partners of the SERA JRA4 team are also working on collecting damage and exposure data related to past events across Europe (e.g. 1976 Thessaloniki earthquake, 1999 Kocaeli earthquake) for further tests of the fragility and vulnerability models.

7 Concluding remarks

A thorough review of the attributes that influence the performance of buildings has been undertaken in this deliverable in order to identify the characteristics that are not accounted for in exposure modelling (by collapsing attributes in the building taxonomy), and that thus need to be included in the vulnerability assessment. Through this review, a number of attributes have been identified that should (and will) be included in future updates to the GEM Building Taxonomy (Brzev et al., 2013; Silva et al., 2018).

A summary of the current status of capacity, fragility and vulnerability modelling in Europe has also been undertaken thanks to the development of the SERA.REVIEW database. Through the subsequent

post-processing of the gathered data, the effect of collapsing attributes in the taxonomy was analysed on both the fragility functions and the capacity curves, and a set of statistical distributions that could be used to develop consistent vulnerability models for pan-European building classes was tentatively made. These analyses thus formed the basis of the framework proposed herein for the development of fragility and vulnerability models for the European Seismic Risk Model (ESRM20).

During the last 12 months of the SERA project, risk calculations at the European scale will be undertaken with preliminary results being presented at the European Risk Workshop, which is planned to take place in Istanbul in September 2019. Some preliminary fragility functions based on the proposed framework have been presented herein, and over the coming months the aim will be to expand these to cover all of the building classes in the exposure model, and to replace where possible the Type 1 analyses (that use simple SDOF models) with Type 2 (and thus more refined) models, as per the framework described herein. Finally, a significant effort will be placed on validation of the models based on 'sanity checks' and empirical damage and loss data.

8   References

Ahmad, N., Ali, Q. (2017) Displacement-based seismic assessment of masonry buildings for global and local failure mechanisms, *Cogent Engineering*, 4(1).

Alderighi E., Bayo E., Bianco L., Braconi A., Coscetti C., Dall'Asta A., Filippuzzi P., Fulop L., Gracia J., Hoffmeister Hradil P.B., Karamanos S., Leoni G., Mallardo R., Moller S., Osta A., Salvatore W., Tsintzos P., Varelis G., Vasilikis D. (2010) PREfabriCAted STEEL structures for low-rise buildings in seismic areas. RFSR-CT-2007-00038 project. Final report, European Commission, Brussels.

Araújo, M. (2018) Seismic Safety and Risk Assessment of Existing Steel Buildings. PhD Dissertation. University of Porto, Portugal.

Babič, A., Dolšek, M. (2016) Seismic fragility functions of industrial precast building classes. Engineering Structures, 118, 357-370.

Balkaya, C., Kalkan, E. (2004) Seismic vulnerability, behaviour and design of tunnel form building structures. Engineering Structures, 26(14), 2081-2099.

Bal, I. E., Crowley, H., Pinho, R. (2008) Displacement-based earthquake loss assessment of Turkish masonry structures. In Proceedings of the 14th world conference of earthquake engineering (WCEE), Beijing, China.

Bal, I.E., Crowley, H., Pinho, R., Gulay, G. (2008) Detailed assessment of structural characteristics of Turkish RC building stock for loss assessment models. Soil Dynamics and Earthquake Engineering 28, 914–932.

Bal I.E., Bommer J.J., Stafford P.J., Crowley H., Pinho R. (2010) The influence of geographical resolution of urban exposure data in an earthquake loss model for Istanbul, *Earthquake Spectra*, 26(3), 619-634.

Beilic, D., Casotto, C., Nascimbene, R., Cicola, D., Rodrigues, D. (2017) Seismic fragility curves of single storey RC precast structures by comparing different Italian codes. Earthquakes and Structures, 12(3), 359-374.

Borzi, B., Crowley, H., Pinho, R. (2008a) Simplified Pushover-Based Earthquake Loss Assessment (SP-BELA) Method for Masonry Buildings. International Journal of Architectural Heritage, 2(4), 353-376.

Borzi, B., Pinho, R., Crowley, H. (2008b) Simplified pushover-based vulnerability analysis for large-scale assessment of RC buildings. Engineering Structures, 30(3), 804-820.

Brzev, S., Scawthorn, C., Charleson, A.W., Allen, L., Greene, M., Jaiswal, K., Silva V. (2013) GEM Building Taxonomy Version 2.0, GEM Technical Report 2013-02 V1.0.0, 188 pp., GEM Foundation, Pavia, Italy, doi: 10.13117/GEM.EXP-MOD.TR2013.02.

Calvi, G. M., Pinho, R. (2004) LESSLOSS: a European integrated project on risk mitigation for earthquakes and landslides. University of Pavia, Structural Mechanics Department.

Caprio M., Tarigan B., Worden C.B., Wiemer S., Wald D.J. (2015) Ground motion to intensity conversion equations (GMICEs): A global relationship and evaluation of regional dependency, *Bulletin of Seismological Society of America*, 105(3), 1476-1490.

Casotto, C., Silva, V., Crowley, H., Nascimbene, R., Pinho, R. (2015) Seismic fragility of Italian RC precast industrial structures. Engineering Structures, 94, 122-136.

CEN (2004) Eurocode 8: Design of structures for earthquake resistance - Part 1: General rules, seismic actions and rules for buildings. Comité Européen de normalization, Brussels, Belgium.

Chiou, B., Darragh, R., Gregor, N., Silva, W. (2008) NGA project strong-motion database, Earthquake Spectra 24, 23–44.

Coburn, A., Spence, R. (2002) Earthquake Protection, 2nd Edition, John Wiley & Sons Ltd, Chichester.

Coburn, A., Spence, R., Pomonis, A (1992) Factors Determining Casualty Levels in Earthquakes: Mortality Prediction in Building Collapse, Proceedings of the 10th World Conference on Earthquake Engineering, Madrid, Spain.

Colombi, M., Borzi, B., Crowley, H., Onida, M., Meroni, F., Pinho, R. (2008) Deriving vulnerability curves using Italian earthquake damage data, Bulletin of Earthquake Engineering 6(3), 485–504.

Crowley H., Pinho R. (2004) Period-height relationship for existing European reinforced concrete buildings, Journal of Earthquake Engineering, 8, Special Issue 1, 93-119.

Crowley, H., Borzi, B., Pinho, R., Colombi, M., Onida, M. (2008) Comparison of two mechanics-based methods for simplified structural analysis in vulnerability assessment. Advances in civil Engineering, 2008, 438379.

Crowley H., Colombi M., Silva V. (2014) Epistemic Uncertainty in Fragility Functions for European RC Buildings. In: Pitilakis K., Crowley H., Kaynia A. (eds) SYNER-G: Typology Definition and Fragility Functions for Physical Elements at Seismic Risk. Geotechnical, Geological and Earthquake Engineering, vol 27. Springer, Dordrecht.

Crowley, H., Despotaki, V., Silva, V., Pitilakis, K., Pitilakis, D., Hancilar, U., Bursi, O., Wenzel, M., di Filippo, R., Castro, J.M. (2017) *Deliverable D26.1 Taxonomy of European residential, commercial, industrial buildings and industrial plants*, SERA Deliverable, Available at URL: https://eu-risk.eucentre.it/exposure/..

Crowley, H., Rodrigues, D., Despotaki, V., Silva, V., Covi, P., Pitilakis, K., Pitilakis, D., Riga E., Karatzetzou, A., Romão, X., Castro, J.M., Pereira, N., Hancilar, U. (2018) *Deliverable D26.2 Methods for Developing European Residential Exposure Models*, SERA Deliverable, Available at URL: https://eu-risk.eucentre.it/exposure/.

Crowley, H., Rodrigues, D., Despotaki, V., Silva, V. (2019a) *Deliverable D26.3 Methods for Developing European Commercial and Industrial Exposure Models and Update on Residential*, SERA Deliverable.

Crowley, H., Despotaki, V., Rodrigues, D., Silva, V., Toma-Danila, D., Riga, E., Karatzetzou, A., Fotopoulou, S., Zugic, Z., Sousa, L., Ozcebe, S., and Gamba, P. (2019b) Exposure Model for European Seismic Risk Assessment, *Submitted to Earthquake Spectra.*

Crowley, H., Silva, V., Despotaki, V., Rodrigues, D., Weatherill, G., Danciu, L. (2019c) *Deliverable D26.7 Framework for European integrated risk assessment*, SERA Deliverable.

D'Ayala, D., Speranza, E. (2003) Definition of Collapse Mechanisms and Seismic Vulnerability of Historic Masonry Buildings, *Earthquake Spectra*, 19(3), -509.

D'Ayala D., Meslem, A., Vamvatsikos, D., Porter, K., Rossetto, T., Crowley, H., Silva, V. (2014) Guidelines for analytical vulnerability assessment of low/mid-rise buildings—methodology. Vulnerability Global Component project.

De Luca, F., Verderame, G. M., Gómez-Martínez, F., Pérez-García, A. (2014) The structural role played by masonry infills on RC building performances after the 2011 Lorca, Spain, earthquake. Bulletin of Earthquake Engineering, 12(5), 1999-2026.

Deyanova, M., Pampanin, S., Nascimbene, R. (2014) Assessment of single-storey precast concrete industrial buildings with hinged beam-column connections with and without dowels. In Proceedings of the 2nd European conference on earthquake engineering and seismology, Istanbul, Turkey.

DPC (2018) Da.D.O. (Database di Danno Osservato). Available at: http://egeos.eucentre.it/danno_osservato/web/danno_osservato)

Eads, L., Miranda, E., Lignos, D. (2015) Average spectral acceleration as an intensity measure for collapse risk assessment. Earthquake Engineering and Structural Dynamics, 44(12), 2057-2073.

Erdik, M., Uckan, E. (2014) Earthquake damage and fragilities of industrial facilities. In Seismic Design of Industrial Facilities (pp. 3-13). Springer Vieweg, Wiesbaden.

FEMA (2004) *HAZUS-MH Technical Manual*, Federal Emergency Management Agency, Washington DC.

FEMA (2012) Seismic Performance Assessment of Buildings. Methodology and Implementation, Tech. Rep. FEMA P-58-1, Federal Emergency Management Agency, Washington DC.

Faenza, L., Michelini, A. (2010) Regression analysis of MCS intensity and ground motion parameters in Italy and its application in ShakeMap. Geophysical Journal International, 180(3),1138–1152.

GEM (2018) Available at www.globalquakemodel.org/gem.

Grünthal, G. (1998) European macroseismic scale 1998. European Seismological Commission.

Gülkan, P., Langenbach, R. (2004) The earthquake resistance of traditional timber and masonry dwellings in Turkey. In 13th World Conference on Earthquake Engineering: 1-6.

Hak, S., Morandi, P., Magenes, G., Sullivan, T. (2012) Damage control for clay masonry infills in the design of RC frame structures. Journal of Earthquake Engineering, 16(sup1), 1-35.

Jalayer, F., Cornell, C. (2002) Alternative nonlinear demand estimation methods for probability-based seismic assessments, Earthquake Engineering and Structural Dynamics, 38, 951–972.

Jaiswal, K., Wald, D., Hearne M. (2009) Estimating casualties for large worldwide earthquakes using an empirical approach, US Geological Survey Open-File Report 1136.

Jaiswal, K., Wald, D. (2013) Estimating Economic Losses from Earthquakes Using an Empirical Approach, Earthquake Spectra, 29(1), 309-324.

Luzi, L., Puglia, R., Russo, E., ORFEUS WG5 (2016a). Engineering Strong Motion Database, version 1.0. Istituto Nazionale di Geofisica e Vulcanologia, Observatories & Research Facilities for European Seismology. doi: 10.13127/ESM

Luzi, L., Puglia, R., Russo, E., D'Amico, M., Felicetta, C., Pacor, F., Lanzano, G., Çeken, U., Clinton, J., Costa, G., Duni, L., Farzanegan, E., Gueguen, P., Ionescu, C., Kalogeras, I, Özener, H., Pesaresi, D., Sleeman, R., Strollo, A., Zare, M. (2016b) The Engineering Strong‐Motion Database: A Platform to Access Pan‐European Accelerometric Data. Seismological Research Letters, 87(4), 987–997.

Kappos, A., Panagopoulos, G., Panagiotopoulos, C., Penelis, G. (2006) A hybrid method for the vulnerability assessment of R/C and URM buildings. Bulletin of Earthquake Engineering 4(4), 391–413.

Karantoni, F., Papadopoulos, M., Pantazopoulou, S. (2016) Simple seismic assessment of traditional unreinforced masonry buildings. International Journal of Architectural Heritage, 10(8), 1055-1077.

Kohrangi, M., Bazzurro, P., Vamvatsikos, D., Spillatura, A. (2017a) Conditional spectrum-based ground motion selection using average spectral acceleration. Earthquake Engineering and Structural Dynamics, 46(10), 1667-1685.

Kohrangi, M., Kotha, S.R., Bazzurro, P. (2017b) Ground motion models for average spectral acceleration in a period range: direct and indirect methods, Bulletin of Earthquake Engineering, 16(1), 45-65.

Kosič, M., Fajfar, P., & Dolšek, M. (2014) Approximate seismic risk assessment of building structures with explicit consideration of uncertainties. Earthquake Engineering and Structural Dynamics, 43(10), 1483-1502.

Lagomarsino, S., Giovinazzi, S. (2006) Macroseismic and mechanical models for the vulnerability and damage assessment of current buildings. Bulletin of Earthquake Engineering, 4(4), 415-443.

Lagomarsino, S., Cattari, S. (2014) Fragility Functions of Masonry Buildings, in SYNER-G: Typology Definition and Fragility Functions for Physical Elements at Seismic Risk: Buildings, Lifelines, Transportation Networks and Critical Facilities, K. Pitilakis, H. Crowley, and A.M. Kaynia, Editors., Springer Netherlands: Dordrecht.

Maio, R., Tsionis, G. (2016) Seismic fragility curves for the European building stock: review and evaluation of existing fragility curves. Joint Research Centre, Ispra, Italy. 10.2788/586263.

Mariniello, C. (2007) Una procedura meccanica nella valutazione della vulnerabilità sismica di edifici in c.a., Ph.D. Thesis in Ingeneering of materials and production, University of Naples "Federico II".

Martins, L. (2018) Earthquake damage and loss assessment of reinforced concrete buildings. PhD Dissertation. University of Porto, Portugal.

Martins L., Silva V. (2018) A Global Database of Vulnerability Models for Seismic Risk Assessment, Proceedings of the 16th European Conference on Earthquake Engineering, Thessaloniki, Greece.

Martins, L., Silva, V. (2019) A Global Database of Vulnerability Models for Seismic Risk Assessment, *In preparation*.

McKenna, F., Fenves, G., Scott, M., Jeremic, B. (2000) Open System for Earthquake Engineering Simulation (OpenSees). Pacific Earthquake Engineering Research Center. University of California, Berkeley, CA.

Mouroux, P., Le Brun, B. (2006) Presentation of RISK-UE Project. Bulletin of Earthquake Engineering 4, 323–339.

MunichRe (2019) NatCatService - Natural catastrophe statistics online. Available at: https://natcatservice.munichre.com/ Accessed on the 03/01/2019.

Pitilakis, K., Franchin, P., Khazai, B., Wenzel, H. (Eds.) (2014) SYNER-G: systemic seismic vulnerability and risk assessment of complex urban, utility, lifeline systems and critical facilities: methodology and applications (Vol. 31). Springer.

Porter, K., Farokhnia, K., Vamvatsikos, D., Cho, I. (2014) Guidelines for component-based analytical vulnerability assessment of buildings and non-structural elements. Global Earthquake Model Foundation, Pavia, Italy: GEM Technical Report 2014-13.

Riahi, Z., Elwood, K.J., Alcocer, S.M. (2009) Backbone Model for Confined Masonry Walls for Performance-Based Seismic Design, Journal of Structural Engineering, 135(6), 644-654.

Rodrigues, D., Crowley, H., Silva, V. (2018) Earthquake loss assessment of precast RC industrial structures in Tuscany (Italy). Bulletin of Earthquake Engineering, 16(1), 203-228.

Rossetto, T., A. Elnashai (2003) Derivation of vulnerability functions for European-type RC structures based on observational data. Engineering structures, 25(10), 1241-1263.

Rossetto, T., Ioannou, I., Grant, D. (2013) Existing empirical vulnerability and fragility functions: compendium and guide for selection. Pavia: GEM Technical Report, The GEM Foundation.

Schnedler, W. (2005) Likelihood Estimation for Censored Random Vectors. Econometric Reviews, 24(2), 195-217.

Senel, S., Kayhan, A. (2010) Fragility based damage assessment in existing precast industrial buildings: A case study for Turkey. Structural engineering & mechanics, 11(1), 39.

Singhal, A, Kiremidjian, S. (1997) A method for earthquake motion–damage relationships with application to reinforced concrete frames. Tech. Rep. NCEER-97-0008, State University of New York at Buffalo, USA.

Silva, V. Crowley, H., Colombi, M. (2014) Epistemic Uncertainty in Fragility Functions for European RC Buildings. 10.1007/978-94-007-7872-6-4.

Crowley, H., Colombi, M., & Silva, V. (2014). Epistemic uncertainty in fragility functions for European RC buildings. In SYNER-G: Typology Definition and Fragility Functions for Physical Elements at Seismic Risk (pp. 95-109). Springer, Dordrecht.

Silva, V., Crowley, H., Varum, H., Pinho, R., Sousa, R. (2014b) Evaluation of analytical methodologies used to derive vulnerability functions. Earthquake Engineering & Structural Dynamics, 43(2), 181-204.

Silva, V., Yepes-Estrada, C., Dabbeek, J., Martins, L., Brzev, S. (2018) GED4ALL - Global Exposure Database for Multi-Hazard Risk Analysis – Multi-Hazard Exposure Taxonomy, GEM Technical Report 2018-01, GEM Foundation, Pavia, Italy.

Silva, V., Amo-Oduro, D., Caldero, A., Costa, C., Dabbeek, J., Despotaki, V., Martins, L., Pagani, M., Rao, A., Simionato, M., Viganò, D., Yepes-Estrada, C., Acevedo, A., Crowley, H., Horspool, N., Jaiswal, K., Journeay, M., Pittore, M. (2019) Development of a Global Seismic Risk Model, *Submitted to Earthquake Spectra*.

Silva, V., Horspool, N. (2019) Combining USGS ShakeMaps and the OpenQuake-engine for damage and loss assessment, Earthquake Engineering and Structural Dynamics, doi: 10.1002/eqe.3154

So, E., Pomonis, A. (2012) Derivation of globally applicable casualty rates for use in earthquake loss estimation models, Proceedings of 15th World Conference on Earthquake Engineering, Lisbon, Portugal.

STREST (2015) Guidelines for performance and consequences assessment of multiple-site, low-risk, high-impact, nonnuclear critical infrastructures exposed to multiple natural hazards. Deliverable report D4.3. Harmonized approach to stress tests for critical infrastructures against natural hazards.

Silva, V., Crowley, H., Varum, H., Pinho, R., Sousa, L. (2015) Investigation of the characteristics of Portuguese regular moment-frame RC buildings and development of a vulnerability model. Bulletin of Earthquake Engineering, 13(5), 1455-1490.

Verderame, G. M., Polese, M., Mariniello, C., Manfredi, G. (2010) A simulated design procedure for the assessment of seismic capacity of existing reinforced concrete buildings. Advances in Engineering Software, 41(2), 323-335.

Villar-Vega, M., Silva, V. (2017) Assessment of earthquake damage considering the characteristics of past events in South America, Soil Dynamics and Earthquake Engineering, 99, 86-96.

Villar-Vega, M., Silva, V., Crowley, H., Yepes-Estrada, C., Tarque, N., Acevedo, A., Hube, M., Santa María, H., Coronel, G. (2016) Development of a Fragility Model for the Residential Building Stock in South America, Earthquake Spectra, 33(2), 581-604.

Yepes-Estrada, C., Silva, V., D'Ayala, D., Rossetto, T., Ioannou, I., Meslen, A., Crowley, H. (2016) The Global Earthquake Model Physical Vulnerability Database, Earthquake Spectra, 32(4), 2567-2585.

Contact

Project lead	ETH Zürich
Project coordinator	Prof. Dr. Domenico Giardini
Project manager	Dr. Kauzar Saleh
Project office	ETH Department of Earth Sciences
	Sonneggstrasse 5, NO H62, CH-8092 Zürich
	sera_office@erdw.ethz.ch
	+41 44 632 9690
Project website	www.sera-eu.org

Liability claim

The European Commission is not responsible for any use that may be made of the information contained in this document. Also, responsibility for the information and views expressed in this document lies entirely with the author(s).